CHARACTERISATION OF A PUBLIC T CELL CLONOTYPE ENRICHED IN *M.tb* INFECTED INDIVIDUALS WHO DO NOT PROGRESS TO TUBERCULOSIS.

MOTSHIDISI MATELA

Thesis Presented for the Degree of

MASTER OF SCIENCE

in the Department of Pathology

Faculty of Health Science

UNIVERSITY OF CAPE TOWN

27/06/2024

Supervisor: Dr Munyaradzi Musvosvi

Co-supervisor: Professor Thomas Scriba

Declaration

I, Motshidisi Matela, hereby declare that the work on which this dissertation/thesis is based is my original work (except where acknowledgements indicate otherwise) and that neither the whole work nor any part of it has been, is being, or is to be submitted for another degree in this or any other university.

I empower the university to reproduce for the purpose of research either the whole or any portion of the contents in any manner whatsoever.

Signature: Signed by candidate

Date: 27/06/2024

Acknowledgements

What a challenging but rewarding journey this has been. I have surely learned a lot!

Firstly, I would like to thank God for giving me the strength to persevere and complete my thesis despite all the personal and academic challenges I faced.

I would also like to thank my wonderful family and friends for their unwavering support. I dedicate this thesis to my parents.

I am profoundly grateful to my supervisor, Dr Munyaradzi Musvosvi. His knowledge, experience, and guidance have enabled me to persevere through the challenges of this project. His encouragement, patience, and understanding throughout this study are deeply appreciated. It has been a pleasure working with him.

I also extend my gratitude to my co-supervisor, Professor Thomas Scriba, for his invaluable guidance that helped shape this project and the write-up.

Many thanks to Constance Scheuder and Lungile Jaxa for training me on various techniques and being a tremendous help in the laboratory. I am also grateful to Onke Nombida for assisting me with retrieving samples from the liquid nitrogen tanks.

To my colleagues, thank you for your support and for making the office a fun space.

Special thanks go to all the adolescents and adults who participated in the Adolescents Cohort Study, Grand Challenge Study, and the MRC-ship pilot study.

Finally, I would like to thank the National Institutes of Health and the Bill & Melinda Gates Foundation for funding this study. I also appreciate the financial support from the National Research Foundation, UCT Vice Chancellor's Scholarship, and the Canon Collins Scholarship towards my degree.

List of Figures

List of Tables

List of Equations

List of Abbreviations

ACS	Adolescent Cohort Study
APC	Antigen Presenting Cell
BB7	MHC Class II-restricted T cell Hybridoma
BCG	Bacille Calmette-Guerin
BCR	B cell Receptor
BTN3A1	Butyrophilin Subfamily 3 Member A1
CCR	Chemokine Receptor
CD	Cluster of Differentiation
CDR	Complementary determining region
CFU	Colony Forming Units
CLRs	C-type Lectins
DC	Dendritic Cell
DNA	Deoxyribonucleic acid
DNM3	Dynamin-3
dPCR	Digital Polymerase Chain Reaction
DURT cells	Donor Unrestricted T cells
ELISA	Enzyme-Linked Immunosorbent Assay
EPTB	Extrapulmonary Tuberculosis
FACS	Fluorescence-Activated Cell Sorting
FBS	Fetal Bovine Serum
FCI	Flow Cytometry Immunophenotyping
FCS-A	Forward Scatter-Area
GC6-74	Grand Challenge
GEM	Germline-encoded mycolyl lipid reactive T cells
HAT	Hypoxanthine-Aminopterin-Thymidine
HK	Heat-killed
HLA	Human leukocyte Antigen
IFN-γ	Interferon gamma
IL	Interleukin
iNKT	Invariant Natural killer T cells
IP	Inducible Protein
LAM	Lipoarabinomannan
LLO	Listeriolysin O
mAb	Monoclonal Antibody
MAIT	Mucosal-Associated Invariant T cell
MCP-1	Monocyte Chemoattractant Protein
MFI	Median Fluorescence Intensity
MHC	Major Histocompatibility Class
MOI	Multiplicity of Infection
MR1	Major Histocompatibility Class-related protein
M.tb	Mycobacterium tuberculosis
MTBC	Mycobacterium Tuberculosis Complex
NETs	Neutrophil Extracellular Traps
NHP	Non-Human Primate
NKs	Natural Killer cells
NO	Nitric Oxide

PAMPs	Pathogen-Associated Molecular Patterns
PBMCs	Peripheral Blood Mononuclear Cells
PBS	Phosphate buffered saline
PCR	Polymerase Chain reaction
PD-1	Programmed Cell Death Protein
Pen-strep	Penicillin-Streptomycin
PLZF	Promyelocytic Leukemia Zinc Finger Protein
PRR	Pattern Recognition Receptors
QFT	QuantiFERON
qRT-PCR	Quantitative-Real time Polymerase Chain Reaction
RAG	Recombination-Activating Gene
rBCG	recombinant Bacille Calmette-Guerin
RLR	RIG-1-like receptors
RNA	Ribonucleic Acid
ROI	Reactive Oxygen Intermediates
ROS	Reactive Oxygen Species
RPMI	Roswell Park Memorial Institute
RT	Room Temperature
SSC-A	Side Scatter- Area
TB	Tuberculosis
Tc	Cytotoxic T cells
TCR	T cell receptor
Tfh	T cell follicular helper
Th	T cell helper
TLR	Toll Like Receptors
TNF	Tumor necrosis factor
TRB	T cell receptor Beta locus
Treg	T regulatory cell
V(D)J	Variable (diversity) joining rearrangement
WHO	Word Health Organisation
γδ T cells	Gamma-delta T cells
°C	Degrees Celsius

Abstract

Introduction: T cells are known to play an important role in controlling *M. tuberculosis* (*M.tb*) infection, but it is not known if specific T cell clones contribute to the outcome of *M.tb* infection. We recently completed a bulk T cell receptor (TCR) sequencing screen and observed that frequencies of a particular donor-unrestricted T cell (DURT) clone were higher in healthy, *M.tb* infected individuals who controlled infection (controllers), than individuals who progressed to tuberculosis (TB) (progressors). This clone expresses a common complementarity-determining region 3 (CDR3) α sequence, which we termed "kiif.tb". Frequencies of kiif.tb T cells were also higher in healthy *M.tb* infected individuals than TB patients in another bulk T cell TCR sequencing screen in a different cohort.

Objective: In my project, we aimed to confirm if healthy, *M.tb* infected individuals (i.e. IGRA+) have higher frequencies of kiif.tb expressing T cells compared to healthy uninfected individuals (i.e. IGRA-) or individuals with active TB. We also aimed to identify cost-effective methods for detecting kiif.tb T cells in peripheral blood mononuclear cells (PBMCs) and assess the activation phenotype of kiif.tb in IGRA-, IGRA+, and TB patients.

Methods: A custom-designed digital PCR (dPCR) assay was used to quantify the frequencies of total T cells and kiif.tb T cells from IGRA-, IGRA+, and TB patients. Identification and characterisation of kiif.tb T cells by flow cytometry was performed using a custom flow cytometry-compatible RNA hybridization assay (PrimeFlow^{TM}) and custom monoclonal antibodies were generated from mice immunised with kiif.tb sequence.

Results: Total T cell frequencies measured by dPCR in all participants correlated strongly with both bulk TCR sequencing (rho = 0.74, p-value = 0.02) and flow cytometry (rho = 0.75, p = $5x10^6$). However, the correlation between kiif.tb T cell frequencies measured by dPCR and kiif.tb CDR3a measured using bulk TCR sequencing was modest (rho = 0.48, p-value = 0.01). Kiif.tb T cell frequencies were not significantly higher in IGRA+ individuals with recent or remote *M.tb* infection compared to IGRA- controls (p = 0.4 and 0.31, respectively), nor when compared to individuals with TB disease (p-value = 0.39 and 0.27, respectively). Frequencies of kiif.tb T cells, quantified by custom monoclonal antibody (clone39A9D4) staining, were not different across study groups. However, active TB patients had higher frequencies of kiif.tb T cells expressing HLA-DR compared to IGRA- controls (p-value = 0.02). We did not include IGRA+ individuals, because only a single individual in this group had sufficient kiif.tb cells for phenotyping. Frequencies of bulk T cells expressing HLA-DR were also higher TB patients than to IGRA+ individuals (p-value = 0.05).

Discussion: Our results suggest that kiif.tb-specific T cell frequencies measured by dPCR, or monoclonal antibodies were not different between the clinical groups, contrary to our hypothesis. The custom dPCR assay may only accurately detect targets at higher abundances, like total T cells (30-70%), limiting accuracy for quantifying kiif.tb T cells, which occur at abundances 1000-fold lower (0-0.04%).

Next steps involve validating initial findings using bulk TCR sequencing and further optimizing the monoclonal antibody staining for kiif.tb T cell quantification by flow cytometry. Notably, our HLA-DR data suggest that kiif.tb T cells are highly activated in patients with active TB, which may suggest that these DURT cells recognise *M.tb* antigen. With further optimization, such an antibody could useful for developing novel T-cell-based TB biomarkers.

Chapter One

Literature review

1.1 Introduction

Tuberculosis (TB) is one of the deadliest infectious diseases globally.[1] In 2022, the World Health Organization (WHO) estimated that around 10.6 million people worldwide were diagnosed with tuberculosis (TB), resulting in approximately 1.4 million deaths attributed to the disease. Tuberculosis is the second leading cause of death from infectious agents after COVID-19.[2] However, with the waning of the COVID-19 pandemic, TB is likely to return to being the leading cause of death from an infectious agent. This disease is caused by members of the *Mycobacterium tuberculosis* complex (MTBC), which include *Mycobacterium africanum*, *Mycobacterium bovis, Mycobacterium canettii, Mycobacterium microti*, *Mycobacterium tuberculosis (M.tb),* and these cause TB in both humans and animals.[3]

Initially, it was thought that infection only occurs following inhalation of aerosol microdroplets coughed up by an individual with active pulmonary tuberculosis.[4] However, it is important to note that cough-independent aerosolization is possible and has been shown to result in a higher production of bacilli compared to coughing.[5] These microdroplets can remain in the air for several hours, and given the small diameter of respiratory bronchioles, only the smallest aerosol droplets containing one or two bacilli can effectively reach the alveolar space.[6] This means a small number of bacterial cells can establish an infection.

Approximately 5-10% of individuals who are infected will progress to develop active TB disease, either due to progressive primary infection, re infection or through reactivation, which can occur long after the initial infection.[7] The progression to active TB disease is typically seen as a failure of the host's immune response to control the infection, a condition shaped by the immune status and genetic makeup of the host. This is usually observed in immunocompromised individuals and children under the age of five years.[8] Pulmonary TB is the most common form of the disease and is the only form likely to transmit, while TB can also affect other organs such as lymph nodes, bones, and meninges, known as extrapulmonary TB (EPTB).[9] Symptoms of

pulmonary TB include chronic cough, sputum expectoration, severe weight loss, fever, and night sweats.[10]

The spread of *M.tb* through aerosols, combined with its ability to be infectious in small quantities, makes it a significant health concern, especially in developing countries. These regions often have higher population densities, poor living conditions, inadequate nutrition, and a higher prevalence of immune-compromising diseases. Furthermore, without an effective vaccine for adolescents and adults understanding why individuals respond differently to *M.tb* may help develop effective therapeutics and a vaccine for all generations.

1.2 General Immunology

Immunology is the field of study dedicated to understanding the immune system, specifically its responses to pathogens, tissue damage, and its role in the pathogenesis of diseases, including cancer, where immune responses can influence tumour development and progression.[11] The immune system is composed of tissues, cells, and molecules that provide resistance to various infections.[12] These elements of the immune system work in unison to defend the body against invaders like bacteria, fungi, viruses, toxins, and parasites.[13] The immune system is comprised of two main classes: the innate and the adaptive immune system.[14]

1.2.1 The innate immunity

The innate immune system is the first line of defence against invading pathogens and provides early, and rapid host protection from infections.[13] It consists of anatomical and physiological barriers (such as skin and gastric pH), antimicrobial peptides, proteins, and humoral components.[15, 16]

This system also comprises cellular components derived from myeloid progenitors, including phagocytes (such as macrophages, dendritic cells (DC), and neutrophils), as well as mast cells, eosinophils, and basophils. Additionally, it includes natural killer (NK) cells derived from lymphoid progenitors.[2, 13] Cells that make up the innate immune system mostly rely on the expression of various receptors termed pattern recognition receptors (PRRs) to recognise pathogens. These receptors (Toll-like receptors (TLR), C-type lectins (CLRs), and RIG-1-like receptors (RLR)) recognise a wide range of pathogen-associated molecular patterns (PAMPs), that are expressed and shared by a large group of microorganisms.[13] While these receptors allow for rapid

immune responses to various classes of pathogens, the innate immune system is a relatively non-specific host immune response.[17]

Macrophages are typically among the first cells to engulf and ingest invading pathogens upon recognition through their PRRs. These PAMPs stimulate the differentiation of macrophages into a classical M1 or alternative M2 phenotype.[18] However, it is important to note that the M1/M2 phenotype distinction is largely observed in murine studies, and in humans, the biology of macrophages is rather complex. The M1 phenotype is associated with the production of pro-inflammatory cytokines, chemokines, nitric oxide (NO), reactive oxygen intermediates (ROI), and the initiation of an immune response that recruits other cells.[18] In contrast, the M2 phenotype promotes cell proliferation and tissue repair.[18]

The secreted pro-inflammatory cytokines such as Interleukin (IL)-12 and IL-18 by macrophages can prime NK cells.[19] These effector lymphocytes of the innate system have cytolytic functions through the release of cellular granules such as perforin and granzymes, thus leading to the direct killing of the viral infected cells or bacteria.[20] Secondly, these cells can produce cytokines such as interferon (IFN)-γ and chemokines such as CXCL1 which leads to recruitment and activation of neutrophils.

Similarly, to macrophages, neutrophils mediate pathogen clearance through phagocytosis and the production of reactive oxygen species (ROS).[21] Furthermore, the neutrophils release granules which are the main storage sites of the most toxic mediators, including elastase, myeloperoxidase, cathepsins, and defensins. [22] These mediators are mobilized to the phagosome promptly after the ingestion of invaders, thereby ensuring the effective killing of the pathogen within the phagosome. In addition, upon activation, these cells release neutrophil extracellular traps (NETs) which are a network of extracellular strings of deoxyribonucleic acid (DNA) that bind microorganisms.[23] This mechanism can lead to immobilizing and sometimes killing of invading microorganisms.

The recruited dendritic cells and macrophages function as professional antigen-presenting cells (APCs). [13] Macrophages facilitate the maturation, differentiation, and migration of DCs. Dendritic cells can play a key role in the transportation of antigens from the site of infection to the draining lymph nodes.[13] In the lymph nodes, these cells present antigens to naïve T cells, thereby priming the adaptive cells. Therefore, DCs

and macrophages are important in linking the innate and adaptative immune system.[13,24]

1.2.2 The Adaptive immunity

Similar to NK cells, T and B cells are derived from the lymphoid progenitor.[14] Both these cells are produced in the bone marrow. However, the T lymphocytes develop in the thymus, whereas B lymphocytes continue their development in the bone marrow.[25]

In contrast to the rapid and non-specific innate response, the adaptive immune system, through mechanisms such as clonal selection and expansion, provides a delayed, antigen-specific, and antigen-dependent host immune response.[2,11] Interestingly, while the initial response is delayed, it is the secondary responses (memory responses) that are faster and larger. In addition, the antigen-specific surface receptors expressed on both these cells are the main contributors to the T and B cell antigen-specific immune responses.

1.2.2.1 T lymphocyte receptor repertoire diversity

T cells express unique T cell receptors (TCR), which are antigen-binding receptors on their membranes. These TCRs are heterodimers, comprised of the α and β chains (TCR-αβ) or γ and δ chains (TCR-γδ), with γδ T cells constituting 1-10% of the T cell repertoire. Most of the TCR-αβ receptors recognise specific antigens presented by APCs in the context of major histocompatibility complex (MHC).[2, 26] TCR diversity is a remarkable and fundamental property of an effective antigen-specific T cell response, and it is required to recognise and mount a response to control infections.[27]

This diversity is generated by V(D)J gene rearrangement, which is a mechanism of somatic recombination that occurs during the early stages of T cell development. A variable (V), joining (J), and constant (C) region make up the TCR α- and γ- chains, while the TCR β- and δ-chains are also made up of a V, J, C regions and an additional diversity (D) region.[27, 28] This site-specific recombination process is directed by lymphoid-specific recombination-activating gene (RAG), which is composed of RAG1 and RAG2.[29].

Each TCR chain is comprised of three complementary determining regions (CDR), namely CDR1, CDR2, and CDR3.[35] The first two complementary determining regions 1, and 2 are germline-encoded Variable gene segments. These regions are involved in MHC interactions.[35]

CDR3 is recombined with either an additional nucleotide and/or deletion of some nucleotide at the joints.[36] CDR3 is the primary site of epitope (antigen) contact. This region is mostly affected by recombination compared to the other two CDRs, and this region in the β chain accounts for most of the variation observed within the T cell repertoire of an individual.[36]

Surprisingly, some TCRs are simple and highly conserved among individuals, and cells that express these TCRs are termed donor-unrestricted T (DURT) cells.[30] DURT cells include mucosal-associated invariant T cells (MAIT), human leukocyte antigen (HLA)-E restricted T cells, invariant natural killer T cells (iNKTs), group 1 cluster of differentiation (CD) 1-restricted T cells, germline-encoded mycolyl lipid reactive (GEM) T cells, and gamma-delta (γδ) T cells.[31] The characteristics of these cells are the TCR-chain's invariant variable (V) and joining (J) gene combinations, as well as the widely distributed canonical TCR-amino acid sequences that are prevalent in many individuals and conserved across species.[32] These alpha chains are usually paired with a limited number of TCR-β chains, except for gamma delta T cells.

1.2.2.2 Conventional T lymphocytes

T cells can be broadly categorized into two subtypes based on the presence of CD4 and CD8 surface markers. CD4 T cells secrete various cytokines that activate other cells and are commonly referred to as helper or inducer T cells.[25] In contrast, CD8 T cells produce a range of cytokines and have the ability to eliminate target cells through direct cell contact or by releasing effector molecules, earning them the designation cytolytic T cells.[33]

CD4 Th subsets

In earlier studies, it was observed that antigen-specific CD4 T cells can be differentiated into T helper (Th1) or Th2 subsets. This differentiation of naïve T cells into different Th subsets is influenced by the cytokines present during and after antigen presentation. Additionally, Th1 and Th2 cells can be distinguished by the unique sets of cytokines they express, known as type 1 and type 2 cytokines. Th1 responses are characterized by type 1 cytokines such as IL-2, IFN-γ, and tumor necrosis factor (TNF). In contrast, Th2 responses are marked by the presence of type 2 cytokines, including IL-4, IL-5, IL-10, and IL-13. More recently, additional T helper subsets, including Th17 and T regulatory (Treg) cells, have been identified. Furthermore, mice

knock-out studies have been essential in shedding light on the transcription factors associated with the differences.

Th1 subset

T-bet is a member of the T-box family of transcription factors that are expressed primarily in immune cells only. This transcription factor is rapidly induced in developing Th1 cells, which plays an important role in eliminating intracellular pathogens.[34] A study by Szabo *et al*. showed that CD4 T cells from mice homozygous for T-bet deletion differentiated into Th2 cells and increased the production of Th2 cytokines.[34] Furthermore, these cells were unable to supress IL-4 and IL-5, even when stimulated under Th1 inducing conditions. This suggested that T-bet may override a pathway that leads to Th2 cells to induce Th1 cells.

Furthermore, expression of this transcription factor correlates with IFN-γ expression, this cytokine is associated with Th1 cells and plays a significant role in the activation of macrophages leading to bacterial clearance. The Szabo *et al.* study further revealed that mice that had T-bet deletion had a marked decrease in IFN-γ production even in the presence of IL-2, a potent inducer of IFN-γ production.[34] The lack of T-bet impairs the production of type 1 cytokines, and this leads to defective control of intracellular infection and may lead to poor control of intracellular pathogens and viruses.

Th2 subset

Unlike Th1 cells, Th2 cells play a role in eradicating extracellular infections. These cells play a role in initiating and sustaining the humoral, or antibody-mediated, immune response against extracellular parasites, bacteria, toxins, and allergens.[35]

The transcription factor associated with this T cell subset is GATA-3, a member of the GATA family of transcription factors.[35] The expression of this transcription factor is associated with IL-4 production, which is essential in regulating antibody production. A study by Granato *et al.* showed that IL-4 stimulates in vitro B-cell maturation and modulates B cell receptor (BCR) signalling in developing B cells.[36]

GATA-3 knock-out studies have highlighted that, CD4 T cells of GATA-3 deficient mice, differentiate into Th1 cells and display increased IFN-γ production.[35, 37] Interestingly, even under Th2 stimulating conditions, mature CD4 T cells from these

mice differentiated into Th1 cells. This suggests that GATA-3 is required in developing Th2 cells for optimal Th2 differentiation and maintenance of the Th2 response.[35, 37]

Th17 and Treg subsets

RORγt is a member of the nuclear receptor family of transcription factors.[38] It is mainly expressed in differentiated Th17 cells and correlates with the expression of IL-17 and IL-22, This transcription factor was identified through analysis of IL-17A in mice deficient for specific transcription factors.[38] It is believed that these cells evolved to protect the host against microbes that Th1 or Th2 immunity is less effective against, such as extracellular bacteria and certain fungi. According to findings by Pelletier *et al.* supernatants derived from activated Th17 cells were found to secrete CXCL8, a chemokine, which attracted neutrophils to the site of infection. This effect of Th17 in recruiting neutrophils may explain how these cells assist in the elimination of extracellular bacteria. However, it is important to note that, like other cytokines, excessive levels can be detrimental. The excessive recruitment of neutrophils by Th17 cells may cause damage to the host.[39]

The generation of a protective immune response is critical to clear infections and protect individuals from pathogens. However, it is equally important to regulate the response to maintain homeostasis.[40] This mechanism prevents host tissue damage and is implemented by Treg cells. These cells are characterized by high expression of the transcription factor Foxp3.[40] This transcription factor stimulates the production of immunosuppressive cytokines, including IL-10 and TGF-β.[40] Additionally, these cells secrete cytotoxic substances such as perforin and granzyme to eliminate effector cells. Findings by Grossman *et al.* revealed that human CD4, $CD25^+$ natural T regs express granzyme A after activation. Furthermore, these cells were able to kill purified autologous CD4 and CD8 in a perforin-dependent manner.[30]

Other subsets of CD4 T cells, like Th9, express the Pu.1 transcription factor, which is believed to inhibit the expression of Th2-associated GATA-3 and Th1-associated T-bet.[41] Like Th2 cells, Th9 is believed to contribute to defence against helminths and to facilitate airway constriction and mucus production in allergic asthma. Furthermore, other important subsets include Th22 cells which express granzyme B and are associated with host defence and remodelling of tissue, they express the RORγt and AhR transcription factors.[42] Lastly, the other subset is T follicular (Tfh) which

expresses the BCL-6 transcription factor and these cells are essential for germinal centre formation.[43]

CD8 Tc subsets

Interestingly, the same transcription factors are expressed in CD8 T cells, allowing these cells to differentiate into distinct cytotoxic T cell (Tc) subsets, each associated with different effector functions.

Tc1/Tc2 subsets

Like CD4 Th1, type 1 cytokine such as IL-12 activate T-bet, which induces a CD8 Tc1 differentiation, and these cells are essential in immunity against intracellular pathogens and tumors.[34] These cells express IFN-γ which is a key mechanism by which these cells combat viral infections. However, this transcription factor plays a role in IFN-γ gene transcription within the CD4 T cell lineage but not within the CD8 T cell lineage.[34] According to findings by Szabo *et al.* IFN-γ production was not affected in T-bet knockout mice.[34] Furthermore, CD8 T cells from knockout mice displayed equivalent cytotoxic activities comparable to CD8 T cells of wild-type mice. These findings suggest that the presence of T bet may play a distinct role in C8 T cells than that observed in CD4 T cells.[34]

In contrast to Tc1, the differentiation of Tc2 is driven by the interaction of type 2 cytokines such as IL-4 and the transcription factor GATA-3.[35] Findings by Pai *et al*. show that optimal production of Tc2 cytokines and suppression of Tc1 cytokine depends on GATA-3.[35] These cells play a role in the propagation of Th2 cell-mediated allergy. However, they display low levels of cytotoxicity compared to Tc1.[44]

Although these cells are induced by different cytokines and transcription factors, both subsets are cytotoxic via the perforin and Fas pathway. Therefore, both subsets can protect the host and induce inflammation.[45]

Other major subsets of CD8 T cells produced by the different cytokine milieu include Tc9, Tc17, Tc22, Tfh, and CD8 T regs and these subsets express different transcription factors such as IRF-4, RORγt, Ahr, BCL-6 and Foxp3, respectively (*Table 1*).[44]

Table 1: A summary of the characteristics of each of the CD4/CD8 T cell lineages

	T cell subset	Polarizing cytokines	Transcription factor	Effector cytokines
CD4	T_H1	IFN-γ, IL-12	T-bet	IFN-γ, TNF, IL-2
	T_H2	IL-4	GATA-3	IL-4, IL-13, IL-5
	T_H9	IL-4, TGF-β	Pu.1, IRF4	IL-9
	T_H17	TGF-β, IL-6, IL-1β	RORγt	IL-17, IL-22
	T_H22	IL-6, IL-23, IL-1β, TNF	RORγt, AhR	IL-22, IL-26, IL-1β, TNF, Granzyme B
	T*fh*	IL-6, IL-21, IL-12	BCL-6	IL-21
	Treg	TGF-β	Foxp3	IL-10, TGF-β
CD8	Tc1	IL-12	T-bet	IFN-γ, TNF
	Tc2	IL-4	GATA-3	IL-4, IL-13, IL-5
	Tc9	IL-4, TGF-β	IRF4	IL-9
	Tc17	IL-6, TGF-β	RORγt	IL-17, IL-22
	Tc22	IL-6, TNF	AhR	IL-22, TNF
	Tfc	IL-6, IL-21, IL-23, TGF-β	BCL-6	IL-4, IL-2, IFN-γ
	Treg	TGF-β	Foxp3	IL-10, TGF-β

(Polarizing cytokines induce different signalling cascades that lead to activation of specific transcription factors, leading to differentiation into one of the T cell subsets. These subsets are characterized by distinct cytokine production.)

1.2.2.3 Donor-unrestricted T cells

While conventional T cells (CD4 and CD8 T cells) are activated through a limited MHC-dependent process, several non-peptide-responsive T cell subsets in humans are activated independently of MHC, using non-polymorphic presentation systems.[46] These systems include CD1, MHC-related protein (MR1), butyrophilin subfamily 3 member A1 (BTN3A1), and the non-classical MHC class 1b family member HLA-E.[31,46]

As a result, the T cell responses that ensue can exhibit similarity across genetically diverse populations. Thus, the donor-unrestricted aspect of antigen presentation introduces an intriguing possibility for vaccine development, where a single vaccine antigen could be formulated to effectively target the entire global population, unaffected by host genetic factors, in contrast to MHC-restricted responses.[46]

MAIT cells

These cells are present in peripheral blood but are highly abundant in barrier tissues such as the lungs, liver, and kidneys, where they possess tissue resident phenotypes.[47] MAIT cells express a semi-invariant TCR and detect antigens presented by the MR1 molecule.[47] MR1 molecules present biosynthetic derivatives of riboflavin synthesis. Riboflavin is required for a broad range of bacterial cellular activities, and most bacteria have functional riboflavin production pathways.[28] Thus, these cells can recognise a variety of different bacteria.

Notably, in the absence of TCR-mediated antigen recognition, these cells can be triggered by cytokines like IL-18 and IL-12, expanding the spectrum of pathogens to which MAIT cells can react, including viruses.[48] However, these two modes of activation seem to have distinct results, in terms of the expression of transcription factors, cytokines, and cytotoxic molecules produced by these cells. Lamichhane *et al*. revealed that upon TCR activation, these cells upregulate the expression of T-bet and RORγt transcription factors, whereas cytokine activation only led to upregulation of T-bet.[48] The expression of distinct transcription factors affects the cytokine profile of these cells. TCR stimulation leads to the production of multiple cytokines such as IFN-γ, TNF, IL-17, and IL-22, while cytokine stimulation results in increased production of IFN-γ but not TNF. This effect makes TCR stimulation result in a rapid immune response as compared to an immune response from cytokine activation.[48]

Even though these cells play a key role in indirect killing of target cells by secreting cytokines that recruit and activate phagocytes, it is important to note that they are capable of directly killing infected cells. Upon both modes of activation, these cells can produce cytotoxic molecules such as perforin and granzymes.[49] However, the level of expression of genes and production of these cytotoxic molecules differs between the two modes of activation. Lamichhane *et al.* further showed that Granzyme A, B, and perforin were found in the culture supernatants of both TCR and cytokine stimulation,

with higher levels of granzyme A observed in the supernatants of cytokine-treated MAIT cells.[48] Furthermore, the differences were also observed in the gene expression of granzyme K and M.

Invariant killer T cells (iNKTs)

Unlike MAIT cells, these cells identify self and foreign lipids presented by CD1d as specific antigens.[50] CD1d belongs to a vast family that encompasses CD1a, CD1b, and CD1c molecules, all of which present lipids instead of peptides. These cells are highly enriched in the liver and the fold of the peritoneum connecting the stomach to other abdominal organs, with their numbers intriguingly decreasing in the context of obesity.[50] The iNKT cell subsets can exhibit distinct profiles based on the expression of various transcription factors and their functional responses, particularly regarding the primary cytokine activation following TCR-dependent or cytokine (IL-12 and IL-18) stimulation.[50, 51] In mice, the determination of whether to become iNKT1, iNKT2, or iNKT17 seems to occur in the thymus during development. However, it is still uncertain whether each fate is fixed permanently or can be subject to further modulation.[50]

However, all these subsets seem to express the same transcription factor, promyelocytic leukemia zinc finger protein (PLZF), which is an essential factor for the development and innate function of these cells.[50] Lee *et al.* demonstrated that iNKT1 cells express low levels of PLZF, and elevated levels of T-bet, while iNKT2 express high levels of PLZF and GATA-3. Lastly, iNKT17 expresses intermediate levels of PLZF and high levels of RORγt.[50]

Additionally, the cytokine profiles are different between these subsets, therefore, indicating they may play distinct roles in the immune response. The iNKT1 cells express IFN-γ as the major cytokine and this may enhance macrophage phagocytic and bacterial activities by increasing the production of nitric oxide.[51] On the other hand, iNKT2 expresses IL-4, which may induce an alternative macrophage activation. Lastly, iNKT17 expresses IL-17 as a major cytokine, and this cytokine can directly induce the recruitment of neutrophils, which are phagocytes.[51]

Gamma delta(γδ) T cells

Gamma-delta T cells are a small subset in the peripheral blood but occur at increased frequencies in epithelial and mucosal tissues.[52] In humans, these cellular subgroups

are categorized as Vδ1 and Vδ2, distinguished by their δ-chain usage. The Vδ2 are mainly found in the peripheral blood whereas the Vδ1 cells primarily reside in the gut mucosa, lungs, and female reproductive system.[53]

Both subgroups have the ability to recognize various non-peptide antigens, although the specific TCR-activating ligands for Vδ1 T cells are not yet well understood.[53] Conversely, Vδ2 T cells have been demonstrated to detect phospho-antigens presented by the non-polymorphic molecule, BTN3A1.[53]

Based on the different anatomic locations these cells populate; it is not shocking to observe phenotypic heterogeneity between the two γδ T cell subsets. A highly expected difference between the two cell subsets is the tissue homing receptors.[53] Findings by Sanz *et al.* showed that pronounced differences between these two cell subsets are observed in chemokine receptors involving tissue homing, with chemokine receptor type 7 (CCR7) and CCR5 expressed at higher levels in Vδ1 than Vδ2, respectively.[53] Interestingly, heterogeneity is not limited to phenotype but also the functionality of Vδ1 and Vδ2 T cells. Although both these cells can express cytotoxic molecules upon activation which assist with killing infected cells, the expression levels seem to differ between the two cell subsets.[53] The study by Sanz *et al*. further revealed that upon activation, perforin production was elevated in Vδ2 T cells as compared to Vδ1 T cells.[53]

Additionally, Vδ2 T cells exhibit features resembling those of antigen-presenting cells, such as dendritic cells.[52] These cells are capable of reacting to signals from both microbes and tumors, and they can activate CD4 and CD8 T cells. The study by Branden *et al*. illustrated that only activated Vδ2 T cells induce proliferation and differentiation of naïve CD4 and CD8 T cells.[52] Therefore, it seems these cells play a role in initiating the adaptive response.

1.2.2.4 B lymphocytes

B cells have been extensively examined for their pivotal role in the humoral immune system, primarily in generating antibodies and establishing an antibody-mediated memory response against pathogens.[13, 17] Beyond this, these cells exhibit the capability to generate cell-mediated immunity. B cells express elevated levels of MHC-class II and possess the ability to present antigens to CD4 T cells.[54]

B cells take up BCR-bound and internalized protein antigens using the specialized MHC-II antigen presentation pathway and then deliver specific peptides in complex with MHC-II to CD4 T cells. Both B and T cells are affected by this interaction, which also affects how the immune system responds.

The B and T cell interaction seems to be beneficial to both cells. B cells can be activated via the B cell receptor which has great diversity due to V(D)J rearrangement, and this is the first signal needed to fully activate these cells.[55] The second signal is obtained from a T cell which responds to antigen presented by the B cell via MHC class II. This T cell-dependent activation leads to the production of long-live and high-affinity antibodies with immunological memory.[55]

1.3 Immune Response against *Mycobacter*ium *Tuberculosis*

The immune response driving the development of TB is intricate and not entirely comprehended. However, it is recognised that the progression of TB relies on the interplay between bacterial virulence and the host's immune response.[56] A key aspect of this disease is the ability of *M.tb* to persist within various intracellular environments across different myeloid cell types.

1.3.1 Innate Immunity

Recent research has uncovered that the innate branch of the immune system plays a more significant role in initiating and controlling inflammatory responses during infection than previously believed.[22] Upon inhalation, *M.tb* encounters the formidable defences of the respiratory tract's innate immune system. This initial interaction involves mucociliary clearance, where mucus and ciliary action collaborate to trap and remove inhaled particles, including *M.tb*, preventing their deeper penetration into the lungs.[57] However, should *M.tb* manage to enter the terminal alveoli, antimicrobial peptides like defensins and cathelicidins, which are peptides and proteins released by epithelial cells, counteract *M.tb*.[4, 58] In addition to the secreted antimicrobial peptides, inflammatory responses induced by *M.tb* infection such as the generation of ROS by recruited macrophages and neutrophils are central.[22] ROS acts as a bactericide, damaging bacterial DNA, ribonucleic acid (RNA), and proteins. Furthermore, the release of cytokine and chemokines from infected innate immune cells mediate the recruitment and activation of other immune cells. However, inflammatory processes

may lead to host tissue damage and chronic inflammation, therefore favouring the progression of the disease.[22]

Moreover, these ROS-generating cells are key players in relevant cell death processes that may eliminate the pathogen, such as apoptosis which is an active programmed cell death.[59] Meanwhile, other processes, like necrosis, which is an unprogrammed cell death caused by disturbances in the environment with the uncontrolled release of inflammatory cellular material, favour the survival of the bacteria.

1.3.1.1 The role of resident alveolar macrophages and recruited macrophages in *M.tb* infection.

Prior to being engulfed by phagocytic cells, *M.tb* has been observed to come into contact with the alveolar lining fluid, which is a diverse blend of lipids and proteins containing surfactant proteins and hydrolases that interact with glycolipids on the surface of mycobacteria.[7] The alveolar lining fluid boosts pathogen engulfment and elimination by phagocytes, with its effects on interactions with alveolar epithelial cells showing variability. A study using a murine lung-on-chip infection model investigated the effect of pulmonary surfactants on *M.tb* growth, extended in vitro cultivation causes alveolar epithelial cells a deficient surfactant phenotype. Surfactant deficiency leads to rapid and unregulated bacterial proliferation within both macrophages and alveolar epithelial cells. Conversely, in the presence of normal surfactant levels, a notable reduction in bacterial proliferation is observed. Hence, these findings could elucidate why smokers and individuals with impaired surfactant function are more susceptible to TB.[60]

Alveolar macrophages serve as the primary host cells to encounter *M.tb* and are crucial in initiating an immune response against the pathogen.[19] In an early infection study using mice infected with H37Rv *M.tb* mCherry, a strain expressing a red fluorescent label, examination of lung tissue via microscopy revealed that tissue-resident alveolar macrophages were the predominant cell type infected during the initial two weeks.[61] These cells become activated in response to mycobacterial products like lipoarabinomannan (LAM) and lipoproteins, engaging a range of receptors including Toll-like receptors, scavenger receptors, mannose receptors, and complement receptors. This leads to the engulfment of *M.tb* and triggers a series of processes involving the release of different chemokines like IL-8, monocyte chemoattractant protein (MCP)-1, and inducible protein (IP)-10, which draw

phagocytes such as monocyte-derived macrophages, dendritic cells, and neutrophils to the infection site.[62, 63,64] The recruited phagocytes are stimulated by the released cytokines, and this leads to their activation. In their activated state, they are involved in phagocytosis and antimicrobial activities. This result is a feedback loop, in which more phagocytic cells become activated, and release cytokines and chemokines to recruit and activate other innate immune cells. Subsequently, the activated antigen-presenting cells will travel to the lymph nodes to activate the adaptive immune cells, ultimately initiating the adaptive response.[65]

Macrophages act as the primary cellular environment for the growth and survival of *M.tb.* Nevertheless, these cells also play a pivotal role in triggering protective immune responses, both innate and adaptive, which are essential for managing or eradicating the infection.[19] These cells recognise *M.tb* via TLR-2 and C-type lectins receptors, and this leads to the uptake of bacteria.[7]

Following phagocytosis, the phagosome, a key regulator of both the homeostatic and microbicidal functions of macrophages, undergoes a sequence of maturation stages to develop into a highly acidic compartment.[66] Later this compartment subsequently fuses with a lysosome to develop into phagolysosomes with a low pH.[67] This low pH creates a suitable environment for the production of ROS, and for the activity of digestive lysosomal enzymes; thus, the process is important for the clearance of intracellular *M.tb.* However, upon phagocytosis, *M.tb* can hinder the maturation of the phagosome, thus evading the effects of being transported to the lysosome. According to findings by Vergne *et al*. *M.tb* can hydrolyse a key lipid, phosphatidylinositol 3-phosphate which is necessary for the fusion of the phagosome and lysosome, leading to the formation of the phagolysosome.[68]

In addition, disruption of phagosome maturation inhibits the processing of mycobacterial antigens to generate peptide-MHC class II complexes.[69] These peptide-MHC class complexes are then presented on the surface of the macrophage to activate naïve and memory T cells, therefore linking the innate and the adaptive immune response to efficiently control the infection. Ramachandra *et al.* illustrated that the presentation of Ag85B to MHC class II-restricted T cell hybridoma (BB7) cells in mice required phagocytosis by activated bone marrow macrophages.[70] Furthermore, this study demonstrated that phagosomes containing live *M.tb* contained fewer

peptide-MHC class II complexes as compared to phagosomes containing heat-killed (HK) *M.tb*, indicating that live bacteria inhibit phagocytic antigen processing. Therefore, this prevents a CD4 T cell response which is essential in controlling the infection.[70]

However, most of the time, the actions of macrophages are not disturbed, and phagocytosis occurs resulting in the production of antigens that could be presented to T cells. Additionally, infected macrophages produce cytokines such as TNF which is a primary mediator of granuloma development.[71] This cytokine stimulates macrophages and prompts the expression of chemokines and adhesion molecules crucial for attracting and retaining immune cells at the infection site. Furthermore, during granuloma maturation, activated macrophages can differentiate into epithelioid cells and giant cells that form mature granulomas. Therefore, this leads to successful interactions with T cells to bring about T cell activation in the lungs. These activated T cells release cytokines such as IFN-γ, driving full activation of macrophages by activating feedback inhibitory mechanisms, such as those mediated by IL-10 and STAT3.[19] Hence, allowing activation of NO synthase 2, which generates NO, is crucial, as NO plays a pivotal role in eliminating intracellular bacteria. In summary, the interactions between *M.tb* and alveolar macrophages significantly influence the subsequent progression of infection, determining whether there is clearance of infection or progression to disease. However, it's important to note that the disease state involves more than just the infected macrophage.[19]

1.3.1.2 The role of Neutrophils in *M.tb* infection

The contribution of neutrophils to the immune regulation of *M.tb* has not been extensively studied compared to macrophages.[72] Nonetheless, there is no doubt that these cells participate in the immune response against *M.tb*. Eum *et al*. illustrated that neutrophils constitute the predominant cell populations found in the bronchoalveolar lavage and sputum of individuals with active TB, and these cells are also the primary carriers of bacilli.[73]

Following infection, neutrophils are one of the first phagocytes to be promptly recruited to the lung interstitium through chemotaxis, which is triggered by alveolar macrophages. The uptake of *M.tb* is facilitated by opsonic receptors, such as

complement receptors and Fc-receptor-like proteins, as well as non-opsonic receptors, particularly CLRs.[72]

Following phagocytosis, the phagosome containing bacilli undergoes a maturation process that is different from macrophages.[72] These cells do not possess the conventional endocytic pathway and have a lower abundance of lysosomes compared to macrophages. During the maturation process, the phagosome merges with granules, allowing the contents of both primary and secondary granules to be conveyed into the phagosomes.[72] The primary granules contain potent hydrolytic enzymes such as elastase and myeloperoxidase. Elastase digests bacteria together with microbicidal peptides and ROS generated by NADPH oxidase, while myeloperoxidase catalyses the conversion of hydrogen peroxide to hypochlorous acid.[72] This acid kills bacteria by penetrating the cell wall and inhibiting DNA and protein synthesis, as well as ATP production. However, it seems *M.tb* has evolved to escape this oxidative killing of neutrophils. Corleis *et al*. demonstrated that whether *M.tb* was incubated with or without neutrophils, there was no alteration in colony-forming units (CFU) observed over a 6-hour period in both scenarios, and this was consistent regardless of the multiplicity of infection (MOI) used (0.1 vs 2). Therefore, this suggests that neutrophils are unable to kill the bacteria over time.[74] Furthermore, priming the cells with pro-inflammatory cytokines for enhanced oxidative killing did not alter *M.tb* survival. The study further revealed that *M.tb* induced necrosis of infected neutrophils by defective ROS production, and in the absence of NADPH oxidase and myeloperoxidase, mycobacteria failed to trigger necrosis of neutrophils.[74] The necrotic cells can be phagocytosed by macrophages, which will then recruit more neutrophils to the site, and this can lead to lung immunopathology. The inability of activated neutrophils to eradicate the bacteria indicated that mycobacteria might be targeting neutrophil survival.

Another mechanism involves the creation of extracellular fibrils known as NETs.[75] These structures consist of chromatin adorned with granule proteins, which adhere to and ensnare bacteria. Following activation, NETs are produced as an effect of the cell death process known as NETosis, which, contrary to apoptosis or necrosis, is dependent on ROS generated by NADPH oxidase.[75] While NETs can protect the host against microbes, excessive NETosis can be harmful to the host. [70] However, these NETs are ineffective at eliminating *M.tb*, which is intriguing given that NETs have been

shown to induce the death of other microorganisms.[75] Ramos-Kichik et al. demonstrated that NETs failed to eradicate *M. tuberculosis* H37Rv and *M. canettii* 9600046, despite their differing levels of virulence.[75] This resistance could stem from the intricate structure of its cell wall and evasion tactics. Consequently, this might result in excessive NET formation in TB, contributing to host tissue damage, exacerbating inflammatory responses, and causing lung injury.[75]

1.3.1.3 The role of dendritic cells in *M.tb* infection

Dendritic cells are highly effective as professional antigen-presenting cells for activating naïve T cells, and they are crucial for producing IL-12, which is essential for promoting a Th1 phenotype in the lymph nodes. This process leads to the activation of T cells that produce IFN-γ. [76]

During the initial stages of the *M.tb* response, these cells are prominently present at infection sites. Sertl *et al*. revealed that DCs were present between epithelial cells and appeared toward the lumina of the airways.[77] Immature dendritic cells found in the lung mucosa are specialized in capturing and processing antigens. After encountering *M.tb*, these dendritic cells mature and travel to the lymph nodes. There, they activate T cells by presenting antigens, providing co-stimulatory signals, and secreting immunoregulatory cytokines like IL-12.[77] In a study by Henderson *et al*. it was observed that human DCs infected with live *M.tb* increased the expression of certain co-stimulatory molecules (CD80, CD40, and CD54) and MHC class I. However, the expression of other co-stimulatory molecules like CD58 and CD86, as well as MHC class II, did not show an increase. Interestingly, this upregulation was only seen when cells were infected with live *M.tb*, while infection with heat-killed *M.tb* did not result in increased expression of CD80, CD40, CD54, or MHC class I.[78]

While these cells enhance the cellular response against *M.tb*, the bacterium's impact on their phagocytic activity may result in compromised antigen presentation to T cells. Henderson *et al*. further revealed that human DC phagocytic activity was diminished but not abolished.[78] Furthermore, the mycobacteria have evolved to inhibit DC maturation, mask the presence of the pathogen, and impair its ability to stimulate antigen-specific T cells.[79] This manipulation of DC maturation exemplifies one of *M.tb's* effective strategies, enabling it to establish a foothold in the airways despite its slow growth rate.[79]

Besides their antimicrobial activity and oxidative killing, neutrophils play a role in the indirect priming of T cells during infection. During infection, mice and human studies demonstrated that neutrophils help DCs to process and present *M.tb* antigens on MHC class I to T cells, and this has been shown to play a key role in the immune response to *M.tb*.[80] Neutrophils interact with immature DCs, and activated neutrophils prompt the maturation of DCs, enabling them to stimulate T cell proliferation and activation.[80] Blomgran *et al*. demonstrated that DCs acquiring *M.tb* from infected neutrophils were equally proficient at presenting antigens and stimulating the proliferation of naïve T cells compared to DCs directly infected with *M.tb*.[80]

Although antigen presentation and activation are comparable between directly infected DCs and DCs that acquire *M.tb* from infected neutrophils, *M.tb* infected neutrophils release chemo attractants for DCs.[80] This is an essential mechanism as it overcomes the inhibitory effect of *M.tb,* the mycobacteria decrease the expression of chemokine receptor CCR7 in infected DCs. This chemokine receptor is important in trafficking DCs from the peripheral to the lymph nodes to prime naïve T cells.[80] Blomgran et al. further showed that the medium from infected neutrophils increased DC migration compared to the medium from DCs directly infected with *M.tb* or from uninfected neutrophils.[80]

1.3.2 Adaptive Immunity

An effective adaptive immune response is essential for halting progressive, disseminated TB. When this response is effective, granulomas can control and potentially eliminate the infection, becoming hardened and calcified. In contrast, granulomas in active TB are necrotic and exhibit a caseating appearance.

1.3.2.1 The role of conventional T cells in *M.tb* infection

While murine models may not fully replicate the entire spectrum of *M.tb* infection outcomes and pathologies seen in humans, they have been crucial in elucidating the pivotal role of T cells in controlling the infection. Earlier studies using knockout mice have shown that mice lacking T cells exhibited higher *M.tb* burden and more severe pathology.[81, 82] These cells are vital for mounting a protective host immune response to *M.tb* infection, as they can stimulate the antimicrobial functions of infected phagocytes.[83]

CD4 Th1 cells

Th1 cells appear to be crucial for defending against TB, as the maintenance of the granuloma relies on the local secretion of Th1 type cytokines such as IFN-γ and TNF. These cytokines facilitate sustained activation of phagocytes and the production of reactive nitrogen intermediates.[82] With optimal conditions, the antimicrobial granulomatous response to infection results in complete control of the bacteria.

In particular, mice deficient in CD4 T cells and Th1 type cytokines succumb to early infection with high bacterial loads. Flynn *et al.* demonstrated that IFN-γ knockout mice succumb to infection early with necrotic granuloma formation filled with a high bacterial load.[81] Furthermore, these mice had reduced production of reactive nitrogen intermediates. However, several other types of cells such as NK cells produce IFN-γ during infection.[82] This raised a question of whether IFN-γ from Th1 cells is sufficient to control infection and if Th1 cells play a role in the addition of this cytokine. However, it seems IFN-γ from Th1 cells is necessary for controlling infection.[82] Green *et al*. revealed when CD4 knockout mice were reconstituted with wild-type CD4 T cells during *M.tb* infection, the mice were able to survive longer than mice that did not receive the cells.[82] These results suggest that IFN-γ from CD4 T cells is necessary for optimal long-term control and bacterial burden.

In addition to IFN-γ, Th1 cells also secrete IL-2 and TNF, which interact with dendritic cells to facilitate T cell priming and offer support to B cells.[82] This may explain another mechanism these cells mediate protection besides using IFN-γ. Green *et al.* also demonstrated that at four weeks post-infection, mice lacking CD4 T cells had fewer total cells recovered from the lungs compared to those with CD4 T cells, regardless of whether IFN-γ was produced.[82] Furthermore, fewer CD8 T cells released IFN-γ in CD4 T cell knockout mice. Thus, Th1 cells seem to display different mechanisms to control infection and sustain local immune responses.

CD4 Th17 cells

The data regarding Th17 responses in TB are extensive but not consistent, likely contingent on the model used and the level of inflammation. A study by Okamoto *et al*. illustrated that the bacterial load in the lungs of IL-17 knockout mice was nearly identical to that in wild-type mice following infection with BCG.[71] Conversely, IL-17-deficient mice have been observed to exhibit higher bacterial numbers following

infection with a virulent *M.tb* strain.[71] Therefore, it seems IL-17 might be involved in the protection against virulent strains of *M.tb.*

Additionally, Khader *et al*. showed that wild-type mice showed an upregulation of chemokine-encoding genes, such as CXC19, CXCL10, and CXCL11, 16 days after infection following vaccination.[84] The increased expression of these chemokines correlated with the accumulation of IL-17-producing antigen-specific T cells and the expression of IL-17A.[84] This effect was not observed in vaccinated mice lacking IL-23p19, because IL-23 is required for the generation of IL-17-producing CD4 T cells. Furthermore, administering IL-17 neutralizing antibodies to vaccinated wild-type mice on day 12 after the challenge significantly suppressed the induction of genes encoding the three chemokines.

Moreover, administering IL-17 neutralizing antibodies on days 12 and 14 after the challenge also markedly decreased the frequency of antigen-specific IFN-γ-producing T cells in the lungs of vaccinated wild-type mice.[84] Interestingly, providing exogenous IL-17 to vaccinated IL-23p19-deficient mice on day 12 after challenge, a period when vaccinated wild-type mice demonstrated IL-17 recall responses, reinstated the accumulation of IFN-γ-producing CD4 T cells in the lungs. This effect was exclusive to vaccinated mice and was not observed in unvaccinated IL-23p19-deficient mice.[84] These results suggest that vaccination results in the generation of T cells producing IFN-γ and IL-17. These IL-17 producing T cells populate the lung and respond rapidly to infection, facilitating increased expression of chemokines and recruitment of T cells producing IFN-γ.

IL-17 has also been demonstrated to stimulate the production of chemokines and cytokines crucial for the induction, activation, or survival of neutrophils.[38] In IL-17 deficient mice infected with Bacille Calmette-Guerin (BCG), it has been shown the expression of neutrophil chemokines KC and MIP-2 is significantly impaired. Furthermore, the expression of cytokines such as IL-6 and TNF is also diminished.[85] These findings indicate that IL-17 plays a role in triggering acute neutrophil-mediated inflammation in the lungs of BCG-infected mice. [85]

CD8 T cells

Similar to CD4 T cells, CD8 T cells can produce IL-12, IFN-γ, and TNF, which are cytokines crucial for controlling *M.tb* infection.[86] Importantly, CD8 T cells possess

cytotoxic capabilities to eliminate *M.tb* infected cells through granule-mediated mechanisms (involving perforin, granzymes, and granulysin) or by inducing apoptosis via Fas-Fas ligand interactions.[86] Human CD8 T cells can also produce granulysin, which has the ability to kill *M.tb.* Stenger *et al*. demonstrated that the combination of perforin and granulysin resulted in macrophage lysis and reduced viability of intracellular mycobacteria.[86] Thus, granulysin could kill *M.tb* if perforin or other pore-forming molecules of T cell granules allowed access to intracellular compartments.

1.3.2.2 The role of Donor-unrestricted T cells (DURT cells) in *M.tb* infection

In addition to CD4 and CD8 T cells, DURT cells such as MAIT cells, iNKT, and γδ T cells have been shown to participate in the immune response against *M.tb*.[46] These cells exhibit interesting effector functions such as rapid cytokine production, have a limited polymorphic TCR repertoire, and recognise non-peptide antigens, increasing the recognition diversity of pathogens.[46]

MAIT cells and iNKT cells

In mouse models, both MAIT cells and iNKT cells have been shown to reduce bacterial burden following *M.tb* infection. In a study by Dey et al., the role of MAIT cells in controlling *M.tb* infection was investigated by comparing CAST/EiJ ($MAIT^{hi}$) mice, which naturally have a higher frequency of MAIT cells, with C57BL/6J ($MAIT^{lo}$) mice, which have lower MAIT cell frequencies.[82] The $MAIT^{hi}$ mice exhibited significantly better control of *M.tb* proliferation, with 2.7-fold fewer CFUs in the lungs and 10.3-fold fewer CFUs in the spleen compared to the $MAIT^{lo}$ mice, five weeks post aerosol challenge. Pathological analysis showed fewer and smaller lung tubercles and smaller, less inflamed spleens in the $MAIT^{hi}$ mice. These findings suggest that increased MAIT cell abundance can enhance the host's ability to control *M.tb* infection.[82]

Additionally, results from non-human primates (NHP) indicate that specifically CD8 iNKT cells may play a protective role in preventing *M.tb* pathology. Chancellor *et al*. investigated iNKT profiles in rhesus macaques that were unvaccinated and classified as either controllers or progressors after an *M.tb* challenge.[83] A comparison of peripheral blood iNKT numbers before infection and CD1 tetramer-mediated iNKT fold expansion revealed no differences between the controller and progressor groups. However, subset analysis of antigen-responsive iNKTs showed a trend towards a reduced CD4/CD8 ratio in controllers compared to progressors.[83] While in humans,

the function of MAIT cells after *M.tb* infection appears to vary according to their location in the body, suggesting differences based on anatomical locations. A study by Jiang *et al*. revealed that MAIT cells isolated from tuberculous pleural effusions produced higher levels of IFN-γ, IL-17, and granzyme B compared to MAIT cells from peripheral blood when stimulated with *M.tb* antigens.[87] This indicates that MAIT cells likely play a significant role in *M.tb* infection.

In addition, the frequency of MAIT cells and iNKT cells seem to differ in individuals after *M.tb* infection. Paquin-Proulx *et al*. found that the frequencies of both MAIT cells and iNKT cells were higher in individuals with latent *M.tb* infection compared to those with active TB disease.[88] The difference between individuals with latent *M.tb* infection and those with active TB is not only observed in the frequencies of these cells but also in the expression of certain activation and exhaustion markers.

The study further revealed higher expression levels of HLA-DR and programmed cell death protein (PD)-1 on MAIT cells and iNKT cells in individuals with active TB compared to those with latent *M.tb* infection.[88] Thus, it appears that active TB is characterized by heightened activation and exhaustion of MAIT and iNKT cells compared to individuals with latent *M.tb* infection. Understanding the detailed characteristics of these cells during latent *M.tb* infection and their involvement in the progression to active TB is essential for gaining insights into their role in immunological control against *M.tb.*

γδ T cells

Despite Th17 cells being well-established IL-17-producing cells and having demonstrated protective effects against *M.tb* infection in vaccinated mice, γδ T cells have been shown to be the major IL-17-producing cells at early stages of BCG infection and 4-52 weeks after high or low dose *M.tb* infection.[71]

This cytokine seems not only to play a role in neutrophil recruitment but also inducing granuloma formation in *M.tb* infection. IL-17 plays a role in the immune response against mycobacterial infection, particularly in the formation of granulomas induced by the infection. Thus, γδ T cells are anticipated to be significant producers of IL-17 within the mature granuloma during BCG infection. A study by Okamoto *et al*. analysed IL-17-producing cells in BCG-infected mice at day 28 of the infection.[71] Following stimulation with *M.tb*-derived PPD and PMA plus ionomycin, the number of γδ T cells

producing IL-17 was higher than αβ T cells or CD4 T cells.[71] The study further investigated the role of TCR γδ T cells in the formation of IL-17-dependent granulomas in the BCG-infected lungs of γδ T cell knockout mice. At day 28 of the infection, IL-17-producing cells were undetectable, and the formation of a granuloma was abrogated.[71] Interestingly, when γδ knockout mice were reconstituted with γδ T cells from wild-type mice, the granuloma formation was restored at day 28 of the infection.[71]

1.3.2.3 The role of B cells in *M.tb* infection

Studies on the defence mechanisms against *M.tb* has predominantly focused on T cells. The role of B cells and antibodies in preventing or controlling *M.tb* infection in humans or nonhuman primates remains unclear. A growing body of evidence highlights the crucial role of humoral immunity and B cells in shaping the immune response to *M.tb*. B cells have been shown to contribute to antigen presentation to T cells and influence the overall immune response. This indicates that B cells might control the local proliferation of T cells in the lungs, thereby affecting the extent of granulomatous inflammation in lung tissue.[89] A study by Phuah *et al*. found that administering the anti-human CD20 chimeric monoclonal antibody (mAb) rituximab to macaques two weeks before *M.tb* infection, which reduced B cell numbers, did not impact the number of CD3 T cells or the proportions of CD4 and CD8 T cells in granulomas.[90] Even so, B cells are recognized for their functional interactions with and influence on T cells. Therefore, even though the number of T cells remained unchanged, the function of the T cells in the rituximab-treated macaques might be altered. The study further revealed that when granuloma samples were stimulated with immunodominant *M.tb* antigens ESAT-6 and CPF-10 peptides, the frequency of T cells secreting IFN-γ or TNF in granulomas was similar between rituximab-treated animals and the control group.[90] However, granulomas from rituximab-treated macaques exhibited a higher frequency of T cells secreting IL-17, IL-2, or IL-10 compared to those from the saline control macaques. The altered cytokine expression of T cells observed in rituximab-treated macaques could potentially be due to the absence of specific B cell cytokines resulting from B cell depletion.

1.3.2.4 The formation and function of the Granuloma

Lastly, macrophage-T cell interactions led to the formation of a granuloma.[71] The formation of an *M.tb* granuloma is a hallmark of TB disease and the key role of the granuloma is to create an immune microenvironment to control the growth of

intracellular *M.tb* and limit the bacillary dissemination.[19] During granuloma maturation, the recruitment of phagocytes (neutrophils, macrophages, and dendritic cells) and lymphocytes is orchestrated by various cytokines and chemokines initially produced by the infected macrophages.[71] While crucial for controlling the growth of intracellular bacteria, this structure may also offer the bacteria a niche where they can survive by altering the immune response to ensure their long-term survival without causing damage.[19]

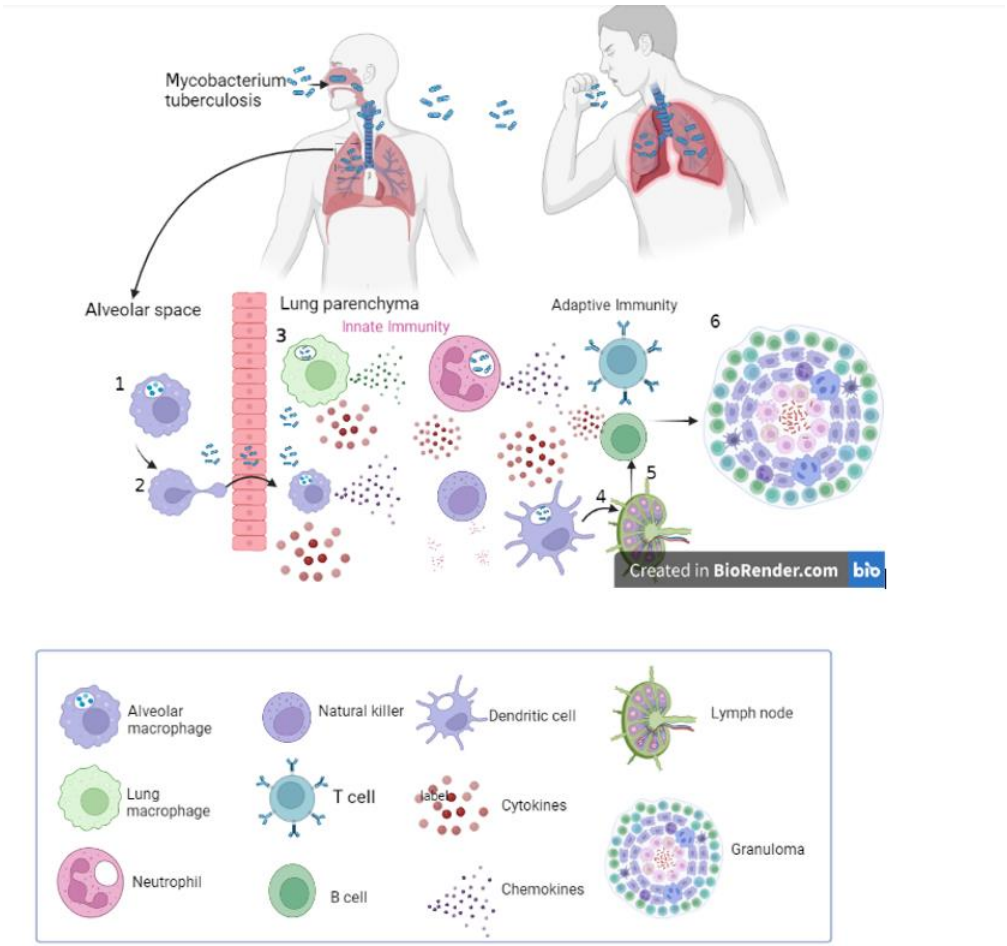

Figure 1: A summary of the immune response against *M.tb* infection. Upon inhalation of aerosols containing the bacilli. **1)** Alveolar macrophages recognise the mycobacteria via PRR and engulf the pathogen. **2)** Alveolar macrophages migrate into the lung parenchyma and start to secrete chemokine and cytokines that recruit and activate other immune cells. **3)** The recruited phagocytes (neutrophils, macrophages, and DC) engulf the bacteria and secrete different cytokines and chemokines that recruit and activate other immune cells. This leads to an amplifying of the immune response. **4)** Once DCs engulf and process the bacterial materials, these cells traffic to and enter draining lymph nodes to prime adaptive immune cells. **5)** The adaptive immune cells migrate out of the lymph nodes to the site of infection, where they start to release cytokines that enhance the function of phagocytes. **6)** The recruitment of immune cells and production of various cytokines results in the formation of a granuloma which contains the bacteria. Image created in BioRender.com

1.4 New approaches toward the development of prevention tools for TB disease

The Bacille Calmette-Guérin (BCG) vaccine has been available for a century and remains one of the most extensively used vaccines worldwide. This vaccine is on the WHO list of essential medicines, and since 2004, around 100 million children have been vaccinated with BCG each year globally. In infants, the BCG vaccine provides protection against all disseminated forms of tuberculosis and reduces overall mortality rates.[91] In contrast, vaccination with BCG in adolescents and adults is inadequate for controlling the tuberculosis epidemic, particularly in terms of protecting against pulmonary TB, the most prevalent form of the disease.[92] TB remains a significant threat to public health, underscoring the urgency to enhance the effectiveness of the BCG vaccine in preventing respiratory TB, the form of the disease that is most easily transmitted. In addition to improving BCG efficacy, the other aim is to develop new, safe, and efficacious TB vaccines that protect against pulmonary TB in adults, and this has been identified as a priority by the WHO. A great challenge in the development of vaccine development against TB is understanding the mechanisms by which *M.tb* evades and escapes the immune response of the host, and host immune responses associated with protection. A primary vaccination strategy focuses on generating T cell responses to *M.tb* antigens, given that various studies suggest T cell-mediated immunity plays a crucial role in controlling infection.

1.4.1 Viral vectored vaccines

Viral vectors offer several advantages over traditional subunit vaccines, including their ability to elicit robust antibody responses and crucially, to stimulate cellular responses necessary for eliminating pathogen-infected cells.[93] Furthermore, viral vectors have the capability to induce durable immune responses, sometimes achieving this effect after just a single dose under certain conditions.[93] The development of MVA85A, a recombinant viral vector vaccine expressing the mycobacterial protein Ag85A, was predicated on the concept that enhancing T cell immunity against a single dominant protein antigen could effectively augment pre-existing immunity induced by BCG vaccination.[46] When administered as a booster vaccine following initial BCG vaccination in South African infants, MVA85A increased the specific CD4 T cell responses targeting Ag85A, characterized by the expression of Th1 cytokines and IL-

17.[94] Despite its ability to induce polyfunctional CD4 T cells, MVA85A failed to prevent *M.tb* infection and disease when compared to BCG vaccination alone.[94]

1.4.2 Live attenuated vaccines

A great deal of effort has been put into developing candidate live vaccines based on attenuating BCG or *M.tb.* An advantage of an attenuated *M.tb* vaccine is that it contains over 120 *M.tb* genes that are not found in the current BCG vaccine, which may include important antigens.[95, 96] Live attenuated vaccines mimic a natural infection often induce robust and durable immune responses, requiring lower vaccine doses for effective protection.[46] This is because live attenuated vaccines can persist longer than inactivated vaccines. Furthermore, this type of vaccine provides non-peptide antigens which could lead to the activation of DURT cells as well increasing the immune response. However, the obstacles faced with live TB vaccines are safety concerns, especially for individuals with weakened immune systems and pregnant women.[97]

One example of a live *M.tb* vaccine is MTBVAC, a live attenuated derivative of a clinical isolate, the *M.tb* Mt103 strain.[98] The virulence genes, PhoP and fadD26, have been eliminated from this vaccine. Crucially, MTBVAC preserves the complete T cell epitope repertoire, encompassing immunodominant antigens such as ESAT-6, CPF-10, and PPE60, which are notably absent in BCG.[98] This preservation of T cell epitopes might enhance the vaccine's potential efficacy by ensuring the inclusion of key immune targets not covered by the existing BCG vaccine.

In a mouse study, MTBVAC appeared to provide protection one month post-challenge with virulent *M.tb* H37Rv via the natural respiratory route of infection.[99] A notably higher reduction in bacterial burden was observed in the MTBVAC group compared to BCG, evident in both the lungs and spleen.[99] Although MTBVAC seemed to be safe and effective in animal models, it is crucial to determine whether comparable findings would hold in humans.

Interestingly, MTBVAC also demonstrated immunogenicity in infants.[100] Those who received the MTBVAC vaccine exhibited durable, dose-independent CD4 T helper 1 cell responses that were antigen-specific and expressed cytokines even a year post-vaccination. Notably, for the highest MTBVAC dose ($2.5x10^5$ CFU), these responses surpassed those generated by an equivalent BCG dose. These differences were consistently observed a year post-vaccination as well.[100] The efficacy of the MTBVAC

vaccine against TB disease is now being assessed in a phase 3 trial in newborn infants.

An alternative to the development of new live attenuated TB vaccines is to modify BCG to improve its immunogenicity and/or safety. VPM1002 is a recombinant BCG (rBCG) in which the urease C gene has been replaced by the gene encoding listeriolysin O (LLO) from *Listeria monocytogenes.*[101] Urease C facilitates the neutralization of phagosomes containing bacteria by producing ammonia, which inhibits phagolysosomal maturation and promotes bacterial survival.[101] Consequently, the absence of urease C allows for quick acidification of phagosomes, facilitating phagolysosome fusion and creating an optimal pH for LLO stability. LLO, a cholesterol-dependent cytolysin, forms transmembrane pores in the phagolysosomal membrane, enabling *Listeria monocytogenes* to escape into the cytosol.[101] Therefore, LLO expression in VPM1002 causes the secretion of antigens and bacterial DNA into the cytosol, which in turn triggers autophagy, inflammasome activation, and apoptosis. This vaccine's primary goal was to increase mycobacteria antigens' accessibility to the MHC class I pathway, which might lead to improved CD8 T cell stimulation.[101]

VPM1002 is immunogenic in humans. Findings from Grode *et al*. demonstrated the vaccine-induced IFN-γ responses by three escalating doses ($5x10^3$, $5x10^4$, $5x10^5$ CFU) of VPM1002 in healthy BCG naïve and BCG immune participants.[102] Additionally, VPM1002 immunization induced antigen-specific CD4 and CD8 T-cell responses. In comparison to BCG, proportions of double- and triple-positive CD4 and CD8 T cells increased following vaccination ($5x10^5$ CFU).

1.4.3 Subunit vaccines

Rather than injecting an attenuated whole organism to trigger an immune response, subunit vaccines such as protein-adjuvant vaccines cannot replicate. Therefore, they may be safer in immunocompromised individuals, as they only contain purified proteins, which have been specially selected for their ability to stimulate immune cells. Antigens of *M.tb* that activate T cells in previously infected individuals are considered promising for vaccine candidates. These types of vaccines have also advanced towards clinical development stages.

For example, the M72 candidate vaccine contains a recombinant fusion protein that is derived from two *M.tb* antigens (*M.tb*32A and *M.tb*39A), combined with the $AS01_E$

adjuvant.[103] In adults infected with *M.tb* who were HIV negative, vaccination with M72:AS01$_E$ provided approximately 50% protection against progression to pulmonary TB disease over a follow-up period of three years.[103]

1.5 Preliminary findings

Understanding the immune response against *M.tb* is crucial for elucidating insights that can inform rational vaccine design or development of novel host-directed immunotherapies, which could offer therapeutic strategies for individuals with drug-resistant TB or with HIV, and TB co-infection.[104] T cells are known to play a vital role in the control of infection, but it is not known to what degree the nature of the *M.tb*-specific T cell repertoire or if specific T cell clones contribute to the outcome of *M.tb* infection. In work performed by supervisors, Drs Munyaradzi Musvosvi and Thomas Scriba, a previously unknown T cell clone was identified that possessed a novel TCR CDR3α sequence that was present in more than 90% of human individuals (*Table 2*). Healthy, *M.tb* infected persons who remained asymptomatic (i.e., did not progress to active disease) during two years of longitudinal follow-up had higher peripheral blood frequencies of this T cell clone than persons who progressed to active disease (progressors) *(Figure 2*). T cells that express this TCR are termed kiif.tb T cells, based on the last four amino acids in the TCRα CDR3 sequence. Furthermore, a separate cohort of healthy *M.tb* infected persons had higher frequencies of kiif.tb T cells compared to persons with active TB disease *(Figure 2*). Taken together, these data provide compelling evidence to support the hypothesis that these kiif.tb T cells are donor-unrestricted T cells and that kiif.tb T cells may play a role in controlling the infection. Should these cells be susceptible to induction or modification by vaccination, they may be a priority target for novel TB vaccines.

Table 2: A public CDR3α sequence was found at higher frequencies in *M.tb infected* individuals who do not progress to active TB disease.

Region	Sequence
CDR3a	CAVNRDDKIIF
V_α	TRAV12-2
J_α	TRAJ30

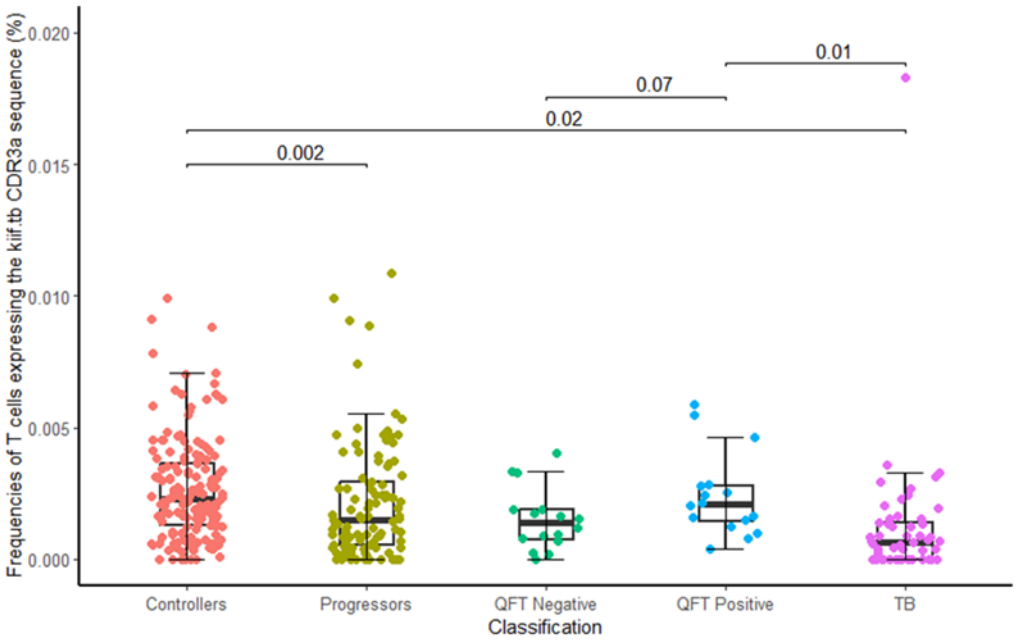

Figure 2: Frequencies of kiif.tb T cells in controllers, progressors, and active TB individuals. Box plot graph showing the frequencies of kiif.tb T cells in controllers, progressors, and active TB individuals. The error bars represent the first quartile (below), the third quartile (upper) and the bars represent the median. Wilcox test was used to compare groups (significant p value<0.05). Results generated by Dr Munyaradzi Musvosvi.

Chapter Two

Application of molecular techniques to measure the frequencies of kiif.tb T cells in our study cohort.

2.1 Background

Characterisation of TCR repertoires is important for gaining insights into the mechanisms of T cell immunity during *M.tb* infection. Yet, the complexity and diversity of clinical manifestations in TB, along with significant inter-individual variation in MHC molecules that dictate antigen presentation to T cells, have posed challenges in characterizing TCR sequences. [105] Additionally, the wide array of TCR diversity even within individual hosts makes it difficult to identify distinct signatures of T cell subsets in TB patients.[105]

The frequencies of mycobacteria-reactive T clonotypes may provide more detailed knowledge and differ amongst *M.tb infected* people. A highly abundant TCR sequence is assumed to be part of an active immune response, where clones that express that TCR have expanded in response to antigen recognition. Conserved TCR sequences found within and between individuals may recognize common antigens. These TCRs can be identified using analytical methods that allow clustering of TCRs based on motifs (CDR3) recognizing similar antigens.[106] Additionally, particular *M.tb* specific T cell clonotypes may be associated with either protection or with risk of disease progression. Musvosvi *et al*. revealed that frequencies of certain similar TCR groups were higher in individuals who controlled the infection, while some TCR groups were higher in those who progressed to TB disease.[105] Therefore, quantification of specific T cell clonotypes frequencies in *M.tb* infected individuals may provide differences between *M.tb* progressors and controllers.

2.2 Techniques used to measure cell frequencies.

The application of polymerase chain reaction (PCR), coupled with the extraction of nucleic acids (DNA and RNA) from peripheral blood mononuclear cells (PBMCs), has been pivotal in elucidating gene expression in immune cells during TB disease. These methods enable the analysis of the changes in gene expression in T cells or other cell frequencies and have revolutionized our understanding of immune response against *M.tb* infection and the diversity of the immune responses observed within *M.tb* infected

individuals. This technique is a highly sensitive enzymatic assay that amplifies specific DNA fragments from a complex pool of DNA, enabling the detection of specific known sequences.

2.2.1 Quantitative real-time PCR (qRT-PCR)

Quantitative real-time PCR (qRT-PCR) provides information that goes beyond simply detecting the presence of a DNA sequence.[107] It indicates the abundance or concentration of a specific DNA or gene sequence in the sample. While the PCR product is being synthesized, qRT-PCR enables both the detection and relative quantification of gene expression.[107] Additionally, the sensitivity of this assay allows quantification of low numbers of target genes. As a result, it might be a useful tool to analyse alterations in the gene-level expression of clonotypes in *M.tb* infected individuals. Quantifying the desired gene during exponential amplification avoids issues associated with end-point PCR, which analyses samples after the final PCR cycle has completed.[107]

Although qRT-PCR is a highly useful technique, it does have limitations. This assay requires standard curves or reference curves.[107] Generating these standard curves is time-consuming, and improper storage or handling may affect the stability of the reference curve over time, potentially altering the measured amount of nucleic acids present.

2.2.2 Digital PCR (dPCR)

Digital PCR is the next generation of PCR technology providing absolute copy number quantification of a targeted sequence.[108, 109] This is accomplished by counting positive amplification signals resulting from the amplification of a single DNA template within samples. Additionally, the sample volume used in the amplification reaction is separated into numerous small volumes using either microdroplets or microwell plates, yielding thousands of partitions.[108] Each partition represents an individual reaction mixture that may contain a few target sequences or none. The fluorescence signal from the reference gene channel determines the validity of each partition in a well. Following this determination, it is labelled positive or negative depending on the presence or absence of the target sequence. The amplification of valid partitioned samples is then completed to the endpoint, and the copy number of positive (fluorescently labelled) and negative valid partitions are counted to determine the sample's target copy number.[108, 109] When the target concentration is high, it is highly

likely that the corresponding valid partition contains two or more targets. As a result, Poisson's Law is applied to accurately count the copy number of target sequences in the total valid partitions generated within that volume.[108, 109] Due to the partitioning of the sample into multiple compartments, the dPCR assay has been found to outperform qRT-PCR in overcoming detection limits. This partitioning contributes to a high signal-to-noise ratio and sensitivity, rendering the assay suitable for detecting rare cell clonotypes sequences and mutations.[108] Moreover, dPCR exhibits strong resistance to PCR inhibitors and is less influenced by variations in PCR efficiency due to sample partitioning and endpoint cycling.[108]

Although dPCR has numerous advantages over qRT-PCR, it does have similar limitations such as unspecific binding of primers to sequences that are similar to the target sequence. Furthermore, at high nucleic acid concentrations, dPCR may be saturated and perform poorly compared to qRT-PCR. [108]

2.2.3 Bulk Sequencing

In contrast to PCR, quantifying the abundances of certain mRNA transcripts by bulk RNA sequencing can provide a higher discovery power and sensitivity.[110] This method is the gold standard for capturing the entire TCR repertoire and estimating frequencies of individual TCRs, thus allowing the detection and quantification of novel TCR sequences of T clonotypes.[110] However, this technique is expensive and is time-consuming.[110]

We wanted to gain a better understanding of differences in frequencies of recently identified T cells expressing the kiif.tb CDR3α between healthy uninfected individuals, healthy infected individuals, and patients with active TB in a separate cohort than the one observed before. Differences in frequencies of particular immune cells have been studied in the context of *M.tb* infection, however, the kiif.tb CDR3α T cell clonotype has not been studied.

This chapter aimed to optimize a custom dPCR assay for the quantification of T cells and kiif.tb T cells in PBMCs by combining a custom multiplex dPCR assay specific for the kiif.tb CDR3α sequence with a published dPCR assay that quantified total T cells in PBMCs. The published dPCR assay took advantage of the dissimilarities between T cells and cells of other origins by measuring the loss of a germline TCR beta locus (TRB). The rearrangement occurs on both alleles at the most immature stage of

human T-cell development, and thus all peripheral T cells have lost the gene. Therefore, instead of counting a whole repertoire of rearranged TCRs, an indirect counting approach was used. The optimised assay was used to accurately measure the frequencies of T cells expressing the kiif.tb CDR3α sequence and compare these between healthy individuals, healthy *M.tb* infected, and individuals with active TB.

2.3 Aims:

2.3.1 To optimize a custom digital polymerase chain reaction assay to measure the frequencies of kiif.tb T cells in peripheral blood.

Hypothesis:

Frequencies of kiif.tb T cells in peripheral blood measured by digital PCR assay will correlate with frequencies measured by bulk TCRα sequencing.

2.3.2 To compare frequencies of kiif.tb T cells in peripheral blood of persons without *M.tb* infection, healthy *M.tb* infected persons, and persons diagnosed with active TB using digital PCR assay.

Hypothesis:

M.tb infected persons will have higher frequencies of kiif.tb T cells compared to M.tb uninfected individuals and individuals with active TB.

2.4 Methods

2.4.1 Study Participant Groups

We assessed PBMC samples collected from adolescents enrolled in the Adolescent Cohort Study (ACS), (UCT HREC 045/2005) conducted in high schools in Worcester and surrounding areas. Adolescents either did not have or had *M.tb* infection, defined by a positive QuantiFERON TB Gold In-tube assay and/or a positive tuberculin skin test. *M.tb* infected participants were divided into two groups based on the QuantiFERON Gold test conducted at baseline and six months after enrolment into the ACS study. Participants who had a negative QuantiFERON Gold result at baseline and then converted to a positive result six months after enrolment were termed recent converters. Participants who had a positive QuantiFERON Gold result at baseline and maintained a positive result throughout the study enrolment were termed persistent QFT-positive participants. Additional PBMC samples from HIV-uninfected TB household contacts living in Cape Town enrolled in the Grand Challenges 6–74 (GC6-74) study (Stellenbosch University Institutional Review Board N05/11/187), and from adults with active TB disease, defined by a positive GeneXpert MTB-RIF test on sputum sampling, enrolled in the MRC-SHIP pilot study (UCT HREC 088/2008) were also analysed.

A sample size of 25 per group was chosen due to limited access to only 25 samples per study group.

2.4.2 DNA extraction

The QIAamp Mini kit (Cat: 51306) was used to extract DNA from PBMCs. The bottom of a 2mL microtube was filled with an aliquot of 20µl of QIAGEN protease. Then 200µl of thawed PBMCs or a Jurkat T cell line that was engineered to express the kiif.tb CDR3α sequence, named “kiif.tb T cells”, was added to the microtube, and 200µl of buffer AL was also added to the microtube. The microtube was then incubated for 10 minutes at 56 degrees Celsius (°C) after which the tube was centrifuged at full speed for 10 seconds at room temperature (RT) to remove any drops from the tube lid. Next, 200µl of ethanol was added to the sample, the sample tube was centrifuged at full speed for 10 seconds at RT to remove any drops from the tube lid. The samples were then pipetted from the 2ml microtube and applied to the QIAamp Mini spin column, and this column was centrifuged at full speed for 1 minute at RT. The QIAamp mini spin column was placed into a clean 2ml collection tube, and the tube containing the

filtrate was discarded. Following this, 500µl of buffer AW1 was added to the open QIAamp mini spin column, and the tube was centrifuged at full speed for 1 minute at RT. Subsequently, the column was transferred to a clean 2ml collection tube, and the tube containing the filtrate was discarded. Next, 500µl of buffer AW2 was added to the open QIAamp mini spin column, and the tube was centrifuged at full speed for three minutes at RT. The column was then placed into a 1.5ml microcentrifuge tube, and the tube containing the filtrate was discarded. After opening the column, 200µl of DNA storage buffer was added and incubated at RT for 5 minutes, followed by centrifugation at full speed for 1 minute at RT. Finally, the sample was transferred to a labelled 2ml screw cap micro tube, and 5µl of the sample was added to a 200µl PCR tube for DNA quantification using the Nanodrop.

2.4.3 Digital PCR assay

To quantify total T cells and kiif.tb T cells accurately, we adapted a published dPCR assay[109] and designed triplex dPCR assays with primers and FAM-, HEX- and Cy5-hydrolysis labelled probes (*Table 3*). The kiif.tb T cell primers and probes were selected using the IDT PrimerQuest™ Tool. The design algorithm included multiple checks to minimize primer dimer formation. Probes directed at the TRB were labelled with Cy5, whereas probes directed at kiif.tb T cells were labelled with FAM. For normalization and calculation of T cells and kiif.tb T cells, it was essential that the reference gene be located in a genomically stable locus. Furthermore, this gene must not be affected by disorders such as malignancy in T cells, as copy number alterations of the reference loci would have misleading effects on the calculations. Based on data from the published dPCR assay, Dynamin-3 (DNM3) was shown to meet these requirements and was used as the reference gene due to its stable copy number, which remains unaffected even in malignantly transformed T cells or tumorous environments. Probes directed to DNM3 were labelled with HEX.

Each reaction consisted of a 40 µL mixture that included 4xProbe PCR Master Mix (Qiagen, Cat: 250102), DNA, nuclease-free water, primers/probes for DNM3, TRB, and kiif.tb, and the restriction enzyme HindIII (10 U/µL, Thermo Scientific™ ER0502), which is necessary for the digestion of genomic DNA > 20 kb (*Table 4*). The 40 µL reactions were then added to a 96-well plate and incubated at 37°C for 10 minutes to allow for DNA digestion (*Table 4*). Following DNA digestion, the 40µl reactions from each of the 24 wells in the 96-well plate were transferred to a 24-well nanoplate,

sealed, and placed in the QIAcuity machine (QIAcuity One, 5plex). Cycling conditions were established, starting with an initial PCR heat activation lasting 2 minutes at 95°C (*Table 4*). This was followed by a two-step cycling process (40 cycles), involving denaturation for 15 seconds at 95°C and combined annealing/extension for 30 seconds at 60°C.

Following the cycling steps, the fluorescence signal in the reference (DNM3) channel was measured by the machine to determine the number of valid partitions in a well. Differences in signal intensities between partitions were then normalized, and the fluorescence signals in the target channels were corrected accordingly. Images of each well were then captured, enabling the visualization of gene expression in individual wells.

The T cell proportion was determined by first calculating the ratio of a copy number of cells expressing TRB to the copy number of cells expressing the stable reference gene (TRB/DMN3). This ratio lies between zero and one. A ratio of zero indicates a total loss of TRB, suggesting that all cells are T cells. In contrast, a ratio of one means that all cells are expressing both the reference gene and the TRB gene, indicating no T cells are found in the sample. This ratio was then subtracted from one, as shown in *Equation 1*. The calculated T cell proportion and a copy number of cells expressing the kiif.tb CDR3α sequence was used to determine the proportion of kiif.tb T cells, as shown in *Equation 2*.

Equation 1: Determining the proportion of total T cells present in a sample.

$$\text{T cell proportion} = 1 - \frac{\textbf{TCB copies}/\mu\textbf{l}}{\textbf{DNM3 copies}/\mu\textbf{l}}$$

Equation 2: Determining the proportion of total kiif.tb T cells present in a sample.

$$\text{kiif.tb T cells proportion} = \frac{\textbf{kiif.tb copies}/\mu\textbf{l}}{\textbf{T cell proportion}}$$

Table 3:The sequences for the primers and probes for each target.

Target gene	Probe sequence	Forward primer	Reverse primer
Kiif.tb	5-TGTGCCGTGAACAGAGATGACAAGA-3	5-CAGTGATTCAGCCACCTACC-3	5-GGGAGAATATGAAGTCGTGTCC-3
TRB	5-TGGACCCTCACAGAGGGAGCA-3	5-GCCATGCACTTTCCCTTTCG-3	5-GGGAGAATATGAAGTCGTGTCC-3
DNM3	5-TGAGCCACCCCTTGCGAATCACCT-3	5-CTAAACACCTCTGCTGATTTCTGC-3	5-CCGCCTTTCATGATGCCAATG-3

Table 4: The reagents and cycling conditions for the dPCR assay.

Reagents used		
Component	**Amount used for a single reaction**	**Master mix amount (26 reactions)**
Master Mix	10µl	260µl
TRB primer[0.8µM] DMN3 primer[0.8µM] Kiif.tb primer[0.8µM]	3.2µl each	83.2µl each
TRB probe [0.4µM] DMN3 probe[0.4µM] Kiif.tb probe[0.4µM]	1.6µl each	41.6 µl each
Restriction Enzyme (HindIII)	1µl	26 µl
DNA	Total 100ng (Variable volume)	Variable
RNAse-free water	Add up to 40µl	Variable
Cycling conditions		
Step	Time	Temperature (°C)
PCR initial heat Activation	2min	95
2 step cycling (40X cycles)		
Denaturation	15s	95
Combined annealing/extension	30s	60

2.4.4 Statistical analysis

R version 4.3.0 (2023.04.21 ucrt) for Windows was used for data analysis and visualization, and p values ≤ 0.05 were considered statistically significant. Correlation between the proportion of T cells or kiif.tb T cells, measured by dPCR, and the proportion, measured by bulk sequencing or flow cytometry were compared using Spearman's rank correlation coefficient test. To test if there were any significant differences in the frequencies of T cells expressing the kiif.tb CDR3α sequence between the cohorts, the Mann-Whitney U test was used. A sample size of 25 in each group provided 70% power to detect higher frequencies of kiif.tb T cells in participants with a positive QuantiFERON TB result and persons with active TB disease. This power calculation was derived from the effect size (cohen's d = 0.62) observed when the frequencies of kiif.tb T cells were compared between QFT-positive and TB samples using the bulk TCR sequencing dataset.

2.5 Results

This study included a diverse sample of adolescent and adult participants (*Table 5*). The sample was further divided into three groups: those diagnosed with active TB, healthy individuals who had *M.tb* infection (QFT-positive), and a control group of healthy, uninfected individuals (QFT-negative).

The uninfected group consisted of 19 adolescents aged 13 to 18 years (median age,15). Eleven were females and eight were males.

In the *M.tb* infected group, 39 adolescents aged 13 to 16 years (median age, 15) were included. Out of the 39 participants, 18 were recent converters while 21 were persistent QFT-positive participants. Overall, this group had more males (24) compared to females (15).

Lastly, the active TB group consisted of adults and adolescents aged 18 to 62 years (median age, 32) who were enrolled in the SHIP pilot study. Only three participants were females and 16 were males.

Table 5: Demographic and clinical characteristics of participants included in the study.

	Uninfected group	***M.tb* infected group**	**Active TB group**
Age,y, median (min-max)	15 (13-18)	15 (13-16)	32 (18-62)
Female	11	15	3
Male	8	24	16
Diagnostics			
QuantiFERON Gold, IFN-g IU/mL, median (min – max)	0 (0-0.09)	5.32 (0.38-35.74)	-
Sputum GeneXpert MTB		-	Positive

2.5.1 The dPCR assay detects different concentrations of kiif.tb-CDR3α expressing Jurkat T cells

The initial objective aimed to evaluate the sensitivity of the custom kiif.tb dPCR assay to detect kiif.tb CDR3α sequences and total T cells. Additionally, it sought to assess the assay's capability to detect differences in the copy numbers of T cells expressing this specific sequence.

To determine the ability of our dPCR assay to quantify frequencies of kiif.tb T cells, kiif.tb-expressing Jurkat T cells were spiked into PBMCs of a healthy donor at varying ratios (*Table 6)*. This deliberate variation in spiked amounts served a dual purpose: firstly, to assess the sensitivity of dPCR in detecting different spiked-in Jurkat T cell proportions, and, secondly, to determine the lowest detection limit that would yield accurate and reliable results. This approach allowed us to monitor the impact of minor fluctuations in Jurkat cell concentrations on the sensitivity of the dPCR assay. The copy numbers of cells/µl expressing DMN3, TRB, and the kiif.tb CDR3a sequences were determined using the dPCR assay (*Figure 3*). The total T cell count in the sample was then calculated by determining the ratio of the copy number of cells per microlitre expressing TRB (non-T cells) to the copy number of cells per microliter expressing DMN3 (reference gene). Subsequently, the total copy number of T cells expressing the kiif.tb CDR3a sequence was obtained by determining the ratio of the copy number of cells per microlitre expressing kiif.tb CDR3α relative to the total T cell count.

Table 6: Serial dilutions and the number of cells added in each condition

TCR-transfected Jurkat T cells added	PBMCs added	Total number of cells	The proportion of TCR-transfected Jurkat T cells (%)	Dilution factor
1 024 500	0	1 024 500	100	1
512 250	48750	561 000	91.3	1:2
256 125	48750	304 875	84.0	1:4
128 062	48750	176 812	72.4	1:8
64 031	48750	112 781	56.7	1:16
32 015	48750	80 765	39.6	1:32
16 007	48750	64 757	24.7	1:64
8 000	48750	56 750	14.0	1:128
4 001	48750	52 751	7.5	1:256
2 000	48750	50 750	3.9	1:512
1 000	48750	49750	2.0	1:1024
0	97500	97500	0	1

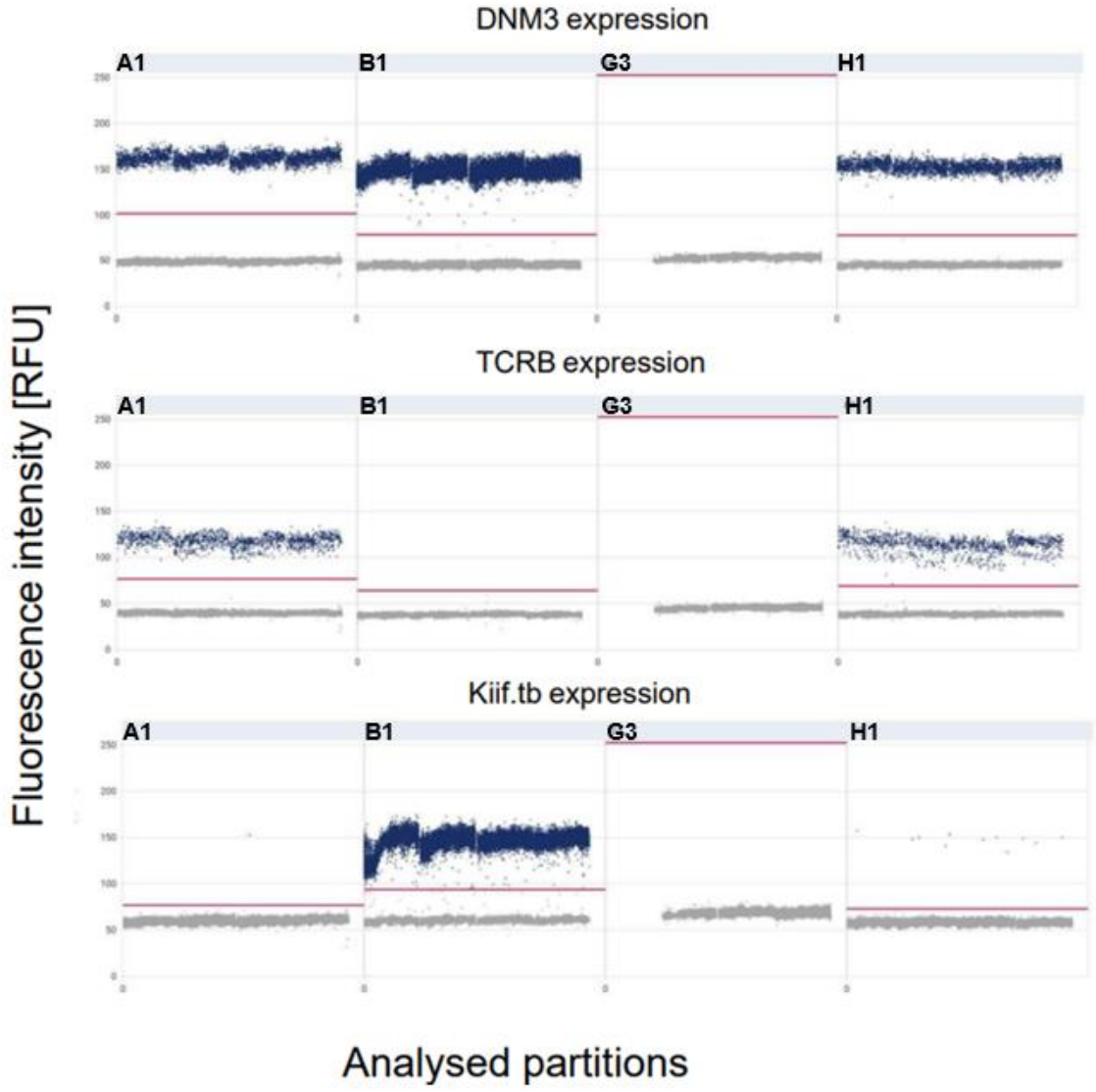

Figure 3: Fluorescence intensity of the DMN3, TRB, and kiif.tb primers for each analysed partition. A scatterplot showing the fluorescence intensity of the DMN3, TRB, and kiif.tb PCR product for each analysed partition which is represented by each dot for four different samples**: A1:** PBMCs only, **B1:** kiif.tb TCR-transfected Jurkat T cells only, **G3:** Negative Control, and H1: 1:64 diluted sample. The red line is the threshold that determines if individual partitions fall above (positive) or below (negative) the signal level that denotes whether the partition contained the gene of interest. The negative control (**G3**) only contained the master mix and no DNA sequence.

The results demonstrated that kiif.tb expressing Jurkat T cells spiked into PBMCs at various amounts could be detected with the dPCR assay (*Figure 3,Figure 4*). Notably, as the amounts of kiif.tb T cells were reduced, so the dPCR assay consistently detected lower counts of the TCR sequence. However, as we added lower amounts (less than 40% of Jurkat T cells) or no Jurkat T cels cells were added, the detection of these cells by dPCR became significantly more difficult *(Figure 4)*. This observation

implies that we had approached the lower detection limit the assay, which was 0.54 copies/µl, obtained when 39.6% of Jurkat T cells were spiked into PBMCs.

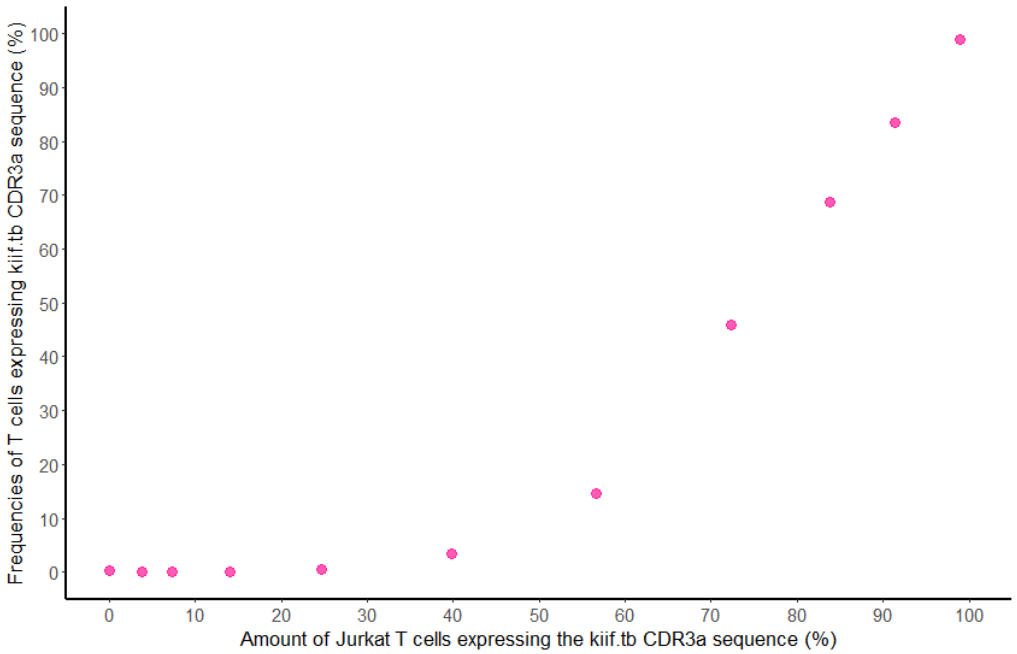

Figure 4: Correlation between the frequencies of Jurkat T cells expressing the kiif.tb CDR3α sequence measured by dPCR and the amount of Jurkat T cells spiked into PBMCs (x-axis). A scatterplot graph displaying the frequencies of T cells expressing the CDR3α sequence measured by dPCR for the different spiked amounts of Jurkat T cells. The proportion of Jurkart T cells spiked in was calculated by dividing the number of Jurkat T cells added over the total number of cells in the sample.

2.5.2 dPCR-quantified frequencies of kiif.tb T cells correlate poorly with frequencies from bulk TCR sequencing

Next, we assessed the accuracy of dPCR in quantifying T cells in PBMCs from the GC6 cohort by comparing it to bulk TCR sequencing. The bulk TCR sequencing was performed on the first vial of PBMCs, while the second vial from the same participant was used for dPCR analysis. The kiif.tb TCR frequencies obtained through dPCR were compared with those previously determined by bulk TCRα sequencing, where the frequencies of total T cells were also quantified. The frequencies of total T cells measured by dPCR and bulk TCR sequencing were highly correlated (rho = 0.73, p-value = 0.021, *Figure 5*). This suggests that our dPCR assay can reliably quantify total T cell frequencies in the samples.

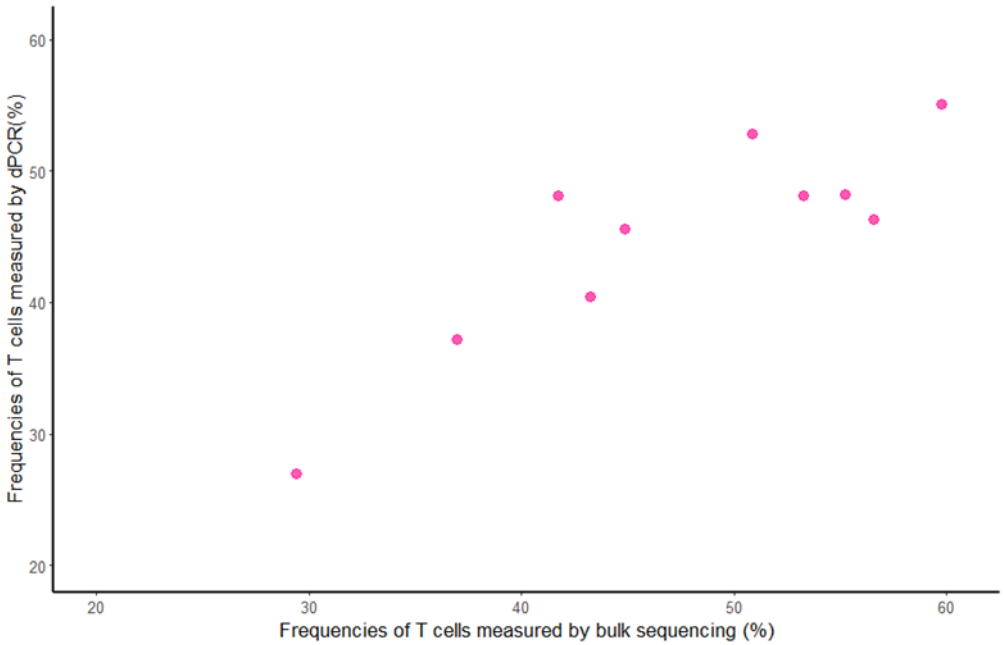

Figure 5: Correlation between the frequencies of total T cells measured by dPCR and bulk sequencing. A scatter plot graph showing the frequencies of T cells measured by dPCR compared to the frequencies of T cells obtained by bulk sequencing in the ACS cohort. The number of samples analysed is 10. The Spearman's rank correlation coefficient, rho, is 0.73, p-value = 0.021.

We were also interested in the correlation between frequencies of specific T cells expressing the kiif.tb T cell CDR3α quantified by dPCR and those quantified by bulk sequencing. Despite the good correlation observed in frequencies of total T cells observed between the two methods, there was no correlation between frequencies of specific T cells expressing the kiif.tb CDR3α sequence measured by dPCR and by bulk sequencing, (rho = 0.07, p-value = 0.8, *Figure 6)*. Moreover, in bulk TCR sequencing, frequencies of kiif.tb T cells were undetectable in two donors, whereas dPCR detected kiif.tb T cells at frequencies well above the detection level. Conversely, in two other donors, dPCR returned zero frequencies of kiif.tb T cells, whereas bulk TCR sequencing detected frequencies above zero.

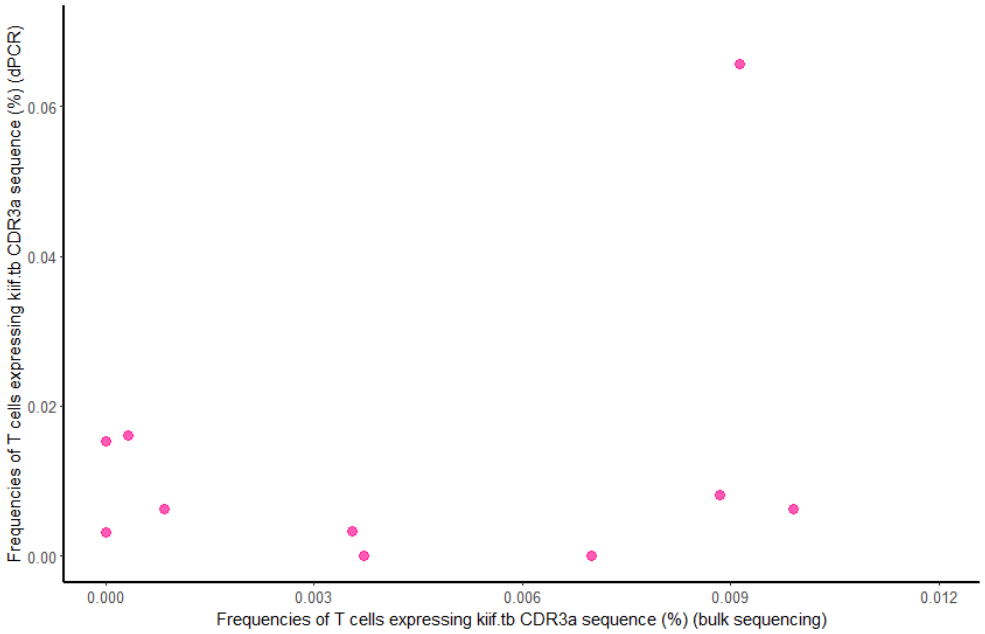

Figure 6: Correlation between frequencies of T cells expressing the kiif.tb CDR3α sequence measured by dPCR or by bulk sequencing. A scatterplot showing the frequencies of T cells expressing the kiif.tb CDR3α sequence measured by dPCR or by bulk sequencing in the ACS samples. The number of samples analysed is 10. The Spearman's rank correlation coefficient, rho, was 0.07, p-value = 0.8.

2.5.3 Hyperwelling improves the correlation between total T cells and those expressing the kiif.tb CDR3α sequence, as measured by dPCR and bulk sequencing

To improve the limits of detection in our dPCR assay, we implemented the hyperwelling technique, distributing our sample across four wells, and taking the sum, which increases the number of partitions where reactions can occur. Thus, whereas a single well generated 26,000 valid partitions, hyper welling increased this number by fourfold to 104,000 valid partitions, except for a few samples that had less than 100,000 valid partitions (*Figure 7*).

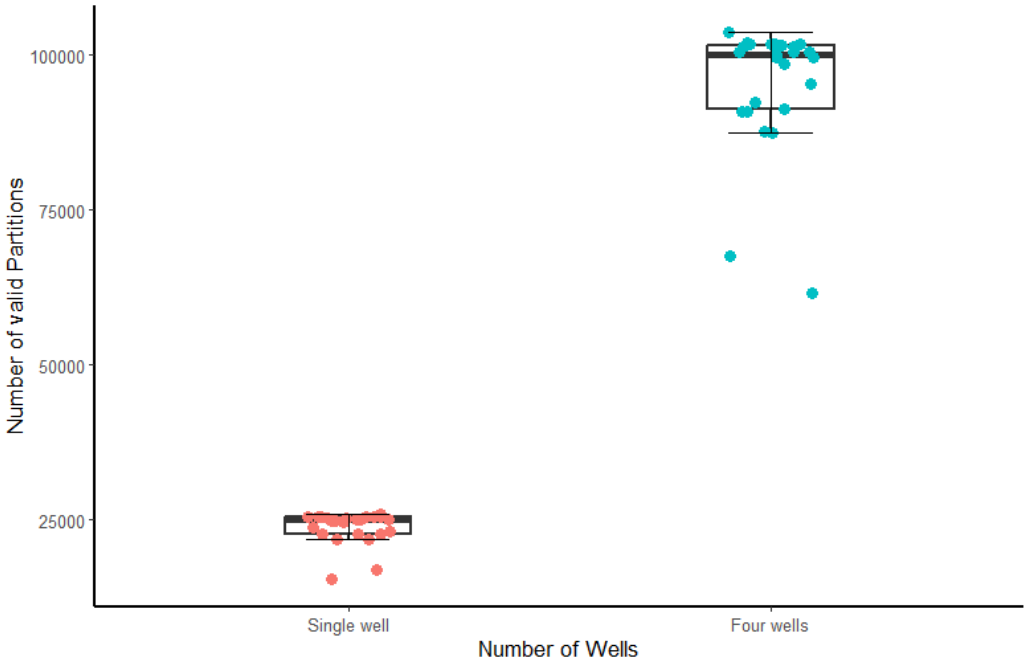

Figure 7: The effect of hyperwelling in the number of valid partitions/reactions. A boxplot showing the number of valid partitions before and after hyper welling using dPCR assay. The error bars represent the first quartile (below), the third quartile (upper) and the middle represents the median The number of samples analysed is 25.

Because the digital PCR spans more reactions, we reasoned that this would improve the sensitivity of the assay to detect kiif.tb CDR3α-expressing cells at lower concentrations. We used samples with known total T cells and kiif.tb frequencies, which were previously determined using bulk TCR sequencing. The samples were then ranked in order of highest to lowest frequencies of T cells expressing the kiif.tb CDR3α sequence based on the bulk sequence readout. Furthermore, we selected samples with a frequency of total T cells greater than 300,000, because the kiif.tb T cells are rare and we needed to sample a large number of T cells to identify them.

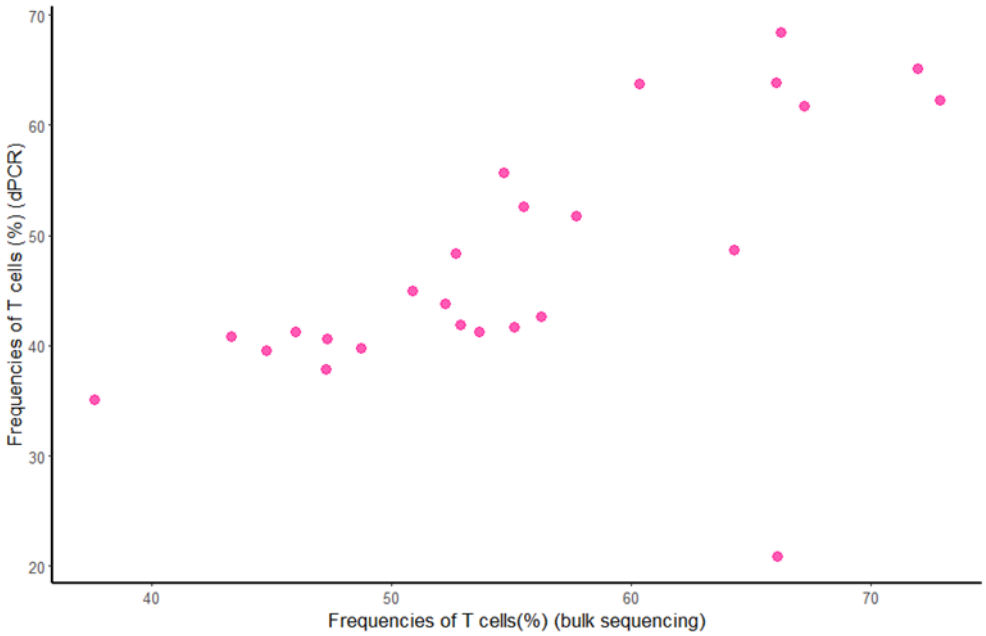

Figure 8: Correlation between T cell frequencies measured by dPCR after hyperwelling and bulk sequencing. A scatter plot graph showing the frequencies of T cells measured by dPCR compared to the frequencies of T cells obtained by bulk sequencing. The number of samples analysed is 25. The Spearman's rank correlation coefficient was 0.74, p-value, 0.02.

We detected a strong correlation between the frequencies of total T cells measured by dPCR and by bulk sequencing using this hyperwelling technique (rho = 0.74, p-value = 0.02, *Figure 8*). Notably, an improvement in the correlation between T cells expressing the CDR3α sequence, as measured by dPCR and bulk TCR sequencing, was observed following hyperwelling (rho = 0.48, p-value = 0.01, *Figure 9*) compared to before hyperwelling (rho = 0.07, p-value = 0.8, *Figure 6*). However, while improved and significant, this correlation was still moderate (rho = 0.48, p-value = 0.01). As observed previously, the frequencies of kiif.tb T cells determined by dPCR, exhibited a higher range compared to the frequencies measured by bulk sequencing.

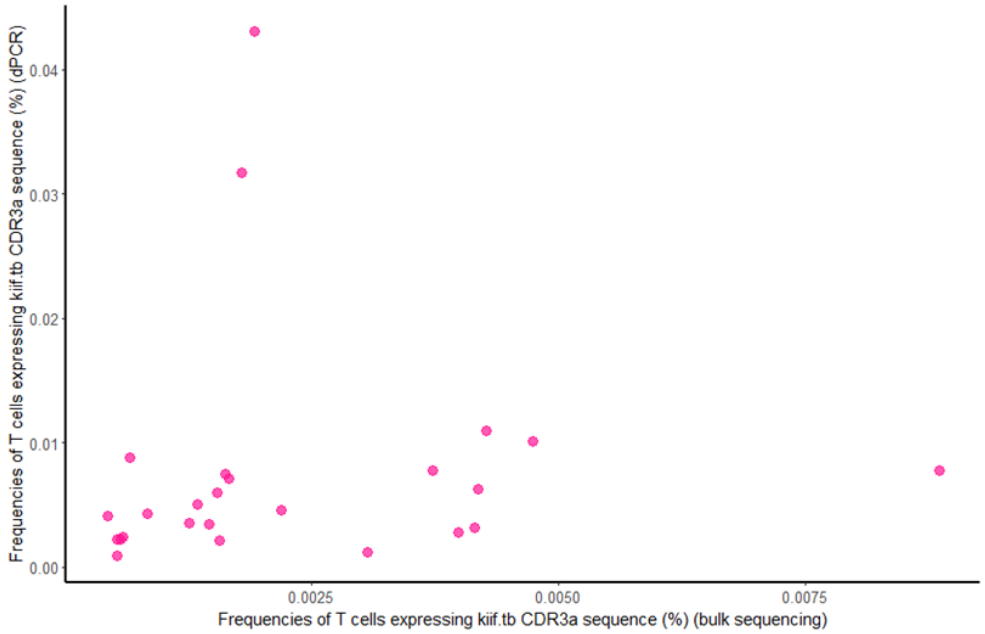

Figure 9: Correlation between T cells expressing the kiif.tb CDR3α sequence measured by dPCR and bulk sequencing after hyperwelling. A scatter plot showing the frequencies of T cells expressing the kiif.tb CDR3α sequence measured by dPCR compared to the frequencies of T expressing the kiif.tb CDR3α sequence obtained by bulk sequencing. The number of samples analysed is 25. The Spearman's rank correlation coefficient was 0.48, p-value, 0.01.

2.5.4 Similar frequencies of T cells expressing the CDR3α sequence in peripheral blood of healthy uninfected individuals, healthy infected, and active TB individuals using the dPCR assay

Previously, we observed significantly higher frequencies of T cells expressing the kiif.tb CDR3α sequence in peripheral blood in controllers, compared with those progressors. Additionally, we also observed higher frequencies of T cells expressing the kiif.tb CDR3a in a separate cohort of QFT-positive individuals compared to those with active TB disease. Given the importance of our previous findings, we wanted to confirm whether the differences in the frequencies of kiif.tb T cells observed between QFT-positive individuals and those with active TB were reproducible using the dPCR-quantification assay in a different cohort. The hyperwelling technique was used, as our previous results indicated that it improves the sensitivity of the assay. Furthermore, our interest extended to assessing the accuracy of the dPCR assay in quantifying the frequency of T cells within our sample cohort. To achieve this, we conducted a comparison between the frequencies of total T cells measured using dPCR and those determined by flow cytometry in a prior study. Likewise, to the correlation between

dPCR and bulk TCR sequencing, we found a significant correlation between dPCR and flow cytometry, (rho = 0.75, p-value = $5X10^{06}$, *Figure 10*).

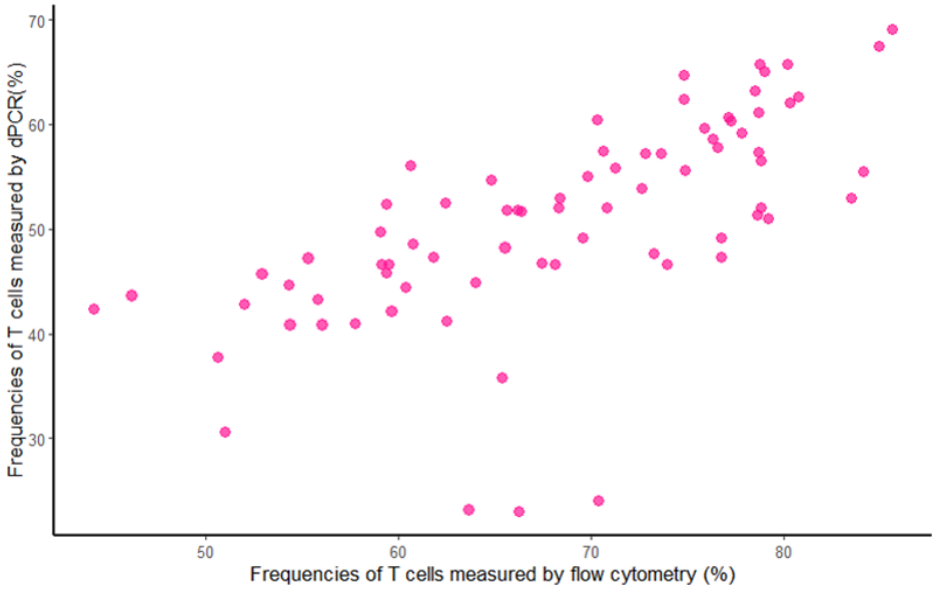

Figure 10: Correlation between T cell frequencies measured by dPCR and flow cytometry. A scatterplot displaying the T cell frequencies measured by dPCR and flow cytometry for the whole sample cohort. The number of samples analysed is n = 77. The Spearman's rank correlation test was performed and the correlation between the two methods was rho = 0.75, p-value = $5x10^{-06}$.

A comparison of the frequencies of T cells expressing the kiif.tb CDR3α measured by dPCR with those obtained from bulk sequencing could not be performed, as this specific method was previously not performed for this sample cohort. Furthermore, in the prior study, flow cytometry analysis was used solely to quantify total T cells and not kiif.tb T cells for this sample cohort. Therefore, we were unable to compare the correlation of these two methods when measuring kiif.tb T cells.

However, our main interest was to determine if the frequencies of kiif.tb T cells were higher in recent QFT converters and persistently QFT-positive individuals compared to individuals with active TB or QFT-negative individuals. Unfortunately, only 77 samples of the possible 100 yielded interpretable results that could be included in our analyses, because some samples had insufficient volume and others had to be excluded due to technical issues with the Qiacuity machine, including failure to capture images for specific wells which precluded visualization and determination of gene copy numbers. Therefore, instead of the full sample size of 25 samples in each group, the sample sizes for each group decreased to a range of 18-21 samples per group.

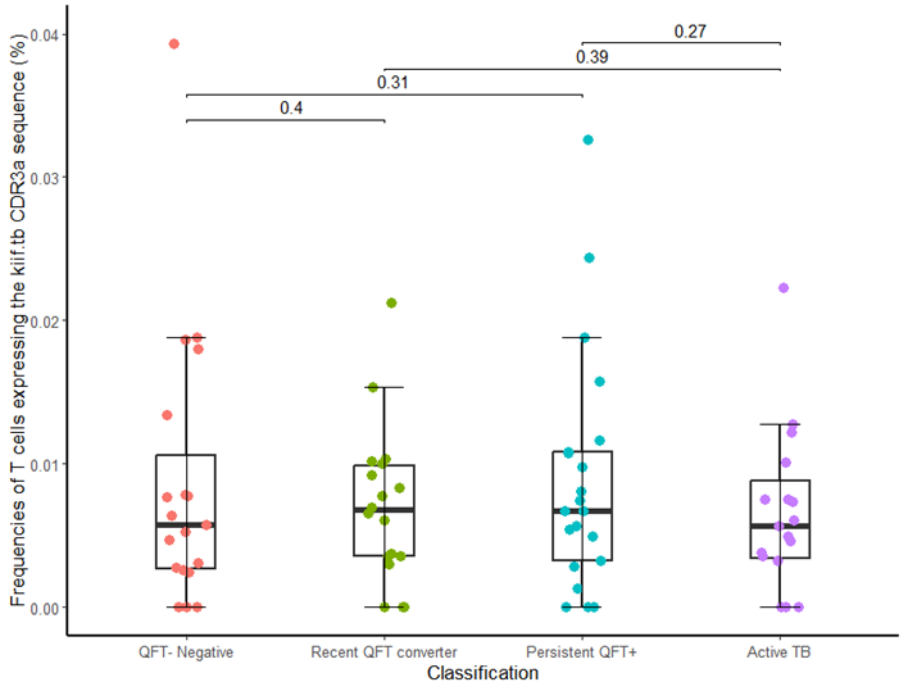

Figure 11: Frequencies of T cells expressing kiif.tb CDR3α sequence in QFT-negative, recent QFT converters, persistently QFT-positive, and active TB individuals. Boxplots comparing the frequencies of kiif.tb T cells in QFT- negative, recent converters, persistent QFT-positive, and active TB individuals. The error bars represent the first quartile (below), the third quartile (upper) and the middle represents the median. Mann-Whitney U test was used to compare groups (significant p value<0.05). The number of samples analysed is i) QFT-negative, n = 19, ii) recent QFT converter, n = 18, iii) persistent QFT-positive, n = 21, iv) active TB, n = 19.

There were no significant differences in frequencies of kiif.tb T cells in recent QFT converters compared to QFT-negative or active TB individuals, (p-value = 0.4, 0.39, respectively, *Figure 11*). Furthermore, frequencies of kiif.tb T cells observed in persistent QFT-positive individuals were not different between QFT-negative and active TB individuals, (p-value = 0.31,0.27, respectively, *Figure 11*).

2.5.5 Effect of the number of valid partitions on the dPCR outcomes

The published dPCR assay we adapted in our study used 50ng of DNA in a final volume of 20µl, which led to 0.75 copies per partition of haploid genomes after partitioning the samples into 20,000 partitions. We followed the same approach to maintain 0.75 copies per partition, as we were also generating around 26,000 reactions. In our study, the final volume was 40µl, so the amount of DNA used was doubled to 100ng. However, there was a concern that this high input amount of DNA

may potentially saturate the microwells, such that many contain more than a single copy of the template. Three target sequences were used in this assay: TRB, exclusively found in non-T cells, its presence in all partitions was not anticipated. Secondly, the kiif.tb sequence is unique to kiif.tb T cells, which are rare, making saturation less likely. For those reasons, we focused on examining the positive partitions for DNM3, a reference gene present in all cells. Each valid partition might contain at least one or multiple copies of DNM3 due to its presence in all cells. As a result, there was a risk that the quantitative ability of the assay would be lost. The following equation is used to calculate the proportion of T cells: ($1 - \frac{TCRB\ copies/\mu l}{DNM3\ copies/\mu l}$). Inaccuracies in the copy number of DNM3 would therefore lead to incorrect quantification of T cells. Moreover, since the calculated amount of T cells is used to determine kiif.tb T cells ($\frac{kiif.tb\ copies/\mu l}{T\ cell\ proportions}$), any inaccuracies could yield inaccurate proportions of kiif.tb T cells. In addition, without a standard reference method to compare our frequencies of kiif.tb T cells to, we opted to assess the range of positive partitions for DNM3 to determine if saturation was occurring. We observed that the proportion of DNM3 positive partitions lay in the range between 25-75% for most samples, with a few below or above this range (*Figure 12*).

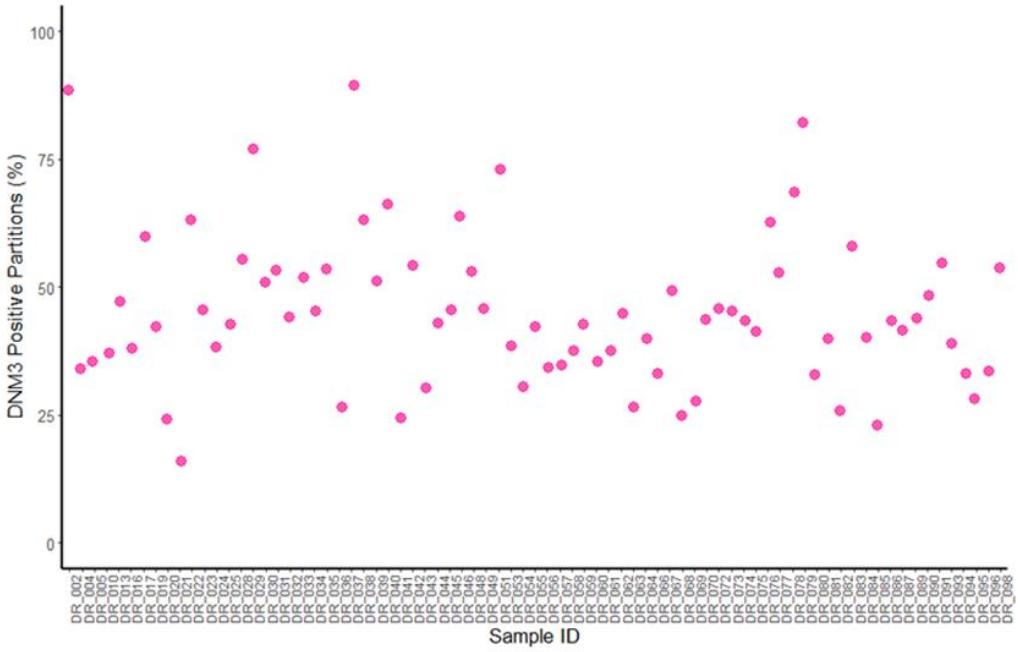

Figure 12: The percentage of positive partitions for the reference gene (DNM3) for each sample. A scatter plot showing the range of positive partitions for DNM3 for each sample. The sample size is n = 77.

Next, we calculated the frequencies of T cells within different ranges to determine a range that is not below the detection threshold but also does not appear to reach saturation. We compared the T cell frequencies measured by dPCR and by flow cytometry at these different ranges for DMN3 positive partitions and first selected samples that had between 15% and 50% DNM3 positive partitions. There was a slight increase in the correlation between frequencies of total T cells measured by dPCR and by flow cytometry (rho = 0.77, p-value = $2.4x10^{-07}$, *Figure 13*) compared to when the correlation for all samples was assessed. Although the correlation was good, it is important to note that we were only comparing 53 samples compared to the initial 77 samples.

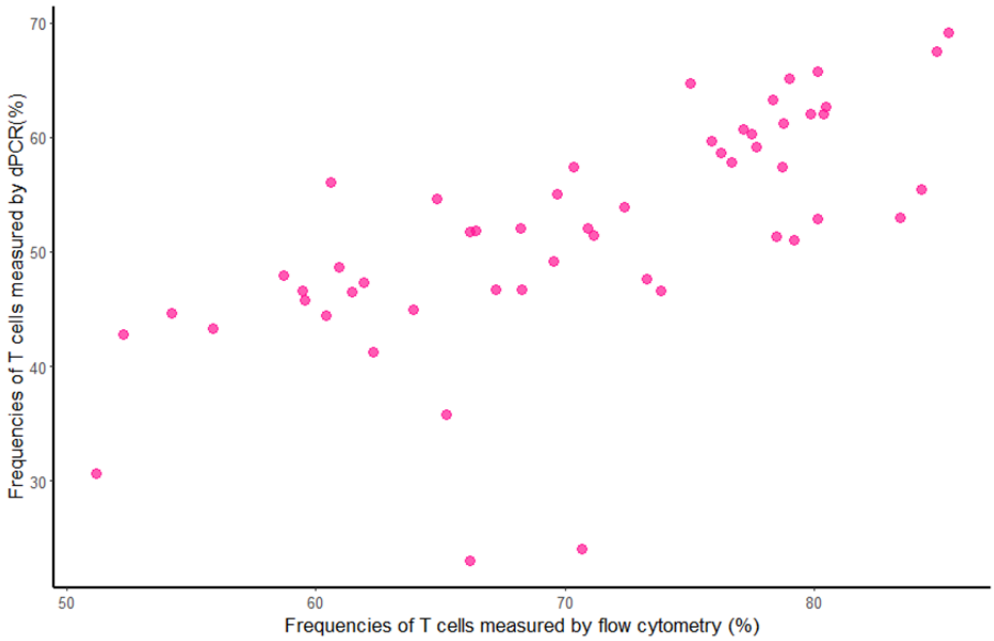

Figure 13: Correlation between total T cell frequencies measured by dPCR and flow cytometry at (15-50%) DNM3 positive partition range. A scatterplot displaying the T cell frequencies measured by dPCR and flow cytometry at 15-50% positive partitions for the reference gene. The number of samples analysed is n = 53 The Spearman's rank correlation test was performed and the correlation between the two methods was rho = 0.77, p-value = $2.4x10^{-07}$

We also compared the frequencies of kiif.tb T cells between the groups in this sub-analysis. The frequencies of kiif.tb T cells in recent QFT-positive were not significantly higher compared to QFT-negative and active TB individuals (p-values = 0.78, 0.71, respectively, *Figure 14*). Additionally, the frequencies of kiif.tb T cells in persistent QFT-

positive were not higher compared to QFT-negative and active TB individuals (p-values = 0.5, 0.36, respectively, *Figure 14*).

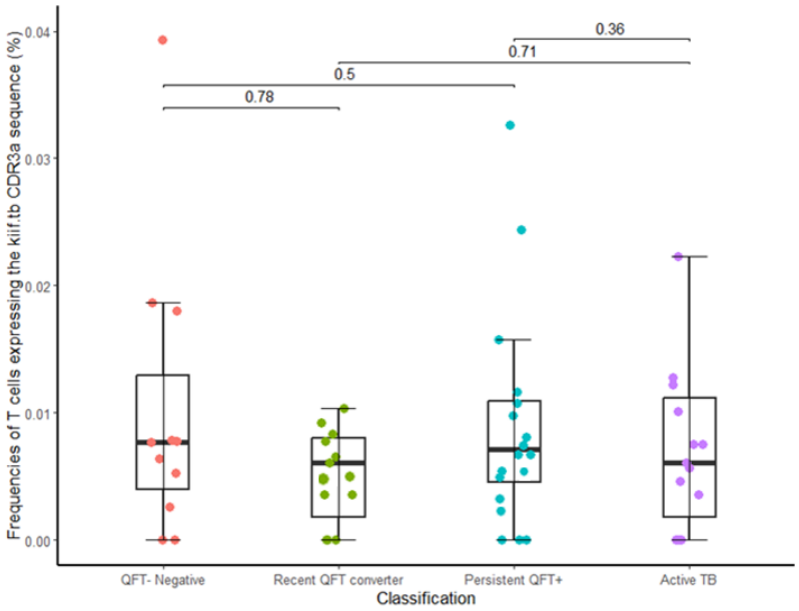

Figure 14: Similar frequencies of T cells expressing kiif.tb CDR3α sequence in QFT-negative, recent QFT converters, persistent QFT-positive, and active TB with 15-50% positive partitions for DNM3. A boxplot comparing the frequencies of kiif.tb T cells in QFT- negative, recent converters, persistent QFT-positive, and active TB individuals at 15-50% positive partitions for the reference gene. The error bars represent the first quartile (below), the third quartile (upper) and the middle represents the median. Mann-Whitney U test was used to compare groups (significant p-value < 0.05). The number of samples analysed is i) QFT-negative, n = 11, ii) recent QFT converter, n = 12, iii) persistent QFT-positive, n = 18, iv) active TB, n = 12.

We also investigated the frequencies of total T cells and kiif.tb T cells in samples with 25 to 75% DNM3 positive partitions. This was a range in which most of the positive partitions lay. The was a slight decrease in correlation between frequencies of T cells measured by dPCR and by flow cytometry (rho = 0.74, p-value = $2.2X10^{-7}$, *Figure 15)*. However, the correlation remained strong. In this range, we only compared 68 samples, which showed that most of our samples lay within this range.

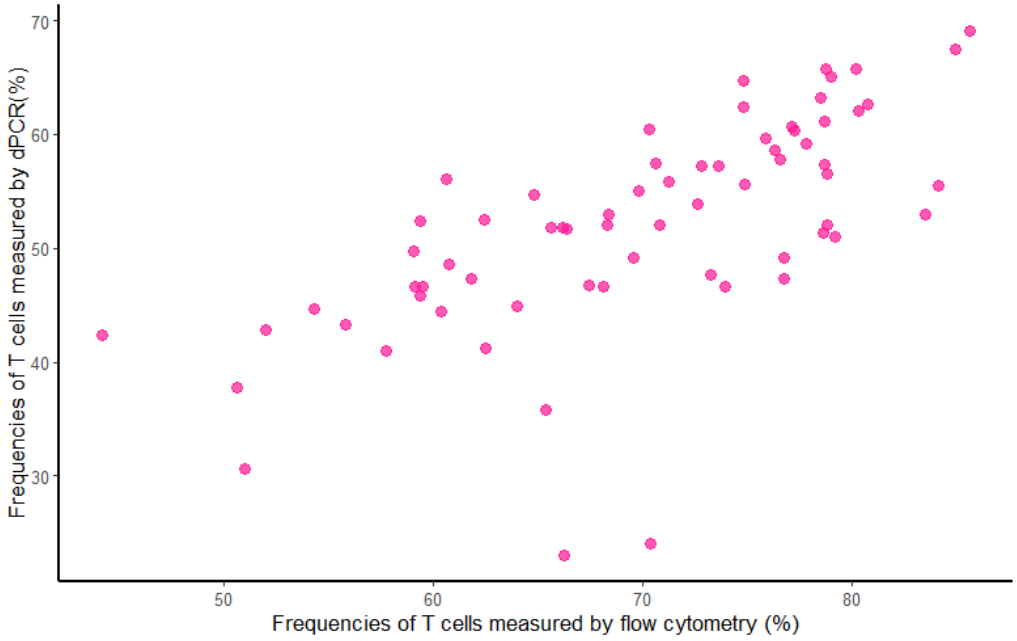

Figure 15: Correlation between T cell frequencies measured by dPCR and flow cytometry at (25-75%) DNM3 positive partition range. A scatterplot portraying the T cell frequencies measured by dPCR and flow cytometry at 25-75% positive partitions for the reference gene. The number of samples analysed is n = 68. The Spearman's rank correlation test was performed and the correlation between the two methods was rho = 0.74, p-value = $2.2x10^{-07}$

In terms of differences in the frequencies of kiif.tb T cells between the groups, a significant difference was still not observed. Frequencies of kiif.tb T cells in recent converters, QFT-negative and active TB individuals overlapped entirely, (p-value = 0.47, 0.75, respectively, *Figure 16*). Similarly, frequencies of kiif.tb T cells in persistent QFT-positive individuals, QFT-negative, and active TB individuals were also not different (p-value = 0.89, 0.66, respectively, *Figure 16*).

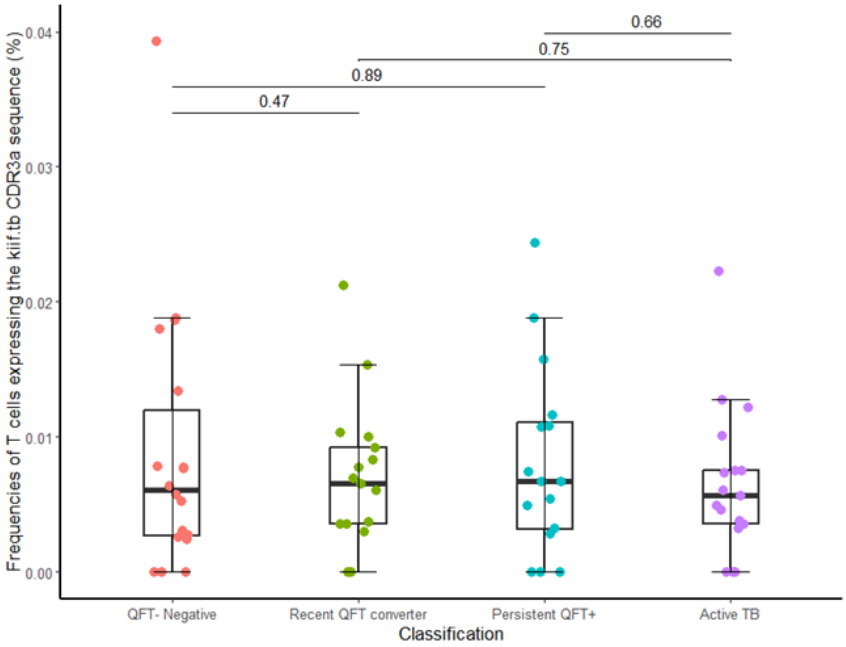

Figure 16: Similar frequencies of T cells expressing kiif.tb CDR3α sequence in QFT- negative, recent QFT converters, persistent QFT-positive, and active TB with 25-75% positive partitions for DNM3. A boxplot comparing the frequencies of kiif.tb T cells in QFT- negative, recent converters, persistent QFT-positive, and active TB individuals at 25-75% positive partitions for the reference gene. The error bars represent the first quartile (below), the third quartile (upper) and the middle represents the median. Mann-Whitney U test was used to compare groups (significant p value<0.05). The number of samples analysed is i) QFT-negative, n = 19, ii) recent QFT converter, n = 17, iii) persistent QFT-positive, n = 16, iv) active TB, n = 16.

Lastly, we looked at samples with 50-75% positive DNM3 partitions. This range represented the above extremities, which might reduce the assay's dynamic range and might also result in inaccurate readouts. The was a decrease in the correlation between T cell frequencies measured by dPCR and by flow cytometry (rho = 0.57, p-value = 0.01, *Figure 17)*. The correlation at this range was poor and only 20 samples were in this range.

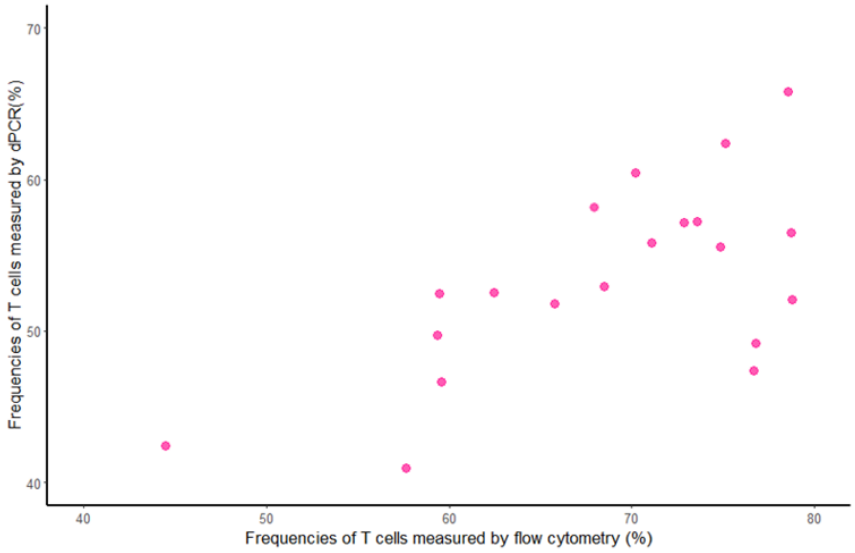

Figure 17: Correlation between T cell frequencies measured by dPCR and flow cytometry in samples within the 50-75% DNM3 positive partition range. A scatterplot portraying the T cell frequencies measured by dPCR and flow cytometry at 50-75% positive partitions for the reference gene. The number of samples analysed is n = 20. The Spearman's rank correlation test was performed and the correlation between the two methods was rho = 0.57, p-value = 0.01

Next, we compared the frequencies of kiif.tb T cells between the groups in samples with 50% to 75% positive partitions of the reference gene. Similarly to all previous findings, no differences between the frequencies of kiif.tb T cells between the four groups were observed, *Figure 18*).

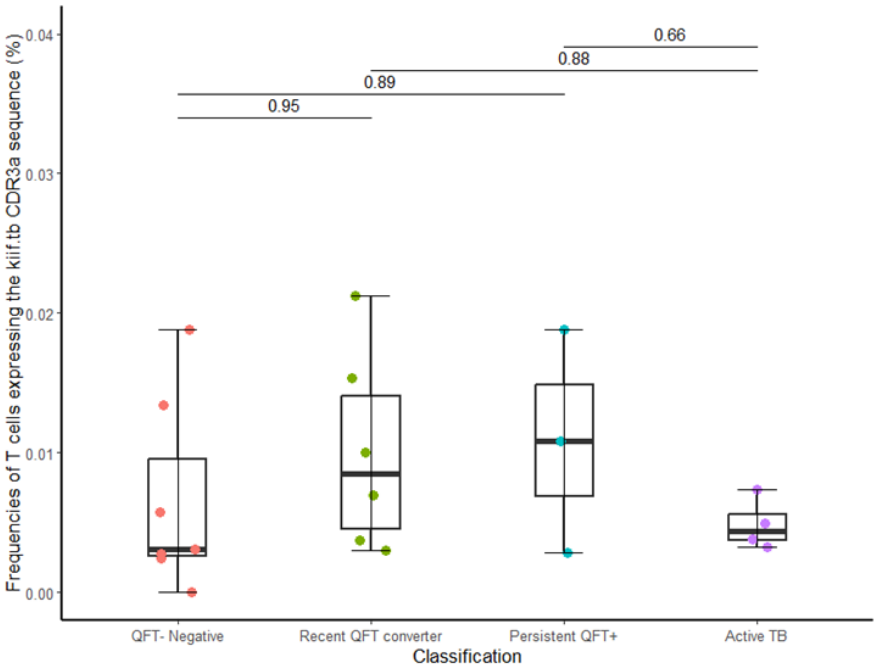

Figure 18: Differences in the frequencies of T cells expressing kiif.tb CDR3α sequence between QFT- negative, recent QFT converters, persistent QFT-positive, and active TB individuals at 50-75% positive partitions for DNM3. A boxplot comparing the frequencies of kiif.tb T cells in QFT-negative, recent converters, persistent QFT-positive, and active TB individuals at 50-75% positive partitions for the reference gene. The error bars represent the first quartile (below), the third quartile (upper) and the middle represents the median. Mann-Whitney U test was used to compare groups (significant p value<0.05). The number of samples analysed is i) QFT- negative, n = 7, ii) recent QFT converter, n = 6, iii) persistent QFT-positive, n = 3, iv) active TB, n = 4.

2.6 Discussion

One of the aims of this study was to optimize a highly sensitive, digital PCR assay for the precise measurement of T cell frequencies and frequencies of T cells expressing the kiif.tb CDR3α sequence in the peripheral blood of distinct participant groups.

The dPCR assay was intended to provide a robust, reproducible, reliable, and cost-effective method for quantifying this particular T cell clonotype within the diverse cohorts. The aim was that the dPCR assay would contribute valuable insights into the dynamics of kiif.tb T cells by quantifying absolute counts and revealing whether frequencies of these cells differ between individuals infected with *M.tb* and those with active TB. In comparison to qRT-PCR, the dPCR assay offers the advantage of absolute quantification of targeted sequences. This is crucial for achieving a higher level of precision and reproducibility in measurements. Notably, when contrasted with traditional PCR methods, dPCR exhibits enhanced sensitivity and precision, making it particularly well-suited for studying T cells expressing specific CDR3α sequences, which are typically present in lower abundance.[109, 111] The dPCR assay accurately identified Jurkat T cells engineered to express the kiif.tb T cells CDR3α sequence at high concentrations. However, challenges arose at lower concentrations, which approached the lower level of detection. Furthermore, a notable discrepancy emerged when comparing frequencies of kiif.tb T cells measured by dPCR with those quantified by bulk TCR sequencing, which is the gold standard for measuring the TCR repertoire and frequencies of individual T cell clonotypes.

To address this limitation hyperwelling was introduced. This resulted in a four-fold increase in the number of valid partitions generated, thereby increasing the sample size of cells that could be assayed by amplifying the number of reactions and broadening the scope for detecting kiif.tb T cells. With the dPCR assay now spanning a greater number of reactions, it allowed sampling of more T cells, and thus low-frequency cells should be detectable, even at very low concentrations.

The introduction of hyperwelling showed a slight improvement in the correlation between kiif.tb T cells measured by dPCR assay and bulk sequencing, but the persistence of a poor correlation raises concerns about the sensitivity of the dPCR assay in detecting kiif.tb T cells. Despite efforts to enhance sensitivity through hyper-welling, a poor correlation was observed in the frequency of kiif.tb T cells measured

by dPCR, compared to bulk TCR sequencing, suggesting limitations in detecting T cells expressing the kiif.tb CDR3α sequence, especially since these cells are found in much lower abundances.

Interestingly, the correlation of total T cell frequencies measured by dPCR compared to bulk TCR sequencing remained modest, regardless of the effects of hyperwelling. Similar findings were observed when the frequencies of total T cells measured by dPCR were compared to those obtained by flow cytometry. A potential explanation for the strong correlation between bulk TCR sequencing and dPCR assay could be that the assay can only accurately detect targets at higher abundances, such as total T cells (in the range of 30-70%). This limitation may affect the assay's accuracy when quantifying T cells expressing the kiif.tb CDR3α sequences, since they are at abundances 1000-fold lower (in the range 0-0.04). It prompts a critical evaluation of the assay's sensitivity range and its applicability to samples with varying cell populations, emphasizing the importance of understanding the dynamic range and limitations of the method.

The challenges observed underscore the complexity of accurately quantifying very low-abundance cell populations using molecular technologies and highlight the need for continued optimization or consideration of alternative methodologies, such as flow cytometry, which is extremely sensitive.[112] Further refinement of the dPCR assay requires validation against other highly sensitive methods, including bulk TCR sequencing and flow cytometry. This validation would help address the existing sensitivity issues and enhance the sensitivity of detection by dPCR, improving its correlation with other established techniques. Ultimately, this approach would facilitate a more reliable analysis of kiif.tb T cell frequencies across diverse cohorts.

Building on our previous study, which revealed higher frequencies of kiif.tb T cells in both peripheral blood and lung tissues among controllers compared to progressors, as well as in individuals who are QFT-positive compared to those with active TB, we aimed to confirm these findings by examining a different study cohort and using an alternative assay— dPCR rather than bulk TCR sequencing. Unlike our prior study, the current study found no statistically significant differences in the frequencies of T cells expressing the kiif.tb CDR3α sequence among the different study groups.

Our findings raise the possibility of assay saturation, given the fixed amount of 100 ng of DNA used—the calculation for the amount of DNA was guided by a published dPCR protocol we adapted in our study.[109] During our analysis, we paid close attention to the ranges of positive partitions for the reference gene, which is found in every cell. This examination was necessary as the determination of T cell proportions in our samples relies on the copy numbers of both the reference gene, DMN3, and the germline TCR gene (TRB). It was likely that each valid partition might contain a copy of DMN3, or even multiple copies, potentially resulting in an inaccurate count of cells expressing the gene. In contrast, it was unlikely for every valid partition to contain a copy of the TRB gene, as mature T cells present in the samples would lack this gene. Furthermore, given that kiif.tb T cells are rare, their copies would not be present in every valid partition. Additionally, a slight error in the quantification of each of the DMN3, TRB, and kiif.tb targets would be when these results are used to calculate the abundance of kiif.tb cells lead to a significantly larger error in quantification.

To evaluate the potential of saturation we performed a sub-analysis of samples with a range of positive DNM3 valid partitions of 15-50% (low), 25-75% (middle), and 50-75% (high). Across various threshold ranges, correlations varied: low thresholds showed increased correlation, middle thresholds decreased slightly, and high thresholds saw a notable drop. However, it is important to note that the sample size in the higher threshold was small, and any differences would be difficult to observe. This suggests a potential overestimation of copy numbers due to multiple gene copies' invalid partitions. Therefore, establishing appropriate thresholds is crucial for accurate and reproducible results using the dPCR assay.

Previous research by Paquin-Proulx *et al*. has demonstrated that frequencies of certain T cell subsets such as iNKTs and MAIT cells were significantly higher in *M.tb* infected individuals compared to those with active TB[88]. We were curious to investigate if this trend applies to kiif.tb T cells, as these cells appeared to be donor-unrestricted T cells due to their presence in virtually all individuals. Interestingly, no significant differences in the frequencies of kiif.tb T cells were observed among the various groups across all three threshold ranges. The frequencies of kiif.tb T cells were not higher in recent QFT converters or individuals maintaining a positive QFT-positive result compared to those with active TB and healthy, uninfected individuals. These results do not support our hypothesis, and the following could be a reasonable explanation. The dPCR assay

lacked the requisite sensitivity to detect these cells, particularly given their very low abundance. This concern is further highlighted by the observation that, even when assessing frequencies of kiif.tb T cells through bulk TCR sequencing, the observed differences between QFT-positive and active TB cases were not massive. Therefore, it appears that a highly sensitive assay is required to accurately detect any changes in the frequencies of these cells. To address this limitation, potential solutions include a comparison of frequencies obtained by dPCR with those obtained through bulk TCR sequencing as this is the gold standard for quantification of T cells with a specific TCR sequence.[109, 111]

However, the absence of significant differences in kiif.tb T cell frequencies in the peripheral blood of our study cohort could be considered valid. This is because we might have lacked the initial power of 70%, as we had fewer than 25 samples in each group. However, the frequencies of kiif.tb T cells between the different groups were overlapping, which might indicate that there is no significant difference between the study cohorts. The initial finding higher kiif.tb T cells in QFT-positive participants compared to TB participants that informed this current study, may have been a chance finding. However, a more detailed analysis of the activation phenotypes of kiif.tb T cells might reveal more notable distinctions, if these cells do engage antigen through their TCR, as previous findings have demonstrated that some donor-unrestricted T cell subsets such as iNKTs and MAIT cells express higher levels of exhaustion and activation markers in individuals with active TB compared to those who are infected.[88] The next chapter aimed to study the differences in the activation states of kiif.tb T cells between healthy uninfected individuals, healthy *M.tb* infected individuals, and those with active TB.

Chapter Three

Optimizing methods Compatible with Flow Cytometry to detect kiif.tb T cells in peripheral blood

3.1 Background

A cell-mediated immune response is widely recognized as crucial for controlling *M.tb* infection, with particular emphasis placed on CD4 T (helper) cells.[113] Among these, Th1 cells are acknowledged for their significant role in controlling *M.tb* infection by producing IFN-γ. However, other cells are also deemed important, such as Th17 and Th1-Th17 subsets. The distribution of these distinct T cell types appears to differ between individuals with *M.tb* infection and those with active TB.[113] A study by Estevez *et al*. demonstrated that Th1/Th2 ratio was lower in individuals with active TB compared to uninfected and *M.tb* infected individuals. Additionally, the Th1-Th17 subset proportions were lower in active TB individuals compared to both uninfected and *M.tb* infected individuals.[113] In a recent study, we identified a T cell clonotype that was more abundant in healthy individuals who controlled *M.tb* infection (controllers) compared to those who progressed to active TB (progressors). Furthermore, we observed in a separate cohort that healthy individuals with *M.tb* infection had higher frequencies of this T cell clonotype compared to those with active TB, suggesting that this clonotype might be associated with protection.

Flow cytometric immunophenotyping (FCI) is increasingly acknowledged as a powerful tool for characterising immune cells, using their surface and intracellular receptors.[114] The capability to measure multiple fluorescence parameters simultaneously enables comprehensive analyses of co-expression or distinct markers. Flow cytometry has emerged as a powerful tool for high-resolution identification and quantification of cell types, along with their functional characteristics. This capability makes flow cytometry invaluable for elucidating inter-individual differences in the immune system.[115]

Based on our preliminary findings, it seemed that peripheral blood frequencies of kiif.tb T cells were higher in QFT-positive individuals compared to QFT-negative and active TB individuals when they were measured using bulk TCR sequencing. However, when we looked at the frequencies of kiif.tb T cells in a different cohort of QFT-positive, QFT-negative, and active TB individuals using a dPCR approach, we did not see any

differences. This raised the possibility that the dPCR assay may not have been sensitive enough to quantify these cells as they are present at low frequencies. We therefore wanted to compare the frequencies of kiif.tb T cells in QFT-positive, QFT-negative and persons diagnosed with active TB using flow cytometry to determine if this method would detect any differences using a more definitive approach.

Additionally, we sought to delve deeper into the distinctions in the activation phenotypes across the categories of healthy uninfected individuals, those who are healthy but infected, and individuals with active TB. Previous studies have indicated variations in the phenotypes of specific T cell subsets between individuals with *M.tb* infection and those with active TB.[116,117,118] Different markers, such as CD27 (expressed on all naive cells and downregulated after TCR engagement) and CD45RO (expressed on memory T cells post-antigen activation), can assist in identifying the activation and memory states of these cells during TB infection.[113]

Furthermore, HLA-DR, which is a member of the MHC class II family typically expressed by antigen-presenting cells, is often used as a marker of T cell activation. In the context of TB, studies have shown that the expression of HLA-DR is elevated in *M.tb* specific T cells from individuals with active TB compared to those who are *M.tb* infected, regardless of their HIV status.[116, 117,118]

The objective of this chapter was to optimize a customized RNA hybridization assay (PrimeFlow), designed to be compatible with flow cytometry, and develop custom monoclonal antibodies to identify and characterise kiif.tb T cells in the peripheral blood of participants in our study cohort. Additionally, we compared the activation phenotype of T cells expressing the kiif.tb CDR3α sequence within our study groups.

3.2 Aims:

3.2.1 To develop and optimize methods compatible with flow cytometry to detect kiif.tb T cells in peripheral blood.

Hypothesis:

Kiif.tb T cells in PBMCs can be detected using the customised PrimeFlow assay and a custom monoclonal antibody.

3.2.2 To compare the frequencies and activation phenotype of kiif.tb T cell between healthy uninfected, healthy *M.tb* infected, and individuals with active TB using the customised PrimeFlow assay or a custom monoclonal antibody.

Hypothesis:

Kiif.tb T cells from healthy M.tb infected will have a less activated phenotype compared to individuals with active TB.

3.3 Methods

3.3.1 Study Participant Groups

The same study samples, described in the previous chapter were used, which include QFT-negative samples and QFT-positive samples from the ACS study, and samples from persons with active TB in the MRC-SHIP study.

3.3.2 PBMC thawing

The complete (R10) media was prepared by adding 44ml of Roswell Park Memorial Institute Medium Lonza BE12-702F(RPMI), 5ml of heat-inactivated Fetal Bovine Serum (FBS-80%), 0.5ml of L-glutamine and 0.5ml of penicillin-streptomycin (Pen-Strep) in a 50 ml falcon tube and was placed in the water bath set at 37°C. A volume of 9ml was added to another 15ml falcon tube and placed in the water bath. Labelled cryopreserved PBMC vials were retrieved from liquid nitrogen storage and thawed in the 37°C water bath by slowly agitating the tubes until cells were nearly completely thawed. For the 1st wash, 1ml of warmed complete media was added to the cells dropwise in the cryovial, and the cells were transferred to the tube containing 9ml of media. The vials were rinsed, and the cells were centrifuged at 400g at RT for 10 minutes. The supernatant was discarded, and for the 2nd wash the pellet was re-suspended with 1ml of warmed complete media then 9ml of the warmed complete media was added. The cells were centrifuged at 400g at RT for 10 minutes. The supernatant was discarded, and the pellet was resuspended in 1ml of warm complete media. The cells were then counted by microscopy using trypan blue to determine viability.

3.3.3 Manual counting of cells

The haemocytometer was pre-cleaned with 70% ethanol and dried using lens paper. An aliquot of 20µl of the thawed cell and 20µl of trypan blue was mixed in a clean tube, and the suspension was allowed to sit for two minutes before loading to the haemocytometer. Approximately 10µl of the well-mixed diluted cell suspension was pipetted at the edge of the coverslip. The haemocytometer was mounted on the microscope and a low-power lens (5X) was used for focus and a higher-power lens (40X) to count the cells was used. Once the cells had settled, a tally counter was used to count the cells in the four large squares that separate viable cells from non-viable cells. The average count from the four large squares was used.

3.3.4 Antibody titration

Antibodies for the flow cytometry panel used (*Table 7*) in the PrimeFlow assay were titrated to determine the optimal volumes needed for optimal resolution. Two-fold dilutions were prepared in fluorescence-activated cell sorting (FACS) tubes. In each tube except the first, 50µl of cell staining buffer (Cat:420201) was added. For the first tube, double the volume of the manufacture's recommended about was added was added and topped up with staining buffer to bring the final volume to 100µl. The solution was mixed and 50µl was taken from the first tube and added to the second tube. The solution was mixed and 50µl was taken from the second tube and added to the third tube. This was repeated for all the remaining tubes.

Table 7: The antibody panel used for identification and characterisation of kiif.tb T cells.

Type of Marker	Fluorochrome	Manufacturer	Catalogue Number	Marker	Titre (µl)	Compensation (µl)
Viability	BUV450	Invitrogen	2286899	Live/dead	0.5	0.2
Kiif.tb T cells	APC	Thermofisher	368738-000	Kiif.tb mRNA	5	5
	PE	Biolegend	405307	Secondary antibody	0.15	2
	-	GenScript	U709BHF060-71FJ1047	Kiif.tb TCRα chain	20	-
Surface markers	APC-H7	BD	560176	CD3	0.5	0.5
	BV786	BD	563877	CD4	0.2	0.2
	BUV805	BD	612889	CD8	0.05	0.05
Activation	BUV563	BD	748340	HLA-DR	0.5	0.5

3.3.5 PrimeFlow assay

Kiif.tb T cells were detected using a customized PrimeFlow assay developed by Dr Munyaradzi Musvosvi. This assay is an in-situ RNA hybridization approach compatible with flow cytometry. The assay uses branched DNA technology, and a clear advantage is that DNA/RNA isolation is not required. Therefore, maintaining single-cell resolution is possible because RNA extraction is not required. DNA/RNA extraction has limitations because it is impossible to determine which cell the DNA/RNA originated from. The PrimeFlow assay utilized a custom-designed probe set

targeting a specific CDR3a sequence, which was designed by Thermo Fisher Scientific. The probe set consisted of five bDNA probes: four Label Extenders (LEs) and one Capture Extender (CE). The Label Extenders (LEs) were specifically designed to bind to the target sequence, covering the region of interest to maximize the signal for detection. These LEs are labeled with fluorophores to facilitate signal amplification.Capture Extenders (CEs) were used to stabilize the target binding, though they are not directly involved in the detection signal. Blockers (BLs) were not necessary in this design, as the LEs provided sufficient coverage and signal strength.

Extracellular staining: After determining viability with LIVE/DEAD™ Fixable Aqua Dead Cell Stain, 50µl of the phenotyping antibody master mix was added to 50µl of cells, and the cells were incubated for 45 minutes at 4°C (*Table 7*). After 45 minutes, 2ml of cell staining buffer was added and the cells were centrifuged at 931g for 5 minutes at RT. The supernatant was discarded, and the cells were resuspended in 1ml of flow cytometer cell staining buffer. The cells were then fixed and permeabilized using the PrimeFlow assay.

Permeabilization and fixation*:* The fixation buffer 1 was prepared by mixing equal parts of PrimeFlow RNA fixation buffer 1A and PrimeFlow RNA fixation buffer 1B. Then 1ml of the prepared fixation buffer was added to each sample, and incubated for 30 minutes at 2-8°C. The samples were then centrifuged at 800g for 5 minutes at 2-8°C, and the supernatant was discarded. A 1X PrimeFlow RNA permeabilization buffer with RNase inhibitors was prepared by diluting the 10X PrimeFlow RNA permeabilization buffer with RNase-free water. Then the RNAse inhibitors (100X) were added at 1/100 dilution, and 1ml of this permeabilization buffer was added to wash cells. The samples were then centrifuged at 800g for 5 minutes at 2-8°C. The wash step was repeated twice to ensure permeabilization of the cells. The cells were fixed again with PrimeFlow fixation buffer 2. The buffer was prepared by adding 125µl of PrimeFlow RNA fixation buffer 2(8X) with 875µl of PrimeFlow RNA wash buffer per sample. A volume of 1ml was added to each sample and inverted to mix, the samples were incubated for 1 hour in the dark at RT. After incubation, the samples were centrifuged at 800g for 5 minutes at RT, the supernatant was discarded, and the cells resuspended in the residual volume by gently vortexing. The cells were then washed in 1ml of PrimeFlow wash buffer and centrifuged at 800g for 5 minutes at RT. The wash step was repeated twice, and the cells were resuspended in the residual volume by gently

vortexing. Target probe hybridization was performed following fixation and permeabilization.

PrimeFlow target probe hybridization*:* Directly to the cell suspension, 100µl of the PrimeFlow RNA target probe diluent with target probes, specific for the kiif.tb mRNA sequence was added at a 1:20 dilution and briefly vortexed to mix. The samples were incubated for 2 hours at 40°C, and after 1 hour the samples were inverted to mix. Following incubation, the samples were washed with 1ml of PrimeFlow wash buffer and centrifuged at 800g for 5 minutes at RT. The supernatant was discarded, and then cells were washed again with 1ml of PrimeFlow wash buffer with RNAse inhibitors. The cells were centrifuged at 800g for 5 minutes at RT, and the supernatant was discarded. Then the cells were resuspended in the residual volume by vortexing gently and stored overnight at 4°C.

PrimeFlow signal amplification: A volume of 100µl of PrimeFlow RNA Preamp mix was added directly to the cell suspension and briefly vortexed to mix. The samples were then incubated for 1 hour 30 minutes at 40°C to allow the preamplifier to hybridize with the target probes. Following incubation, 1ml of PrimeFlow wash buffer was added to the samples and centrifuged at 800g for 5 minutes at RT and the supernatant was discarded. The wash step was repeated three times and cells resuspended in the residual volume. After the wash steps, 100µl of PrimeFlow RNA Amp mix was added to the samples and incubated for 1 hour 30 minutes at 40°C to allow hybridization to the PrimeFlow preamplifier. At the end of incubation, 1ml of PrimeFlow wash buffer was added and the samples were centrifuged at 800g for 5 minutes at RT. The supernatant was discarded, and the cells resuspended in residual volume by gently vortexing, the wash steps were repeated twice. Following the wash steps, 100µl of PrimeFlow RNA label probe diluent and PrimeFlow RNA label probe at a 1:100 dilution was added to the cell suspension. The cells were incubated for 1 hour to allow the label probe to hybridise to the PrimeFlow amplifier, and after 1ml of PrimeFlow wash buffer was added. The cells were centrifuged at 800g for 5 minutes at RT, the supernatant was discarded, and the cells were resuspended by gentle vortexing, and these wash steps were repeated twice. Following the wash steps, 1ml of flow cytometry staining buffer was added to the cells, and centrifuged at 800g for 5 minutes at RT. The supernatant was discarded, and the cells were resuspended in the residual

volume by gently vortexing, and 100µl of flow cytometry staining buffer was added. The cells were then analysed on flow cytometer.

3.3.6 GenScript antibody production

Two amino acid sequences containing the kiif.tb sequence were generated by GenScript and used to immunize mice: a shorter kiif.tb peptide sequence (*LNKASQYVSLLIRDSQPSDSATYL***CAVNRDDKIIF**) and a longer sequence (MHHHHHHQGFPSHDEDGRFTAQ*LNKASQYVSLLIRDSQPSDSATYL***CAVNRDDKI IF**GKGTRLHILPNIQNPDPAVYQLRDSK). Both antigens contained two important sequences: the variable gene usage sequence for the alpha chain of the TCR of kiif.tb T cells (TRAV12-2) labelled in red and underlined, and the kiif.tb CDR3α sequence, which is a very hypervariable region labelled in bold. Furthermore, both peptide sequences were conjugated to an immunogen: keyhole limpet hemocyanin. This was done to elicit a more vigorous immune response. Approximately 6-week-old mice were then immunized with either a shorter or longer kiif.tb peptide sequence to allow the mice to mount an antibody response to the antigens. Following this, the spleens of the mice were harvested for mature plasma cell isolation, and after isolation, the B cells were fused with immortal cancer cell lines to form hybridomas using electrofusion. After fusion, successfully formed hybridomas were isolated from unfused B cells and immortal cancer lines by growing the cells in a hypoxanthine-aminopterin-thymidine medium (HAT), which is a selective medium. The surviving hybridoma cells were then diluted into multi-well tissue culture plates, each in their well, and their supernatants, containing monoclonal antibodies, were subjected to a rigorous screening process using enzyme-linked immunosorbent assay (ELISA) to select for the highest specificity and affinity binders against shorter and/or longer kiif.tb sequence and a negative control TRAV1-2. The hybridoma cells that produced monoclonal antibodies with higher affinity and specificity against the two peptides were then purified and cryopreserved for future production of monoclonal antibodies. This whole protocol was done by Genscript and we received the eight clones.

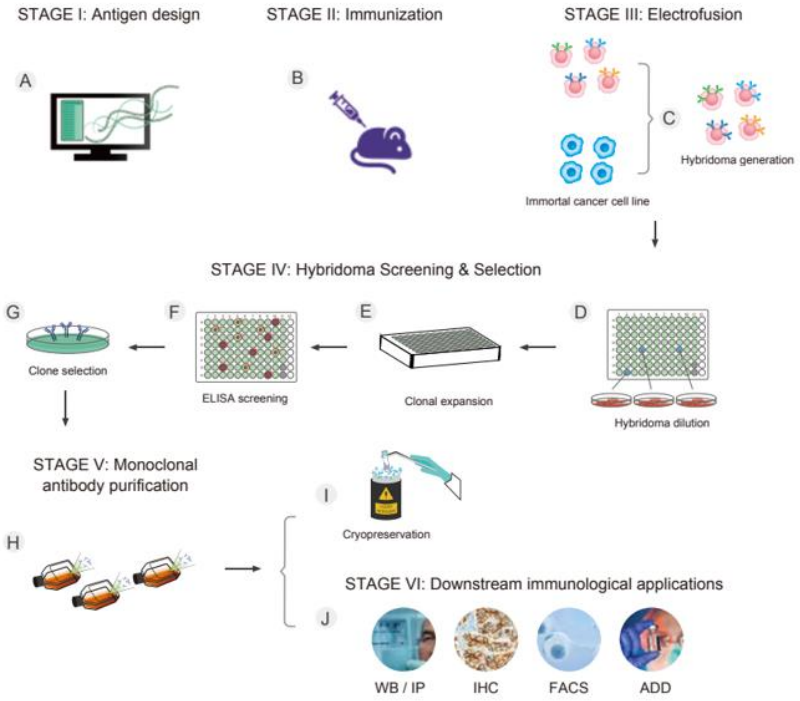

Figure 19: Summary of the method used to develop monoclonal antibodies that recognise the kiif.tb CDR3α sequence. A) Stage 1: Two specific antigens recognizing the variable gene usage of the alpha chain of kiif.tb T cells and the TCR CDR3α were generated. **(B)** Stage 2: Mice were immunized with either a shorter or longer kiif.tb sequence. **(C)** Stage 3: B cells were then isolated from the mice's spleen and fused with myeloma cells to form hybridomas using electrofusion. (D–G) Stage 4: The hybridomas were **(D)** diluted into selective culture medium and plated in multi-well tissue culture plates (1 clone/well), **(E)** individual hybridoma clones were allowed to expand, after which **(F)** tissue culture supernatants that contain monoclonal antibodies were screened via ELISA in order to **(G)** hybridoma clones which produce monoclonal antibodies with higher specificity and affinity for the two specific antigens. (H, I) Stage 5: Selected hybridoma clones were used for **(H)** monoclonal antibody purification, and hybridoma cell lines were **(I)** cryopreserved for future antibody production. **(J)** Stage 6: Purified monoclonal antibodies were used in flow cytometry in our study. (Figure taken from the GenScript white paper, Hybridoma Technology for the Win: An In-Depth Introduction into Hybridoma-Based Antibody Development, https://www.genscript.com/hybridoma-technology-for-the-win.html). This whole protocol was done by GenScript.

3.3.7 GenScript antibody staining

Kiif.tb T cells were detected using an indirect flow cytometry assay, where a primary antibody which targeted the kiif.tb sequence was first used, followed by a secondary antibody labelled with PE, which binds to murine IgG (the primary antibody). Cells were first incubated with LIVE/DEAD™ Fixable Aqua Dead Cell Stain and then washed and resuspended in 200µl of cell staining buffer. The resuspended cells were

split evenly into two FACS tubes labelled primary antibody and no primary antibody (negative control) tubes per sample. Then 20µl of the primary antibody was added into the tube labelled primary antibody, while in the other tube, 20µl of media with no primary antibody was added (negative control). The mixture was incubated in the dark at RT for 30 minutes. Following incubation, 2ml of cell staining buffer was added to each tube, and the cells were centrifuged for 5 minutes at 931g at RT. Next, the secondary antibody was added to both tubes and incubated for 15 minutes at room RT. Subsequently, 2ml of cell staining buffer was added, and the cells were spun at 931g for 5 minutes at RT. This washing step was repeated three times to ensure the removal of unbound secondary antibodies. Then, 50µl of the phenotypic markers antibody master mix was added to cells, and the cells were incubated for 45 minutes at 4°C (*Table 7*). After the 45-minute incubation, 2ml of cell staining buffer was added, and the cells were centrifuged at 931g for 5 minutes at RT. The supernatant was discarded, and the cells were resuspended in 100µl of 1X Phosphate buffered saline (PBS). The cells were then analysed on a flow cytometer.

3.3.8 Statistical analysis

Statistical analysis and representative graphs were performed using R version 4.2.0 and GraphPad Prism 9.3.1(471) for Windows. A Fisher's exact test was conducted to determine whether an individual had a kiif.tb response (responder) or not. The Mann-Whitney test was performed to evaluate the differences between frequencies of PE positive cells detected when no primary antibody or the primary antibody was added. Furthermore, this test was also used to detect the differences in frequencies of kiif.tb T cells/Bulk T cells expressing HLA-DR and the median expression of HLA-DR between our study groups. Differences with a p-value of ≤ 0.05 were considered significant.

3.4 Results

3.4.1 Custom PrimeFlow assay detects Jurkat T cells expressing the kiif.tb CDR3α sequence

Dr Munyaradzi Musvosvi developed customized PrimeFlow probe pairs specifically designed for the kiif.tb CDR3α sequence to identify kiif.tb T cells. Dr Musvosvi prepared a dilution series of kiif.tb-TCR expressing Jurkat T cells in PBMC ranging in proportion from ~3% to 10% of kiif.tb-TCR expressing Jurkat T cells. The PrimeFlow assay stained approximately 73.6% of cells in the 100% kiif.tb-TCR expressing Jurkat T cell preparation, suggesting that some TCR-transfected Jurkat T cell did not express sufficiently high levels of TCR to allow detection. However, although there was some staining, we observed a significant decrease of positive staining in the PBMC-diluted kiif.tb-TCR expressing Jurkat T cell conditions, to much lower levels than expected (*Figure 20)*.

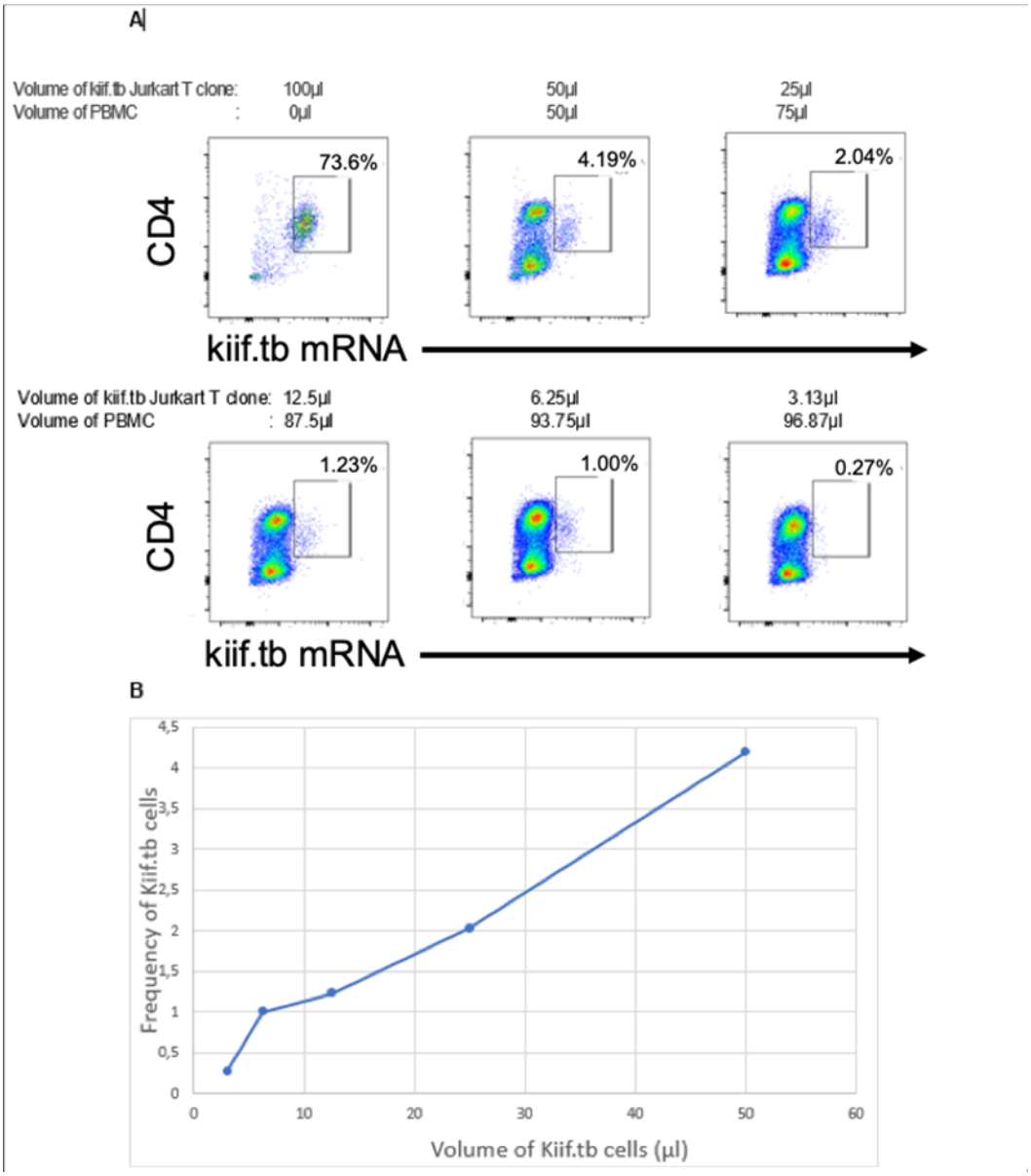

Figure 20: Custom PrimeFlow assay detects kiif.tb-expressing Jurkat T cell line. **A**) The first plot (top left) shows custom kiif.tb PrimeFlow assay staining of a Jurkat T cell line engineered to express the kiif.tb sequence. The next five plots show frequencies of kiif.tb T cells detected by prime flow assay as the proportions of kiif.tb Jurkat T cells among PBMC added were reduced. **B**) A summary line graph showing the frequency of Kiif.tb cells detected using the custom kiif.tb PrimeFlow assay as the proportion of kiif.tb cells added reduced. Results generated by Dr Munyaradzi Musvosvi.

Dr Musvosvi also assessed if the custom kiif.tb-specific PrimeFlow assay could identify cells expressing the kiif.tb sequence in PBMCs collected from a QFT-positive donor. A small population of T cells staining positive for the kiif.tb-specific PrimeFlow assay could be detected *(Figure 21)*. The population of kiif.tb-specific PrimeFlow-positive cells did not express CD8, however, because CD4 was not included in the flow cytometry

antibody panel it was not possible to determine if kiif.tb-expressing T cells express CD4. Overall, the preliminary results suggest that kiif.tb-expressing T cells can be detected using the custom kiif.tb PrimeFlow.

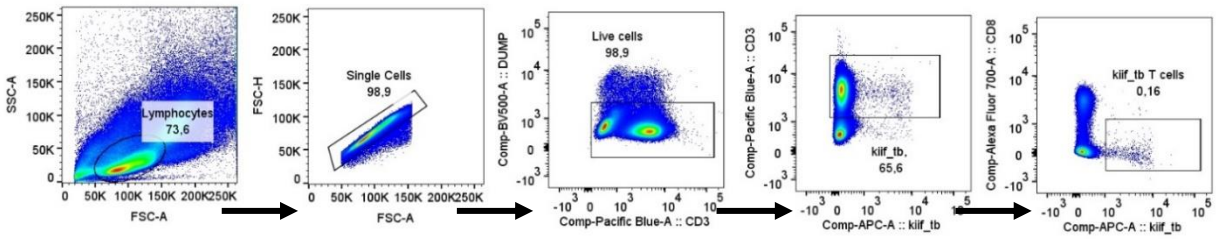

Figure 21: Gating strategy to identify kiif.tb T cells in PBMCs. A population of lymphocytes was first identified, then a population of singlet cells. Next, live cells were identified, followed by T cells, and lastly kiif.tb specific T cells. Two million cells were used in this experiment. Results generated by Dr Munyaradzi Musvosvi.

3.4.2 Optimizing cell retention in PrimeFlow assay for enhanced experimental accuracy

To validate the results generated by Dr Musvosvi, we spiked different amounts of Jurkat T cells expressing the kiif.tb CDR3α sequence into PBMCs to generate samples with varying frequencies of Jurkat T cells expressing the CDR3α sequence. Despite starting with 2,000,000 cells, we only acquired 383 of cells, demonstrating a substantial loss of cells when using the PrimeFlow assay (*Figure 22)*.

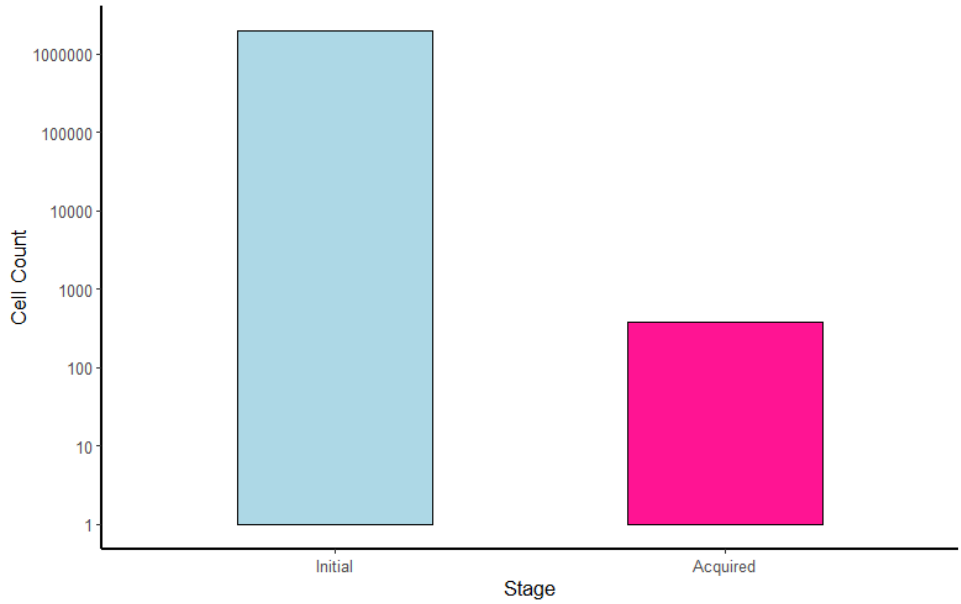

Figure 22: Loss of cells observed follow the PrimeFlow assay sample preparation. A bar graph showing the initial cell count and the acquired cell count. The starting cell count was two million cells of Jurkat T cells. The log scale was used for the y-axis to accommodate the wide range data set.

PrimeFlow assay is a two-day experiment. On the first day, it involves viability dye staining (LIVE/DEAD™ Fixable Aqua Dead Cell Stain) and surface receptor staining, fixation, permeabilization of cells, and target probe hybridization. On the second day, signal amplification takes place. Despite starting with 2,000,000 cells, it appeared that excessive cell loss might be occurring at various stages, as the assay includes a total of 16 washes. To investigate steps in the sample process where cell loss might occur, we performed flow cytometry analyses at varying steps, relative to a control tube (*Figure 23*). This control tube did not undergo PrimeFlow, but only underwent viability and surface marker staining, which is done before starting the PrimeFlow assay. This tube thus had only two washes.

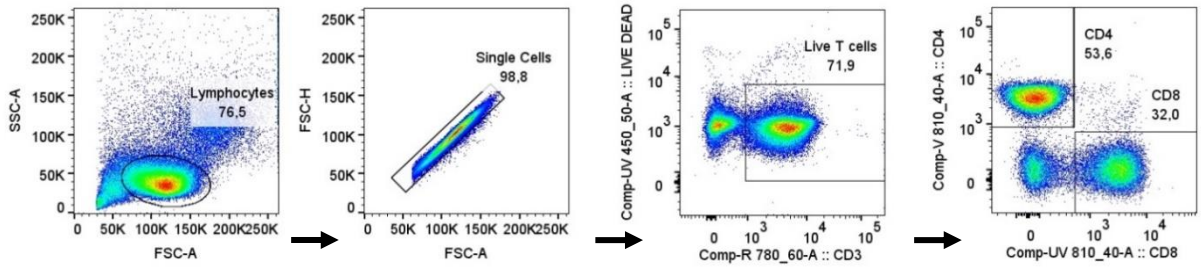

Figure 23: The gating strategy used to determine stages of cell loss. The side scatter (SSC-A) and forward scatter (FSC-A) parameters were used to assess the granularity and size of lymphocytes. A population of lymphocytes was first identified, then a population of single cells. Next, live T cells were identified, followed by T cells expressing CD4 and CD8. A threshold of 30 000 on the FSC-A was used to avoid acquiring debris.

It seemed that the frequencies of live T cells and those expressing CD4 or CD8 were similar to those of the control tube (*Figure 24A)*. However, the frequencies were relative, so we looked at the time it took to acquire 100,000 events as the starting number of cells was a million in each tube. We then compared that to the time it took to acquire 100,000 events in the control tube.

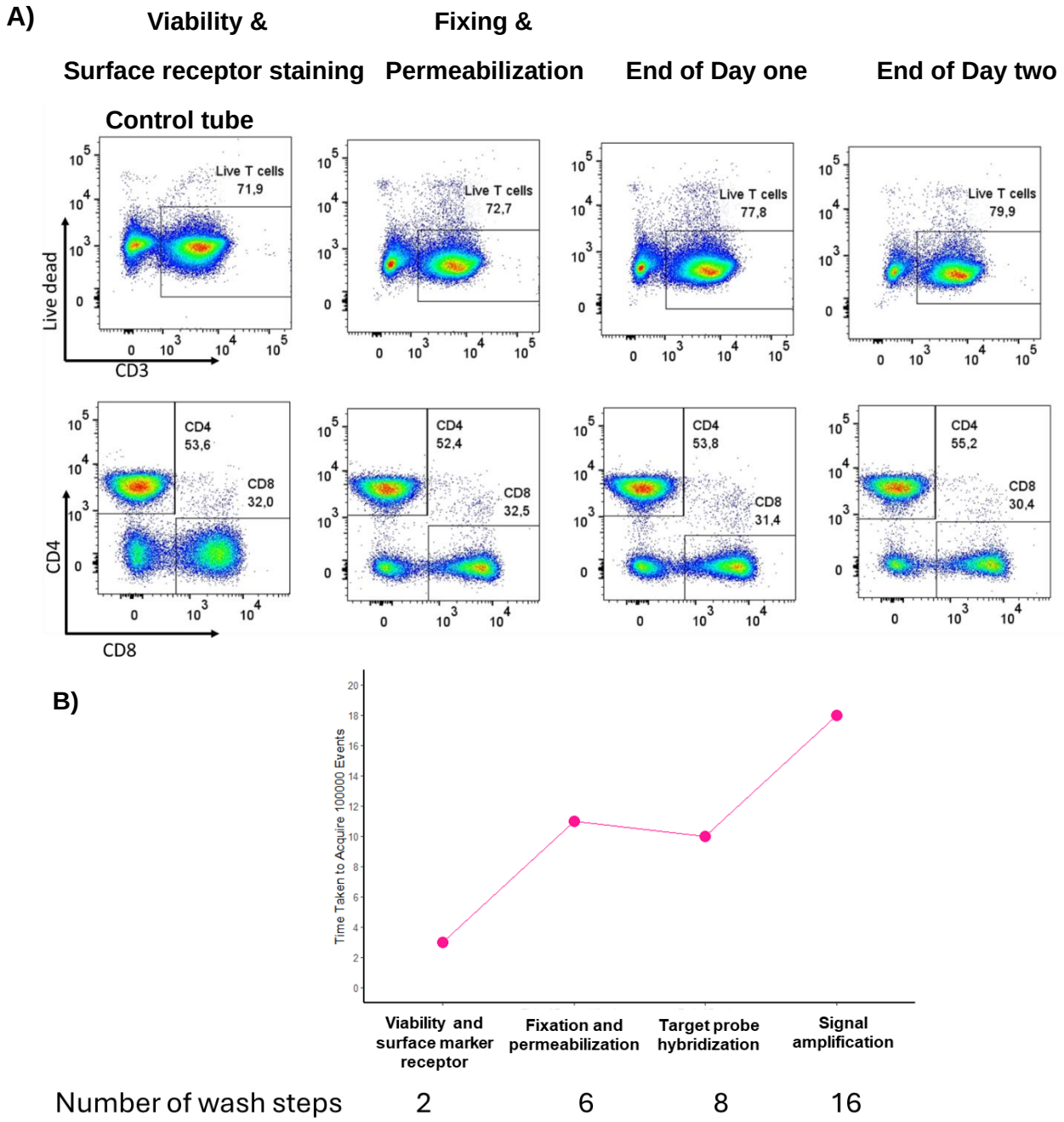

Figure 24: Time taken to acquire 100,000 live T cells, CD4 and CD8 T cells for the different stages of the PrimeFlow assay. A total of one million cells was used in each condition. **A)** In the Viability & Surface receptor staining, there were a total of two washes, while in the fixing & Permeabilization condition, a total of six washes were conducted. During the target probe hybridization stage (End of day one), eight washes were performed, and the signal amplification stage (End of day two) involved a total of 16 washes. A million cells were utilized in each condition, and this experimental setup was duplicated for every stage. **B)** A line graph showing the average acquisition times in minutes for 100 000 events across different stages of the assay and the control.

As expected, the control tube, which underwent only viability and surface receptor staining, had the shortest acquisition time. In comparison the time to acquire 100,000 events increased as the tubes were exposed to more washes, with the tube that underwent the entire procedure taking nine times longer compared to the control tube. This highlights that considerable cell loss occurs during this assay, but it appears that some cells are still present at the end of the assay (*Figure 24A&B*). We proceeded to assess the specificity of PrimeFlow in detecting T cells expressing the kiif.tb CDR3α mRNA sequence.

3.4.3 Poor viability of the Jurkat T cell line and poor resolution of surface markers

Next, we spiked Jurkat T cells expressing the CDR3α sequence into PBMCs at equal proportions. Additionally, we had conditions with only PBMCs or kiif.tb-expressing Jurkat T cells (positive control). The reason for this was that we wanted to determine if the PrimeFlow assay would detect the increase in frequency of kiif.tb T cells when we spiked them into PBMCs. However, the viability of the Jurkat cells was very poor, severely limiting our ability to detect kiif.tb T cells (*Figure 25*).

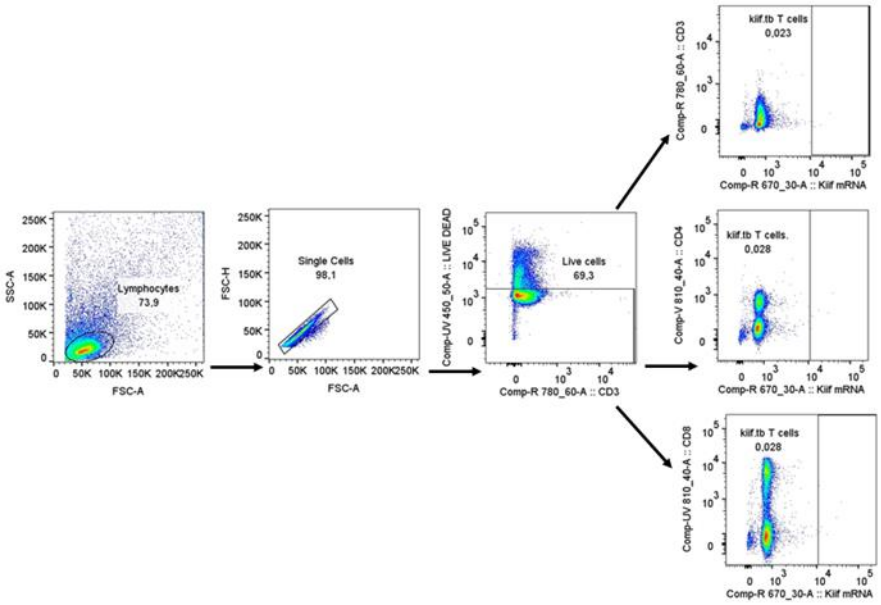

Figure 25: The gating strategy used to identify kiif.tb T cells. A population of lymphocytes was first identified, then a population of singlet cells. Next, live cells were identified, followed by kiif.tb T cells, and then CD4 and CD8 kiif.tb T cells. A threshold of 30 000 on the FSC-A was used to avoid acquiring debris.

Upon spiking Jurkat T cells into PBMCs at equal proportions and gating for live cells, we noticed that most of our Jurkat T cells appeared to stain positive for the Viability dye, suggestive of major cell death (*Figure 26*). We did not detect higher frequencies of kiif.tb PrimeFlow assay-positive cells as expected in our positive control, nor when we spiked Jurkat T cells into PBMCs. Moreover, even after titrating the anti-CD3 antibody to determine the optimal titre, we encountered challenges with optimal resolution when using the assay (*Figure 26*).

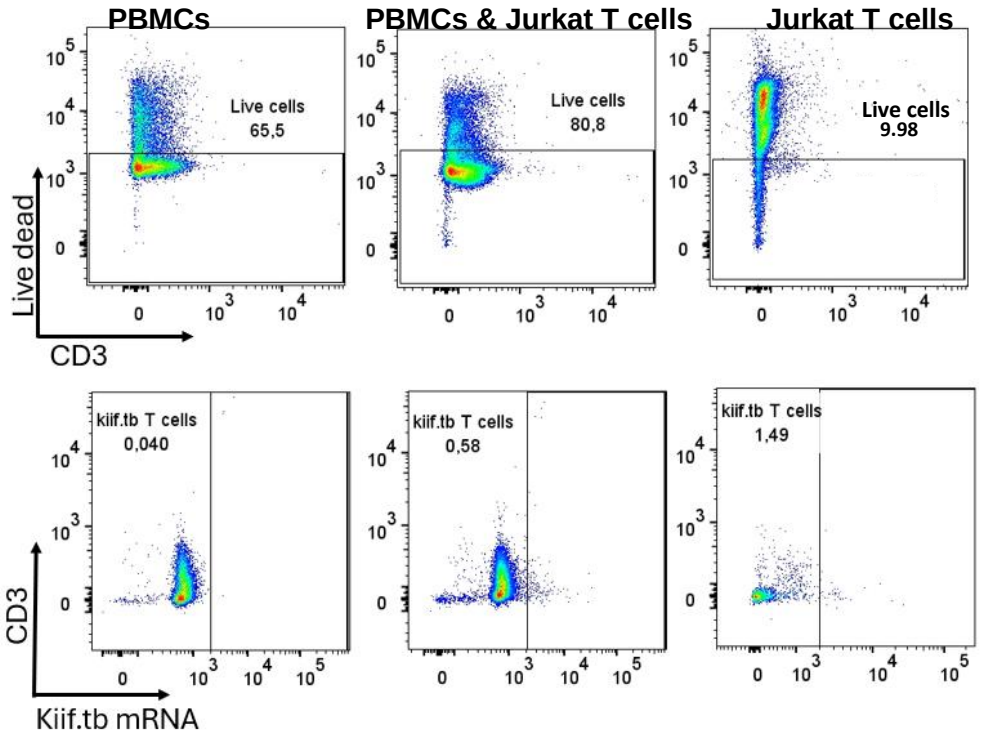

Figure 26: Lower frequencies of kiif.tb mRNA-positive cells observed in PBMCs only compared to PBMCs with Jurkat T cells spiked in, and Jurkat T cells only. A total two million cells were used for each condition. For the spiking one million of PBMCs and one million Jurkat T cells (middle plots) were added to make a total of two million cells.

The initial gating strategy exclusively included live cells (Viability-dye positive cells were excluded); however, upon noticing that a substantial portion of our Jurkat T cells appeared to be dead, we explored modifying the gating strategy to include all cells, regardless of the viability dye staining (*Figure 27*). This adjustment resulted in an increased number of kiif.tb mRNA-positive cells, suggesting that the majority of Jurkat T cell line was dead, but the assay was still able to detect kiif.tb mRNA in the Jurkat T cells (*Figure 27B*). However, when looking at PBMCs and the spiked condition, although an increase was seen in the frequencies of kiif.tb, the separation between kiif.tb negative and kiif.tb positive cells was not good, and it was difficult to detect a clear population of kiif.tb T cells (*Figure 27B*).This was concerning, as the sample type

to compare frequencies of kiif.tb cells in our study cohort were PBMCs. Without a clear resolution of kiif.tb T cells, it was clear that this assay for quantifying kiif.tb T cells would be too challenging.

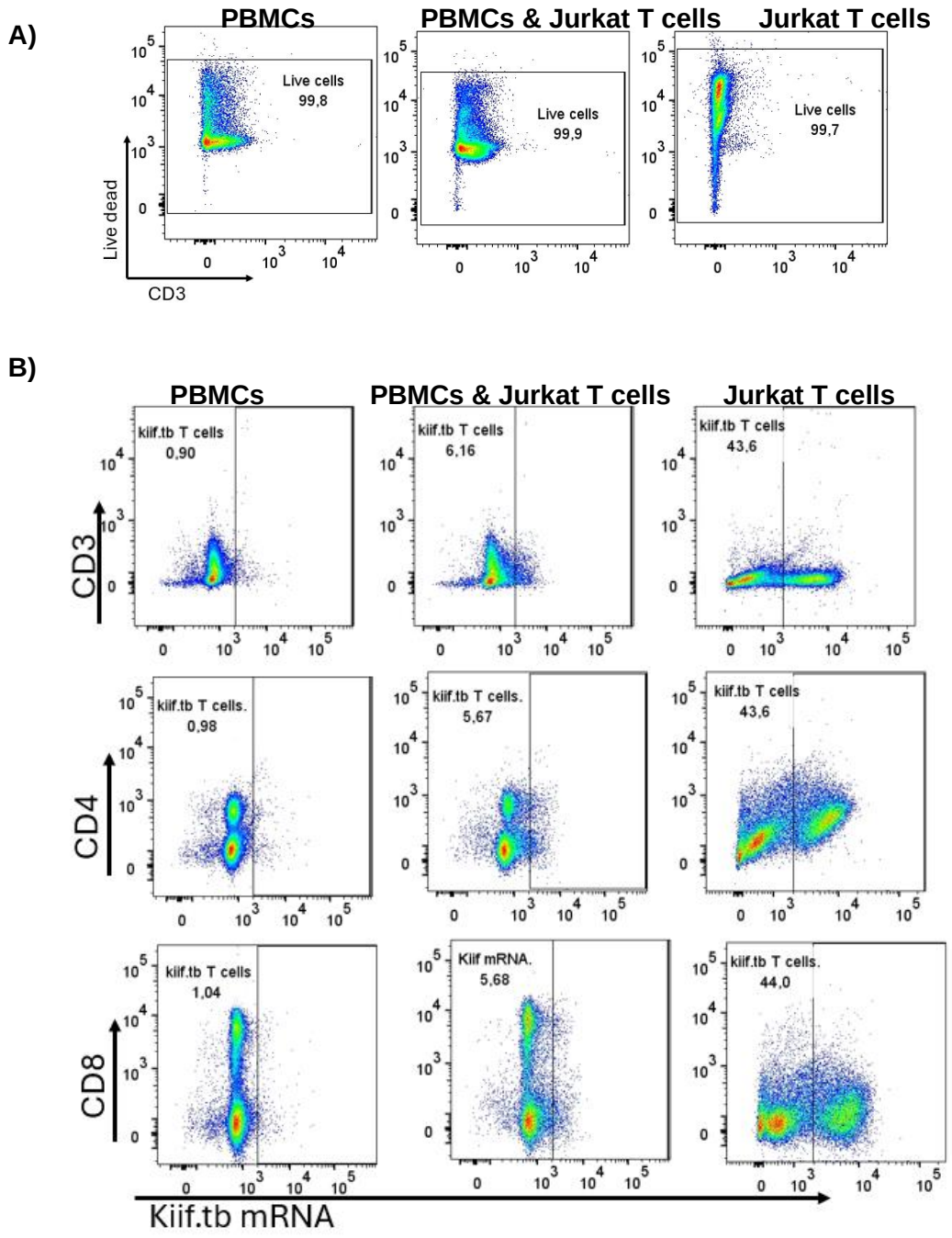

Figure 27:Higher frequencies of kiif.tb mRNA-positive cells observed in PBMCs only, spiked PBMCs with Jurkat T cells, and Jurkat T cells only, when including viability dye-positive cells. A total two million cells were used for each condition. For the spiking one million of PBMCs and one million Jurkat T cells were added to make a total of two million cells (middle plots). The gating strategy was changed to include dead cells. **A)** The gating strategy including all cells**. B)** An increase in the frequencies of kiif.tb T cells in the three different condition

Additionally, poor, or minimal CD4 staining was observed in all conditions *(Figure 28)*. Interestingly, the CD8 staining appeared optimal.

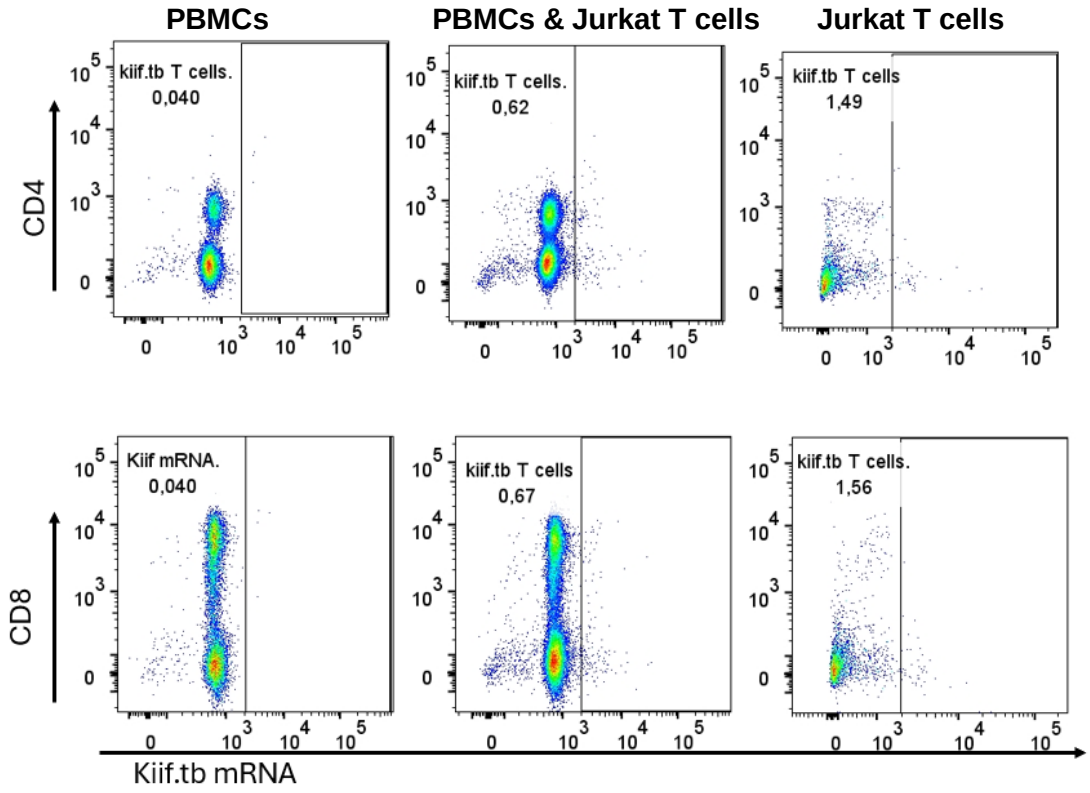

Figure 28: Frequencies of kiif.tb T cells expressing CD4 or CD8 in PBMCs only, spiked PBMCs with Jurkat T cells, and Jurkat T cells only. A total two million cells were used for each condition. For the spiking one million of PBMCs and one million Jurkat T cells (middle plots) were added to make a total of two million cells.

Initially, we used CD3, CD4, and CD8 titres optimised for PBMCs and thought they would be compatible with the PrimeFlow assay. We observed satisfactory resolution of cell subsets using these when testing at which stages of PrimeFlow cell loss occurs (*Figure 24A*). However, during that experiment, we did not incubate cells at 40°C degrees as we thought cell loss might occur due to washes and not incubation, but now we suspected that the 40°C degree incubation might affect our antibody staining quality. We proceeded to titrate the CD4 and CD3 antibodies to determine the optimal antibody volumes for the PrimeFlow assay, including incubation steps at 40°C, that would improve staining resolution. We also investigated whether the volume optimised for standard PBMC surface receptors staining could be used at the end of the assay to avoid any potential interference from the incubation steps and preserve staining quality.

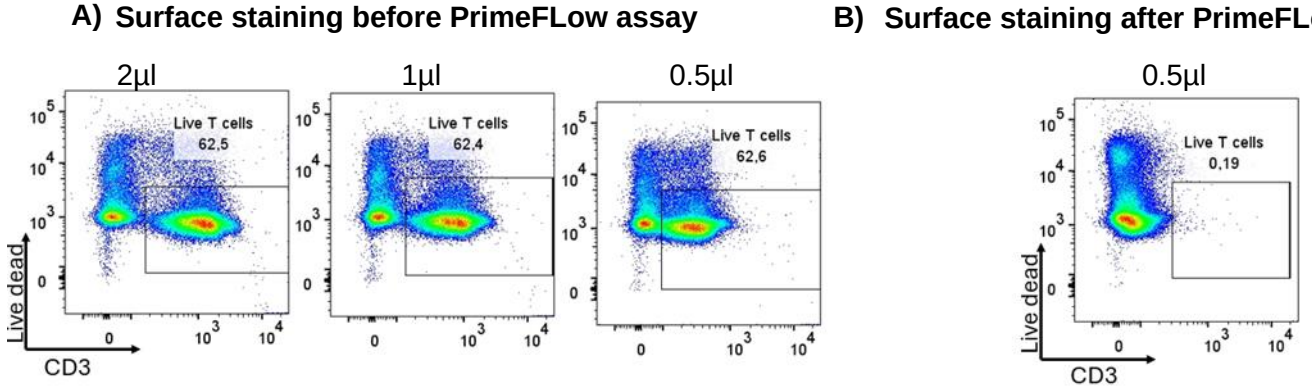

Figure 29: Optimal titre for CD3 compatible with PrimeFlow assay. A 2-fold dilution was performed to determine the optimal titre and a million cells were used. **A)** shows the titrations and the volumes. **B)** shows surface staining after the PrimeFlow with the original titre which was 0.5µl.

In titrating the antibodies, we were able to identify staining volumes that resulted in improved resolution. For CD3, we selected 1µl (*Figure 29A).*Staining after the PrimeFlow assay step was not successful, as we did not observe any CD3-positive staining (Figure 29*B)*. For CD4, we selected 0.4µl as the optimal volume (*Figure 30A*) and similarly, there was no CD4 staining observed after staining following the assay *(Figure 30B*). However, the challenge remained as we did not seem to be detecting kiif.tb+ T cells in using PBMCs using the PrimeFlow approach.

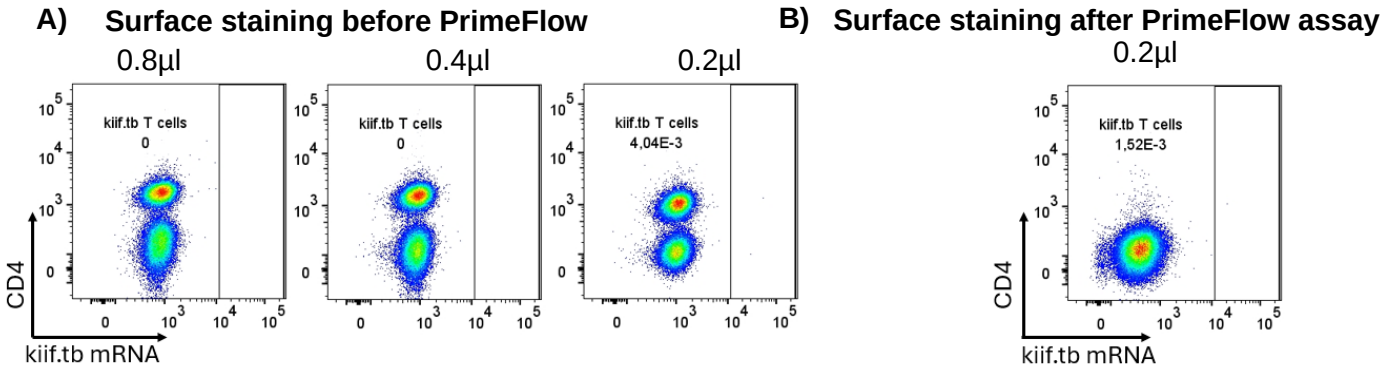

Figure 30: Optimal titre for CD4 compatible with PrimeFlow assay. A 2-fold dilution was performed to determine the optimal titre and a million cells were used. **A)** shows the titration and the volumes used for CD4 **B)** shows staining of CD4 after PrimeFLow with the original titre; 0.2µl.

3.4.4 GenScript primary antibodies recognise the kiif.tb T cell CDR3α sequence in Jurkat T cells

The initial use of the PrimeFlow assay was driven by the lack of available technologies to directly detect the kiif.tb CDR3α sequence. While optimising the PrimeFlow assay, we contacted GenScript to produce monoclonal antibodies that would directly bind to the CDR3α amino acid sequence of kiif.tb T cells. Monoclonal antibodies from eight hybridoma clones were identified by GenScript using indirect ELISA as having specificity for the kiif.tb CDR3α sequence and not for the negative control (TRAV1-2 CDR3α) (*Figure 31)*.

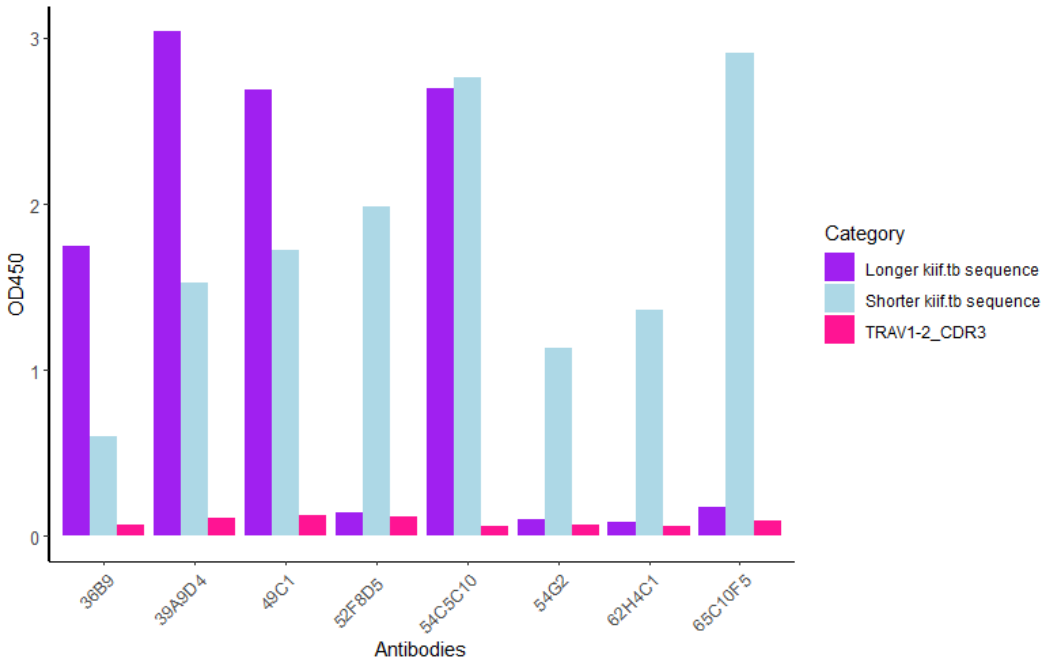

Figure 31: Monoclonal antibodies specific for the kiif.tb CDR3α sequence. An indirect ELISA was performed to determine the specificity of the monoclonal antibodies for the kiif.tb sequence, and 8 monoclonal antibodies were identified as having specificity for kiif.tb T cell sequence. ELISA plates were coated with either the shorter or longer kiif.tb sequence which both contained the kiif.tb sequence (see methods for full the sequences). As a negative control, ELISA plates were coated with a peptide termed TRAV1-2 CDR3, which did not contain the kiif.tb sequences.

The poor viability of the TCR-engineered Jurkat T cells was an ongoing concern, as these cells served as our positive control due to their expression of a TCR containing the kiif.tb CDR3a sequence. Firstly, we were concerned that the non-viable TCR-engineered Jurkat T cells may result in autofluorescence or non-specific staining to the PE-labelled secondary antibody due to the accumulation of cellular debris and breakdown products. Secondly, this presented a challenge as we needed to select an

antibody that binds most effectively to Jurkat T cells. This determination relied on assessing the frequency of cells positive for PE. However, our ability to interpret the data could potentially be compromised if the kiif.tb expressing Jurkat T cells inherently fluoresced at a wavelength overlapping with the PE signal, due to autofluorescence.

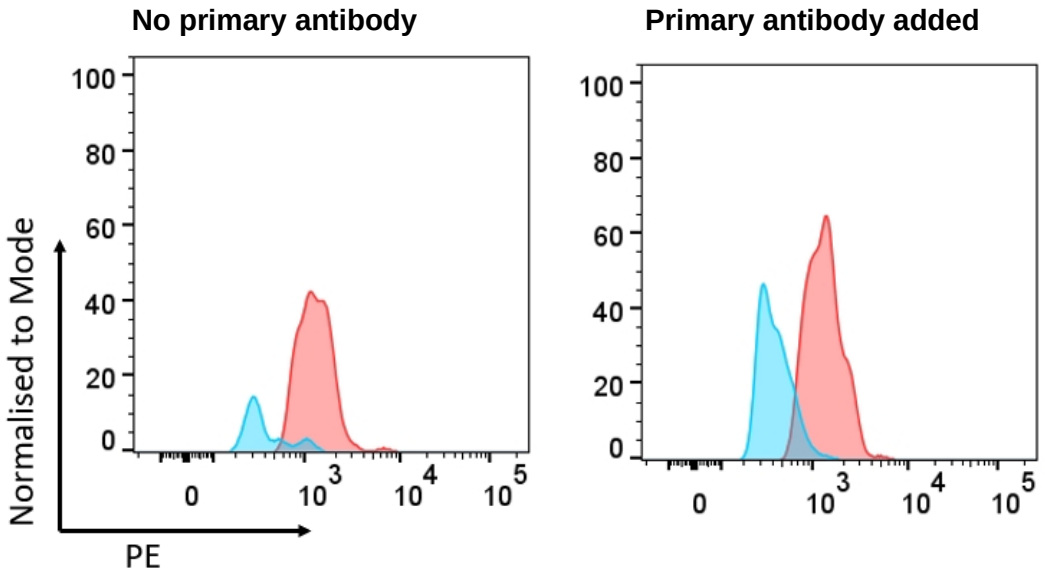

Figure 32: Dead Jurkat T cells have a higher level of autofluorescence. The level of PE fluorescence for dead (pink) or live cells (blue) are plotted. A total of 250 0000 cells was used. The cells were not stained with a secondary antibody labelled with PE.

To determine the extent of PE signal we compared PE fluorescence from live or dead cells without including any PE-labelled secondary antibody. No PE signal should be observed in this case. Dead cells had considerably higher PE signal compared to live cells (*Figure 32)*. Therefore, a decision to gate only on live cells was made, as dead cells are highly auto fluorescent and yield inaccurate results.

Next, we tested the eight monoclonal antibodies on the TCR-engineered Jurkat T cell line to determine which antibody had higher specificity for the kiif.tb CDR3α sequence (*Figure 33*). Despite the suboptimal viability of our Jurkat T cell line, observed consistently whether we used thawed cells or fresh cells from culture, we observed that some of the antibody clones bound the Jurkat T cell line (*Figure 34)*.

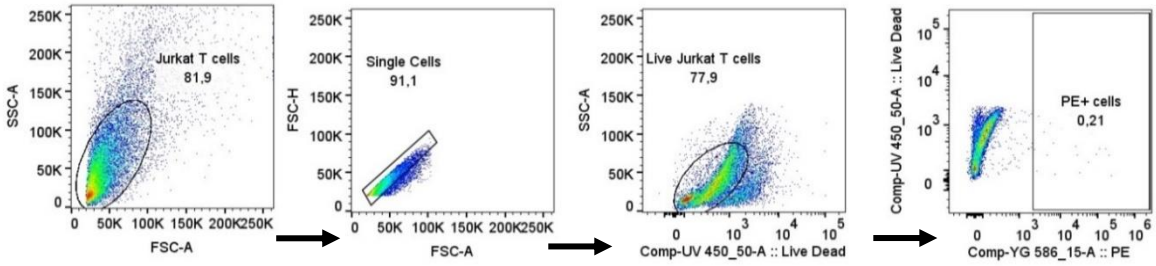

Figure 33: The gating strategy used to determine the frequencies of kiif.tb T cells identified by each monoclonal antibody. A population of Jurkat T cells was first identified and then followed by single cells. Then a population of live Jurkat T cells was identified and lastly a population of Jurkat T cells were the kiif.tb sequence was identified by the different antibodies. A total of 700 000 cells were used to test frequencies of cells binding each clone.

In this experiment, we used only a single negative control, where we did not add the primary antibody but did add the secondary antibody to determine the level of nonspecific signal from the secondary antibody alone. However, we did not include another important negative control: adding the primary antibody without adding the secondary antibody. This control would have shown the level of PE signal due to the primary antibody alone. As anticipated, Jurkat T cells that were not stained with any primary antibody but were stained with the secondary antibody (PE), which recognises the primary antibody, demonstrated low frequencies of cells that were PE positive (*Figure 34)*. This served as a negative control to assess nonspecific binding (background noise). mAb39A9D4 resulted in the highest frequencies of PE+ cells and was selected as the antibody to use on PBMCs to identify kiif.tb T cells.

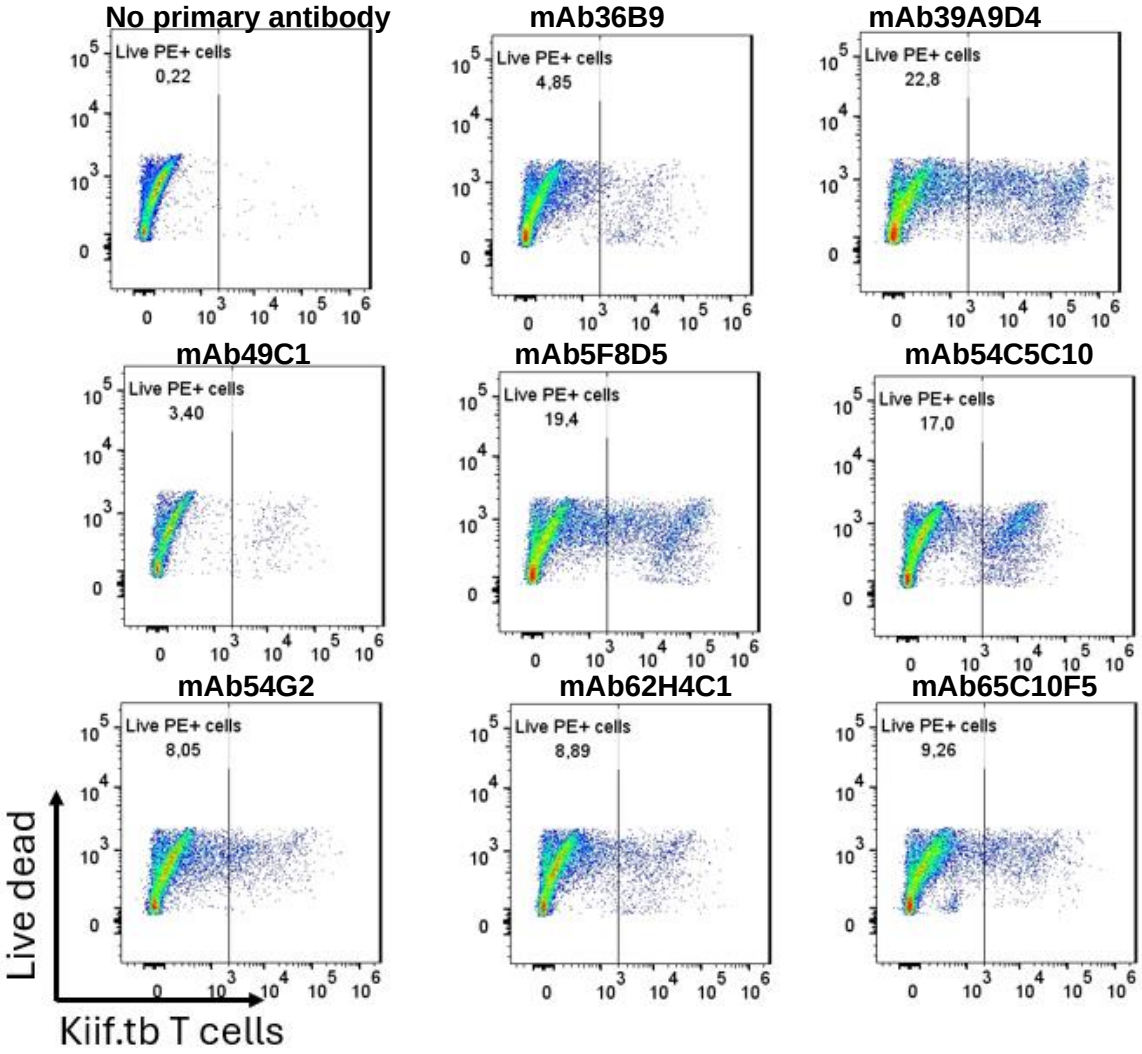

Figure 34: Frequencies of kiif.tb T cells binding to each of the clones. A total of 700 000 cells were used to test frequencies of cells binding each antibody. The negative control was included to determine unspecific binding.

3.4.5 Identification of optimal secondary antibody volume enabling detection of kiif.tb T Cells with minimal background signal

We then assessed the capability of the selected monoclonal antibody (mAb39A9D4) to bind to kiif.tb T cells in PBMCs from various donors (*Figure 35)*. This was done to determine whether the antibody could identify kiif.tb T cells when they are expected to be present at lower frequencies, unlike when using a kiif.tb expressing Jurkat T cell line.

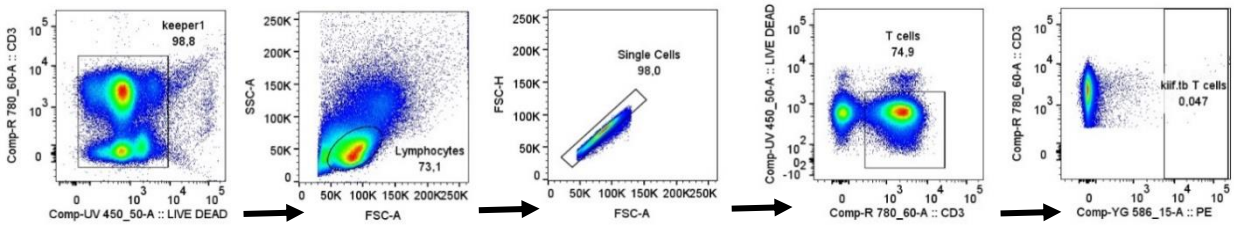

Figure 35: The gating strategy used to determine the frequencies of kiif.tb T cells in PBMCs of different donors. A keeper gate was included to remove debris, then a population of lymphocytes was identified, followed by a population of single cells. Next, live cells were identified, followed by kiif.tb T cells. A threshold of 30 000 on the FSC-A was used to avoid acquiring debris.

The manufacturer's recommended volume for the secondary antibody of 2µl, appeared to be too high because we did not see clear resolution of kiif.tb T cells from other T cells (*Figure 36*). Additionally, in the negative control, where no primary antibody was present but only stained with the secondary antibody (PE), we observed a high frequency of T cells positive for PE. This observation indicated unspecific binding by the PE-labelled secondary antibody.

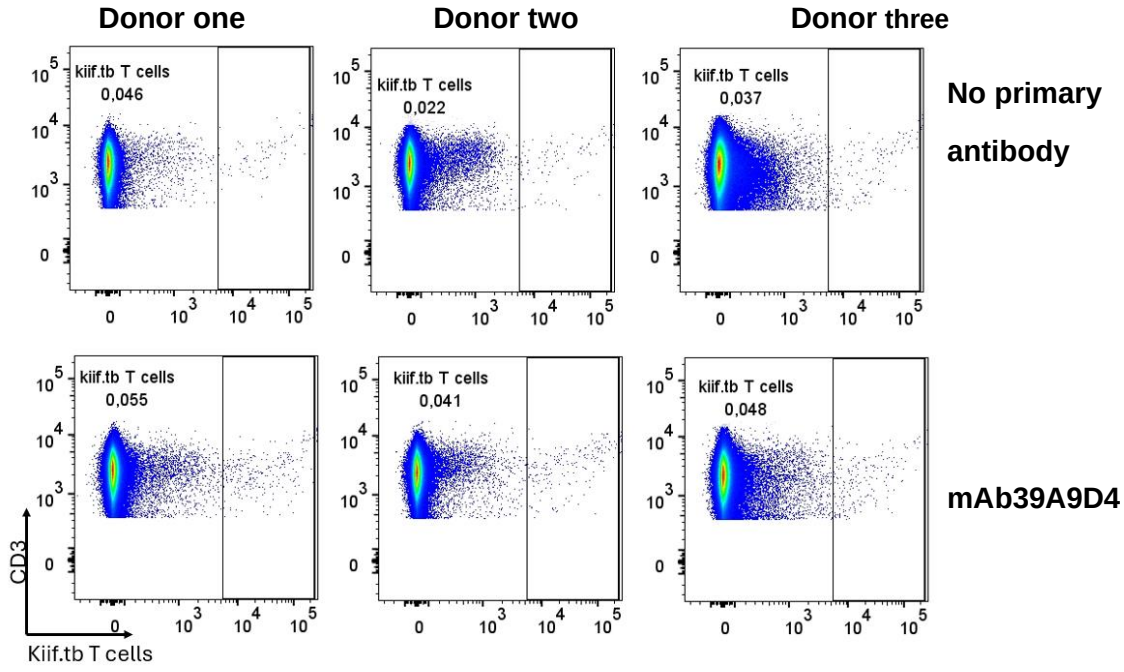

Figure 36: Frequencies of kiif.tb T cells in PBMCs of different donors detected using 39A9D4 antibody. A total of a million cells was used for each donor and each condition (No primary antibody added and when primary antibody is added). The negative control was included to determine non-specific binding

Following this, we then performed a two-fold titration of the secondary antibody (PE), to identify the optimal staining volume We performed this titration under two conditions: PBMCs alone, given the low abundance of kiif.tb T cells and PBMCs spiked with kiif.tb-expressing Jurkat T cells. These conditions allowed us to identify a volume that could discriminate between negative and positive populations, in both conditions where kiif.tb T cells are present in low abundances and/or higher abundances (*Figure 37*). Additionally, we also had two negative controls. The first one was where we did not add the primary antibody but added the secondary antibody to check for nonspecific binding. The second negative control was where we added the primary antibody but did not add the secondary antibody. We did not expect to detect a positive signal in this case, as the signal comes from the secondary antibody. Our objective was to determine a volume that allows clear resolution between negative (other T cells) and positive populations (kiif.tb T cells) in the spiked condition as well as in PBMCs because we wished to observe clear kiif.tb T cell populations in our PBMC samples.

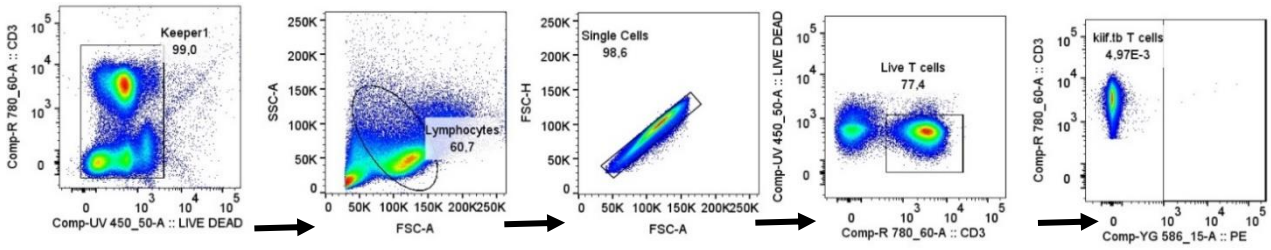

Figure 37: The gating strategy used to determine the optimal titre for the Secondary antibody (PE). A population of lymphocytes and Jurkat T cells was first identified, then a population of single cells. The FSC-A and SSC-A values of PBMC and Jurkat cells were different so the gate was placed this way to be able to detect both PMBC and Jurkat T cells that have been spiked in. Then a population of single cells. Next, live cells were identified, followed by kiif.tb T cells (pink plot). A threshold of 30 000 on the FSC-A was used to avoid acquiring debris.

We selected 0.30µl of the secondary antibody, because this volume resulted in separation of the negative and positive PE populations, while maintaining a low background level of PE in the no-primary antibody control, particularly in the experimental condition with the spiked kiif.tb cells (*Figure 38A&B*). Additionally, at this volume an increase in the frequency of kiif.tb T cells in PBMCs was observed. Although an increase in the frequencies of kiif.tb T cells was noted when higher volumes were used, we were worried that we might also see an increase in nonspecific binding in

the negative control. This volume (0.30µl) was a compromise to limit nonspecific binding but still detect kiif.tb T cells (*Figure 38A&B*).

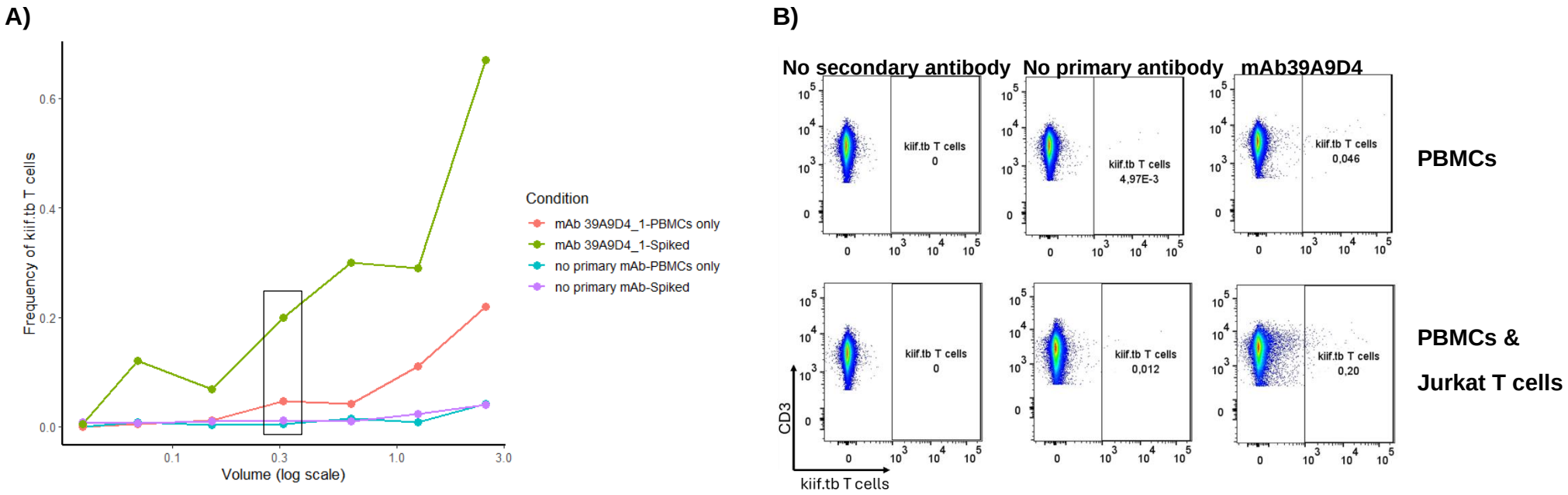

Figure 38: Optimal Secondary antibody (PE) allows detection of frequencies of kiif.tb T cells and has minimal background noise. A two-fold dilution was performed, starting from 2.5µl and reducing to 0µl. In the PBMCs only condition, a total of 500,000 cells were used, while in the spiking condition (250,000 PBMCs and 250,000 Jurkat T cells), the total cell count remained the same. **A)** Frequencies of kiif.tb T cells detected at different volumes for the shown conditions. The box shows frequencies of kiif.tb T cells at the chosen volume of 0.30µl across the different conditions. The log scale was used and zero was given a small value of 0.04. **B)** Flow plots for the different conditions at the chosen volume (0.30µl).

However, when we used this volume of secondary antibody on PBMC samples from other donors, we observed some background PE signal in the negative control (no primary antibody condition), which could lead to inaccurate results due to unspecific binding *(Figure 39*). Therefore, we decided to use a secondary antibody volume of 0.15µl, as this volume also showed better discrimination between mAb39A9D4 stained kiif.tb T cells and the no primary antibody control (*Figure 38*). Although this volume was chosen, we were aware of limitations such as detecting fewer kiif.tb T cells, especially in the spiked condition, as we observed a decrease in frequencies using this volume.

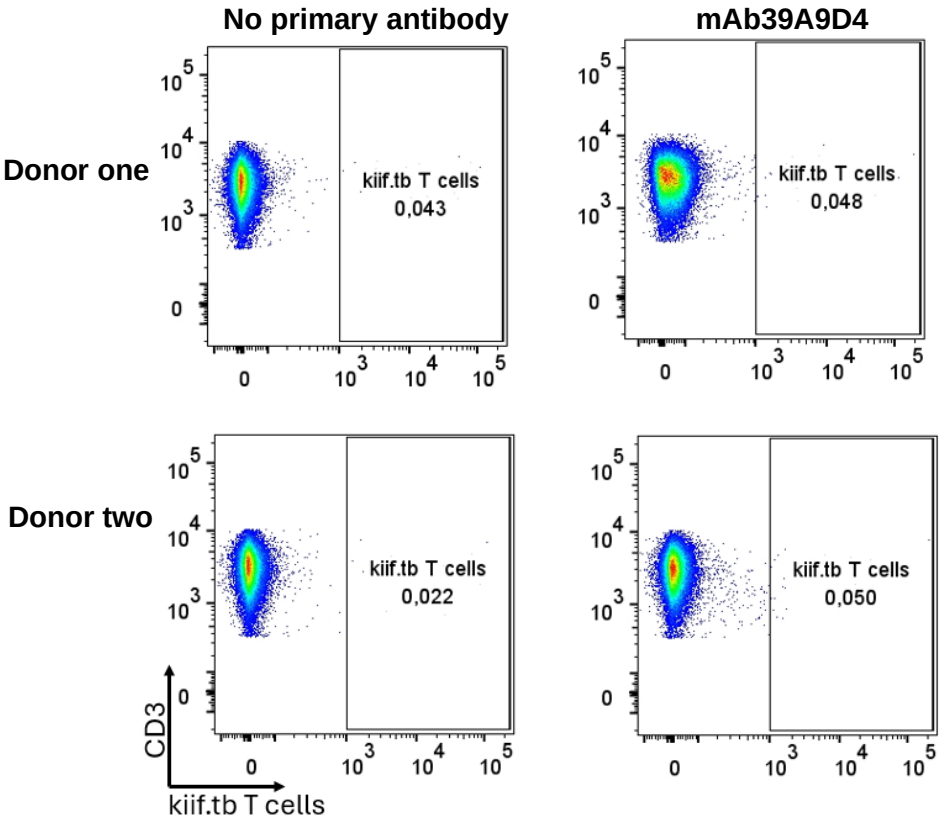

Figure 39: Higher background signal observed in the optimal secondary antibody in other donors. The optimal chosen volume was tested on two donors and a total of a million cells was used in each experimental condition.

3.4.6 Frequencies of T cells expressing the CDR3α sequence in healthy uninfected individuals, healthy infected and active TB individuals are not different

Based on the dPCR results, it appeared that there were no significant differences in frequencies of cells expressing the kiif.tb CDR3a sequence. To address this question using the anti-TCR antibody staining approach. We used monoclonal antibody (mAb39A9D4) to assess the frequencies of kiif.tb T cells in PBMC collected from healthy *M.tb* uninfected, healthy *M.tb* infected individuals, and those with active TB *(Figure 40*).

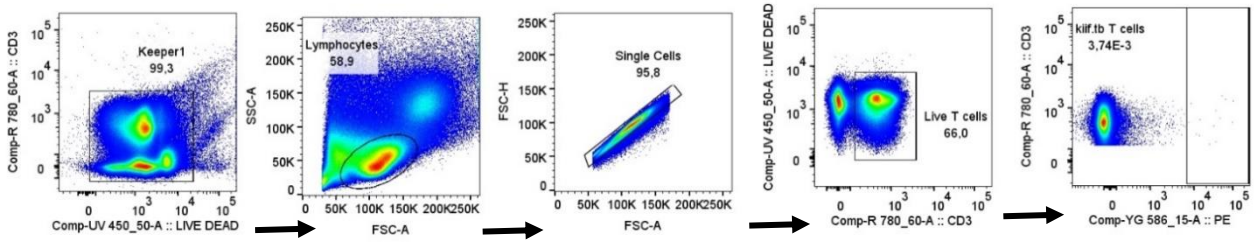

Figure 40: The gating strategy used to determine the frequencies of kiif.tb T cells in QFT-negative, QFT-positive, and active TB individuals. A population of lymphocytes was first identified, then a population of single cells. Next, live T cells were identified, followed by kiif.tb T cells. A threshold of 30 000 on the FSC-A was used to avoid acquiring debris.

Before comparing the differences in the frequencies of kiif.tb T cells between our study cohorts, we first wanted to determine whether the frequencies of kiif.tb cells detected by the primary antibody were higher compared to the negative control in each study group control. Interestingly, samples from QFT-negative and individuals with active TB had higher frequencies of mAb39A9D4-PE+ T cells compared to their corresponding negative controls, which did not contain the primary antibody (p-value = 0.030, 0.050, respectively, *Figure 41A)*. In contrast, in QFT-positive individuals, frequencies detected with the mAb39A9D4-PE antibody were not significantly higher than frequencies observed in the negative controls (p-value = 0.09). We then assessed if the frequencies of mAb39A9D4-PE+ T cells were different in active TB individuals, unhealthy uninfected and *M.tb* infected individuals. There was no significant difference in the frequencies of kiif.tb T cells between our study groups (*Figure 41A)*.

A)

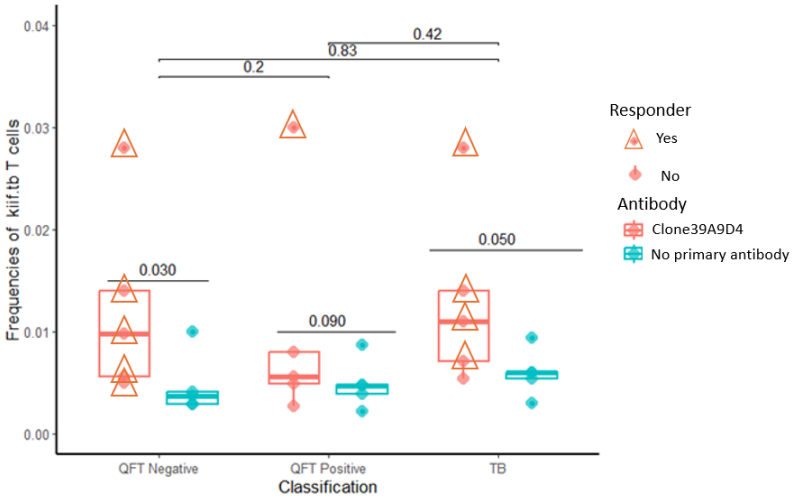

B)

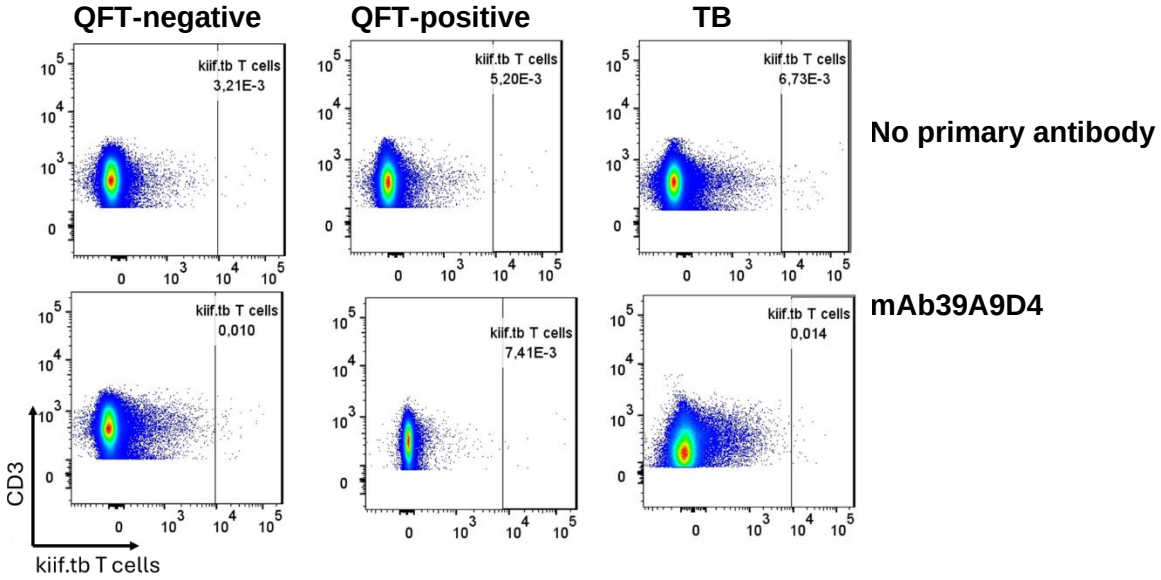

Figure 41: Similar frequencies of kiif.tb T cells between QFT-negative, QFT-positive, and active TB individuals. A) Boxplot comparing the frequencies of kiif.tb T cells in QFT-negative, QFT-positive, and active TB individuals**.** The error bars represent the first quartile (below), the third quartile (upper) and the middle represents the median. Mann-Whitney U test was used to compare groups (significant p-value<0.05). The number of samples analysed is i) QFT-negative = 5, ii) QFT-positive, n = 5, iii) active TB, n = 5. **B)** The representative plots showing from different classifications and the experimental conditions.

Next, we focused on identifying responders, defined as donors having significantly higher frequencies of kiif.tb T cells when stained with the primary antibody (mAb39A9D4) compared to their corresponding negative control (i.e. samples without the primary antibody). We wanted to compare the activation of kiif.tb T cells amongst QFT-negative, QFT-positive, and active TB individuals, and to do this we first had to identify which of the donors had a kiif.tb response. We used Fisher's exact test to compare the number of positive cells vs the total cells in the fully stained vs negative control samples. This approach ensured that we focused on individuals with a significantly higher staining in the presence of the antibody compared to no-antibody controls, aiming to minimize the impact of background signal, which we acknowledge will always be present to some extent. However, it is important to note that this approach only addresses issues of nonspecific binding by the secondary antibody. To also address potential nonspecific binding of the primary antibody, a good control that our study lacked and needed to be added might have been an untransfected Jurkat cell line to check for background staining, as the PE signal could have resulted from nonspecific binding of the primary antibody. All QFT-negative individuals had significantly higher kiif.tb antibody-positive T cells compared to the negative control (*Figure 41A*). Among QFT-positive individuals, only a single individual demonstrated significantly higher kiif.tb antibody-positive T cells, whereas four active TB individuals had higher counts of kiif.tb T cells compared to the negative control (*Figure 41A*).

3.4.7 Higher relative expression and frequencies of kiif.tb T cells expressing HLA-DR in active TB individuals compared to QFT-negative individuals

Due to insufficient responders, defined by a Fisher's exact test, among QFT-positive individuals we could not examine the expression of HLA-DR in kiif.tb T cells because it is not possible to assess phenotypes if the donor does not have a sufficient population of antibody-positive cells. We decided to compare the expression of HLA-DR in QFT-negative and active TB individuals only *(Figure 42).*

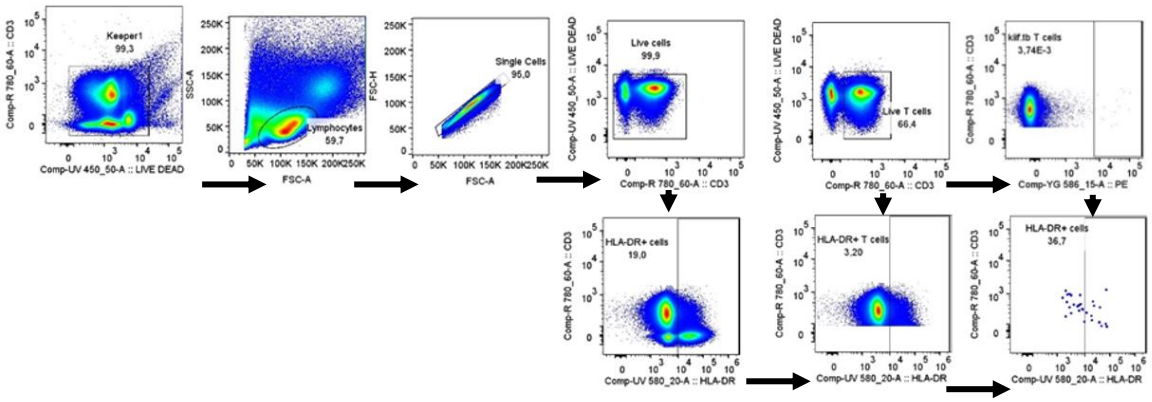

Figure 42: The gating strategy used to determine the frequencies of kiif.tb T cells expressing HLA-DR among QFT-Negative and active TB individuals. A population of lymphocytes was first identified, then a population of single cells. Next, live cells and live T cells were identified, followed by total cells expressing HLA-DR. Then a population of T cells expressing HLA-DR was identified using the threshold set to identify all cells expressing HLA-DR. Lastly, a population of kiif.tb T cells was identified using the HLA-DR threshold. A threshold of 30 000 on the FSC-A was used to avoid acquiring debris.

As expected, active TB individuals had higher frequencies of kiif.tb T cells expressing HLA-DR compared to QFT-negative individuals (p-value = 0.02, *Figure 43A*). Besides examining frequencies, we were also interested in assessing the median fluorescence intensity (MFI), which indicates the relative intensity of HLA-DR expression on kiif.tb T cells. We aimed to determine whether differences in the relative expression of HLA-DR between these two study groups could also be observed. The relative expression of HLA-DR on kiif.tb T cells was also higher in active TB individuals compared to QFT-negative individuals(p-value = 0.03, *Figure 43B)*.

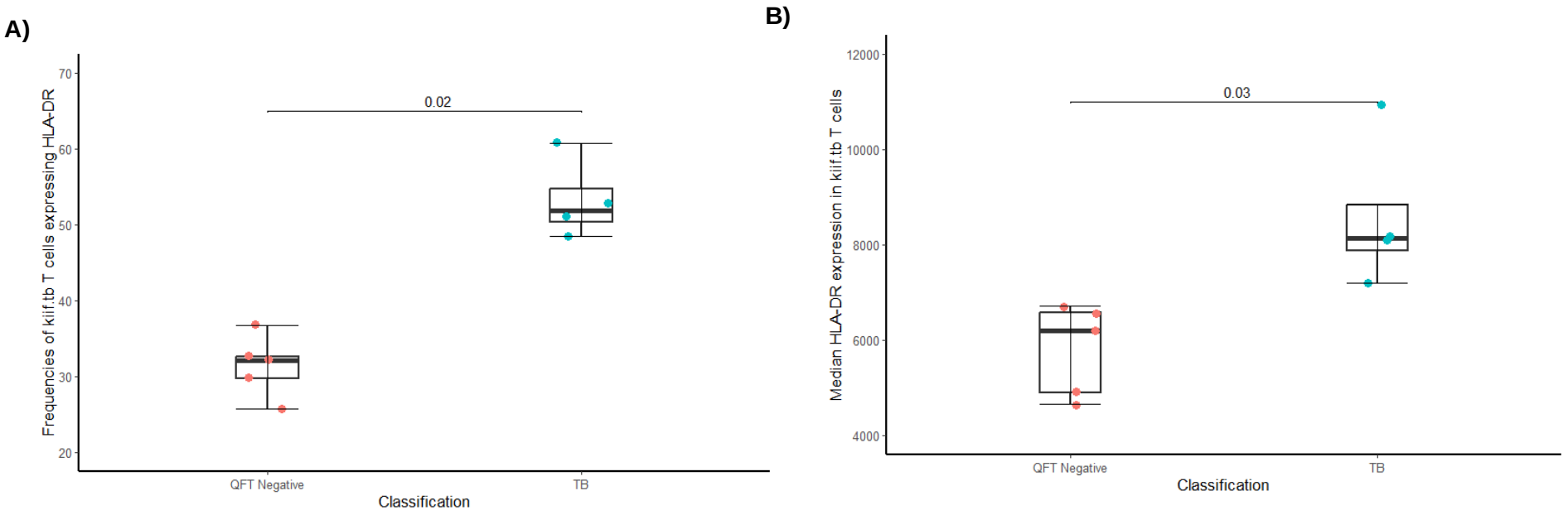

Figure 43: Higher frequencies of kiif.tb expressing HLA-DR and relative expression of HLA-DR among active TB individuals compared to QFT-negative individuals. A boxplot comparing the frequencies of kiif.tb T cells expressing HLA-DR between QFT negative, and active TB individuals. The error bars represent the first quartile (below), the third quartile (upper) and the middle represents the median. Mann-Whitney U test was used to compare groups (significant p-value<0.05). **B)** A boxplot comparing the median of kiif.tb T cells expressing HLA-DR between QFT negative and active TB individuals. The number of samples analysed is i) QFT-negative = 5, ii) active TB, n = 4.

3.4.8 Comparison of the frequencies of bulk T cells expressing HLA-DR and relative expression of HLA-DR among QFT-negative, QFT-positive, and active TB individuals

We also wanted to see if there were any differences in the expression of HLA-DR in bulk T cells as it has been described in the literature (*Figure 44)*.

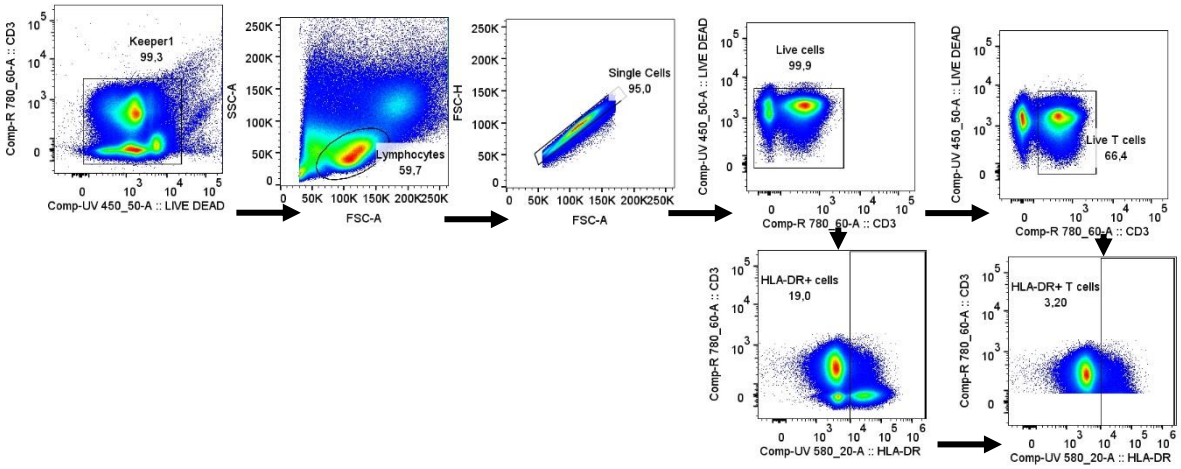

Figure 44: The gating strategy used to determine the frequencies of bulk T cells expressing HLA-DR. A population of lymphocytes was first identified, then a population of single cells. Next, live cells and live T cells were identified, followed by total cells expressing HLA-DR. Then a population of T cells expressing HLA-DR was identified using the threshold set to identify all cells expressing HLA-DR. A threshold of 30 000 on the FSC-A was used to avoid acquiring debris.

Frequencies of bulk T cells expressing HLA-DR were higher in active TB individuals compared to QFT-negative individuals (p-value = 0.05, *Figure 45A*). However, frequencies of bulk T cells expressing HLA-DR were not higher in active TB compared to QFT-positive individuals (p-value = 1). Frequencies of bulk T cells expressing HLA-DR were also higher in QFT-positive compared to QFT-negative individuals (p-value = 0.03, *Figure 45A*). Furthermore, we also measured the MFI and observed a similar trend to that observed in frequencies of bulk T cells expressing HLA-DR. However, the relative differences in intensity of HLA-DR expression in bulk T cells did not reach significance (*Figure 45B*), although the relative intensity of HLA-DR expression in bulk T cells was higher in active TB compared to QFT-negative (p-value = 0.02*, Figure 45B*).

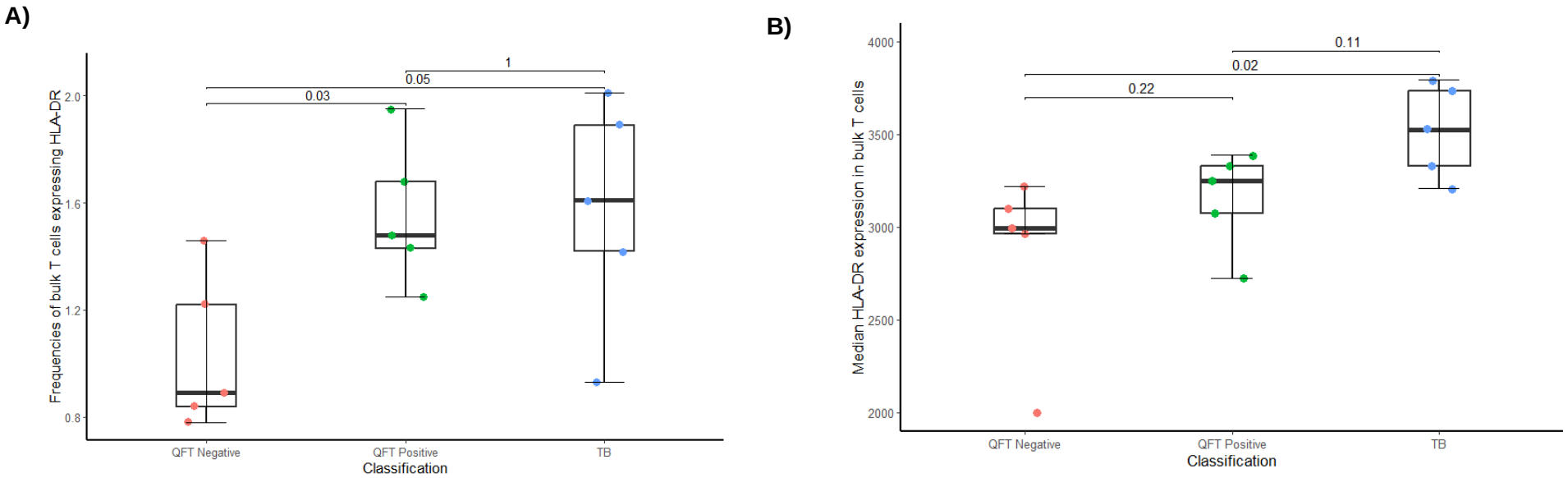

Figure 45: Frequencies of bulk T cells expressing HLA-DR in QFT-negative, QFT-positive, and active TB individuals. **A**) A boxplot comparing the frequencies of bulk T cells expressing HLA-DR between QFT-negative, QFT-positive, and active TB individuals. The error bars represent the first quartile (below), the third quartile (upper) and the middle represents the median. Mann-Whitney U test was used to compare groups (significant p-value<0.05). **B)** A boxplot comparing the median of bulk T cells expressing HLA-DR between QFT-negative, QFT-positive, and active TB individuals. The error bars represent the first quartile (below), the third quartile (upper) and the middle represents the median. Mann-Whitney U test was used to compare groups (significant p-value<0.05). The number of samples is n = 5 in each classification.

3.5 Discussion

The second aim of this study was to develop and optimize methods compatible with flow cytometry to measure the frequencies of T cells expressing the kiif.tb CDR3α sequence and characterise these cells in peripheral blood samples from healthy uninfected individuals, healthy *M.tb* infected individuals, and active TB individuals. Furthermore, we also wanted to examine the activation phenotype, i.e., the frequencies of kiif.tb T cells expressing HLA-DR, within our study cohort.

Our results suggested no significant differences in the frequencies of T cells expressing the CDR3a sequence when measured by dPCR between QFT-negative, QFT-positive, and active TB individuals. However, during the optimization stages, the dPCR assay showed poor correlation of the kiif.tb T cell frequencies measured by dPCR vs bulk TCR sequencing, which is considered the gold standard in measuring the frequencies of certain TCR sequences. This raised questions about the validity of the results or whether there was a sensitivity issue with our dPCR assay.

Therefore, we sought to measure the frequencies of kiif.tb T cells between QFT-negative, QFT-positive, and active TB individuals using flow cytometry. Additionally, we aimed to study the differences in activation phenotypes, as previous studies have shown higher expression of HLA-DR in active TB individuals compared to QFT-positive individuals.[116, 118] We hypothesized that the frequencies of kiif.tb T cells expressing HLA-DR may be higher in active TB compared to QFT-positive individuals.

The PrimeFlow assay, is an in-situ hybridization assay that combines the power of branched-DNA technology with flow cytometry. This assay offers the advantage of simultaneous detection of up to four RNA targets in combination with immunophenotyping for surface and intracellular markers using antibodies. However, in our case, we were interested in detecting a single mRNA target, specifically the kiif.tb CDR3α sequence. This assay used a pair of kiif.tb-specific probes to amplify the detection of kiif.tb mRNA transcripts, achieving 8000-16000-fold signal amplification.

Although in experiments performed by Dr Musvosvi illustrated that the custom PrimeFlow assay was able to detect TCR-engineered Jurkat T cells expressing the kiif.tb CDR3α sequence spiked in PBMCs (*Figure 20,Figure 21*), similar results could not be obtained in our case. Several challenges with the assay were also encountered,

primarily because of loss of the majority of kiif.tb expressing Jurkat T cells during the process, which initially was attributed to the numerous washes involved.

However, upon investigating at which stages of the assay cell loss might have occurred, significant cell loss was not observed. The frequencies of live T cells, CD4, and CD8-positive T cells in the tubes subjected to the PrimeFlow assay were not markedly different to those in the control tube, which did not undergo the PrimeFlow assay. Furthermore, the time required to acquire 100,000 events was also examined. Expectedly, the control tube, which only underwent surface and live/dead staining, had the shortest acquisition time, while the tubes that went through the entire procedure had the longest time. These results suggest that cell loss did occur, but we were still able to acquire enough PBMC.

The second challenge encountered was regarding the viability of the TCR-engineered Jurkat T cells. A significant portion of our cells appeared to be dead, based on staining with our amine group-binding viability dye. Despite our efforts to grow the cells and use Jurkat cells from fresh culture, the viability did not improve. A possible reason for the observed cell death, confirmed by staining with trypan blue and a viability dye, could be the number of passages the cell line underwent. There is a possibility that the cells had reached the replicative senescence stage, where they lost their ability to divide and eventually died.

The viability issue presented a challenge as these cells served as positive controls and were crucial to demonstrating the specificity of the assay in detecting kiif.tb T cells. With dead cells, it became increasingly difficult to showcase the assay's specificity because the cells were dying. Future optimization can look into creating a new kiif.tb clone (i.e., cloning within the kiif.tb clone), cloning the kiif.tb into primary T cells using CRISPR-Cas9, or using a T cell line with better stability than the Jurkat T cell line, such as SUP-T1.

In addition, the frequencies of kiif.tb T cells detected in PBMCs were low, and the resolution was suboptimal when we used the PrimeFlow assay. A possible reason for the poor sensitivity might be that the recommended concentration of the Fixation buffer II used prevented amplification, as demonstrated in some studies to affect mRNA amplification. Henriquez *et al*. demonstrated that loss of Early B cell Factor 1 mRNA amplification was observed after fixing with Fixation buffer II. [119] The loss of Early B

cell Factor 1 was recovered by reducing the concentration of the buffer by half or fixing the cells with the recommended concentration but incubating for half the stated time. These techniques might be adapted in future work to optimize the PrimeFlow assay. Furthermore, issues of poor resolution were also observed in the CD4 and CD3 staining. Initially, it was attributed to the majority of our Jurkat T cells being dead, possibly resulting in downregulated CD4 and CD3 expression. However, even in viable PBMCs, the same poor staining quality was observed. During the optimization of antibody titres, incubation stages at 40°C, required for the PrimeFlow protocol, were not included, and it was clear that incubation at 40°C appear to have affected staining.

After performing titrations, we identified optimal antibody titres. However, the staining quality was still not optimal, especially staining after the PrimeFlow assay. This suggests that the CD3 and CD4 surface receptors may be affected during the incubation stages. Surprisingly, CD8 staining remained good and was not significantly affected by the incubation steps. Considering the challenges mentioned above, we thought a more standard flow assay using custom antibodies would be better.

To overcome these challenges a switch to the use of custom monoclonal antibodies specific for the kiif.tb CDR3α was made. Monoclonal antibodies were generated from mice immunized with either shorter or longer kiif.tb peptide sequence. Both kiif.tb peptide sequences were conjugated to keyhole limpet hemocyanin. This conjugation was done to enhance immunogenicity by specifically targeting the recognition of the kiif.tb CDR3a sequence.

Aware of the viability concerns with Jurkat T cells and the potential autofluorescence from dead cells due to the breakdown of cellular products such as flavins or ROS[120], we observed a shift in the median fluorescence intensity for PE in dead Jurkat T cells compared to live cells, emphasizing the challenge of determining whether the PE signal was due to antibody binding or autofluorescence. We therefore decided to gate only on live cells to avoid any false PE signal when testing the eight monoclonal antibodies to determine which antibody had the highest specificity for kiif.tb expressing Jurkat T cells.

Similar findings to the dPCR assay were observed when using monoclonal antibodies with flow cytometry, as there were no significant differences in the frequencies of kiif.tb T cells among QFT-negative, QFT-positive, and active TB individuals.

Unfortunately, I did not have sufficient time to further investigate each of the possible challenges to further optimise the assay to detect kiif.tb T cells. However, it should be noted that there are several additional avenues for exploring and further optimising the assay. Further titrations of the secondary antibody are needed to determine the optimal volume. It would be useful to conjugate the primary antibody with a fluorophore to avoid the need for two-step staining and decrease the background signal issues observed when using a secondary antibody. Another approach that may improve the performance is additional purification of the monoclonal antibody preparation and increasing the concentration.

Previous studies have indicated that T cells in individuals with active TB express higher levels of HLA-DR compared to those with *M.tb* infection.[116] It was thought that similar differences may be observed in the activation phenotypes of kiif.tb T cells between QFT-negative, QFT-positive, and active TB individuals.

To study the activation phenotypes in kiif.tb T cells, we first had to identify which donors had sufficient numbers of kiif.tb T cells to allow assessment of HLA-DR expression. We compared the proportion of PE+ T cells when PBMC were stained with our custom primary antibody, mAba39AD4, with the proportion of PE+ T cells when cells were not stained with a primary antibody. All five QFT-negative donors and four active TB donors had detectable kiif.tb T cells, whereas only one QFT-positive donor had detectable kiif.tb T cells. Therefore, we did not compare the expression of HLA-DR in kiif.tb T cells amongst QFT-positive individuals because, without differences between the antibody and the negative control, we might compare cells that were positive for PE but are not kiif.tb T cells. This further highlights the need to optimise the secondary antibody volume so that if allows for clear separation of negative and positive populations. As expected, individuals with active TB had higher frequencies of kiif.tb T cells expressing HLA-DR compared to QFT-negative individuals. Not only were the frequencies different, but the median fluorescence intensity of HLA-DR in kiif.tb T cells were higher. Consistent with this, we also observed that the median expression of HLA-DR in kiif.tb T cells was higher in active TB individuals compared to QFT-negative individuals.

As previous studies have revealed that T cells generally express higher levels of HLA-DR expression in individuals with active TB compared to those with *M.tb*

infection.[118,121] We decided to look at bulk T cells to determine if a similar result would be observed. A similar trend was noted, the frequencies of bulk T cells expressing HLA-DR were higher in active TB individuals compared to both QFT-negative and QFT-positive individuals. Furthermore, we observed significantly higher frequencies of HLA-DR+ T cells in persons with active TB compared to and QFT-negative individuals. Additionally, we also observed that QFT-positive individuals had higher frequencies of bulk T cells expressing HLA-DR compared to QFT-negative individuals. However, we noted that some QFT-negative participants had high frequencies of bulk T cells expressing HLA-DR. The high HLA-DR expression by T cells in these QFT-negative participants may be due to other infections that trigger T-cell activation. A study demonstrated increased expression of HLA-DR but not CD38 on CD4 bulk T cells in patients with non-TB respiratory diseases, and this might be due to bystander T cell activation.[116]

It's important to note that we had a limited sample size of only five samples in each group. This was due to time constraints and if we had run more samples, we might have observed different results.

Chapter Four

General Discussion and Conclusions

While T cells are recognized for their pivotal role in infection control, the extent to which the nature of the *M.tb*-specific T cell repertoire or specific T cell clones influences the outcome of *M.tb* infection remains unclear. The original finding that the donor-unrestricted T cell clonotype termed kiif.tb T cells was more abundant in controllers compared to progressors suggested that this T cell might be associated with controlling infection. This study aimed to develop and optimise molecular and immunophenotyping techniques to replicate our prior findings using different quantification methods. Additionally, we wanted to determine if the activation state of these cells was different between healthy uninfected, healthy *M.tb* infected, and persons with active TB.

We used a customized dPCR, which allows absolute quantification, and generated custom monoclonal antibodies to measure the frequencies of kiif.tb T cells between recent and persistent QFT-positive, QFT-negative, and active TB individuals. There were no significant differences in the frequencies of kiif.tb T cells between our study groups, using both the dPCR assay or flow cytometry using customized monoclonal antibodies.

Because of our small sample size and because a single person in the QFT-positive group had sufficient numbers of kiif.tb-positive cells, the expression of HLA-DR in kiif.tb T cells could not be compared to QFT-negative and active TB individuals. Therefore, the proportions of HLA-DR+ kiif.tb cells and the relative surface expression of HLA-DR on kiif.tb cells were investigated between QFT-negative and active TB individuals. The proportion and the relative expression of HLA-DR on kiif.tb T cell were higher in active TB individuals compared to QFT-negative individuals.

Likewise, the expression of HLA-DR on bulk T cells was investigated among our study cohort. Similar trends to those reported in the literature were observed, where individuals with active TB had higher frequencies of bulk T cells expressing HLA-DR compared to QFT-positive individuals. We also observed that QFT-positive individuals had higher frequencies of bulk T cells expressing HLA-DR compared to QFT-negative individuals.

The future work for this project includes several areas of focus. Firstly, it will be important to validate our initial finding of higher kiif.tb T cell frequencies in QFT-positive individuals and those with active TB, using the gold standard of bulk TCR sequencing. It will also be important to determine if QFT-positive have higher frequencies of kiif.tb T cells compared to QFT-negative individuals. In preliminary analysis of bulk TCR sequencing, we observed a trend toward higher frequencies of kiif.tb T cells in QFT-positive individuals compared to QFT-negative individuals ($p = 0.07$). This analysis was performed on a small sample size of ten in each group. We hypothesise that increasing the sample size to 25 per group and performing paired analysis using samples from recent QFT converters, collected before and after the QFT conversion, would provide sufficient statistical power to determine if the frequency of kiif.tb T cells is higher in QFT-positive individuals compared to QFT-negative individuals.

If the results from bulk TCR sequencing highlight significant differences between the study groups, the second area of focus would be to further optimise the custom monoclonal antibodies that specifically bind the kiif.tb CDR3α sequence. We hypothesise that by increasing the antibody purity, concentration, and conjugating a fluorophore directly to the antibody, hence eliminating the need for secondary antibody binding, will improve the performance of the monoclonal antibodies. Once the antibody reagent has been optimized, the subsequent step would be to study the activation state of these kiif.tb T cells and to characterise the transcriptional profile, phenotype, and function of these cells in an expanded sample size of donors per study group.

For example, it will be important to determine whether these cells express CD4 or CD8, or other defining lineage markers. Based on preliminary findings, these cells did not express CD8, but because CD4 was not used in the staining, we could not confidently state that they are CD4-positive cells. Additionally due to the presence of kiif.tb T cells in most individuals confirmed by bulk TCR sequencing, it is thought that these cells are donor unrestricted T cells. We would also like to study their TCR beta chain variable gene usage using antibodies targeting the majority of human class-specific V segments for the TCR β chain (*Supplementary Table 1*). We had titrated the antibodies to do this, but the variable gene usage antibodies were conjugated to PE,

which was the same as our secondary antibody conjugate (*Supplementary Table1, Supplementary Figure 1*). We therefore were not able to complete the optimisation of the assay to complete this due to time constraints. We hypothesize that kiif.tb T cells will have a highly restricted variable gene usage.

Overall, this project laid the foundation for the development of innovative tools in understanding kiif.tb T cells. One particularly intriguing finding was the higher expression of HLA-DR+ on kiif.tb cells, a result that will require further investigation and may be a crucial tool in for a TB biomarker quantifying the activation of *M.tb*-reactive cells. As a foundational project, it has set the stage for subsequent studies, that aim to define the role of kiif.tb T cells.

References

(1) Sulis, G.; Roggi, A.; Matteelli, A.; Raviglione, M. C. Tuberculosis: epidemiology and control. *Mediterr J Hematol Infect Dis* **2014**, *6* (1), e2014070-e2014070. DOI: 10.4084/MJHID.2014.070 PubMed.

(2) World Health, O.; Centers for Disease, C.; Stop, T. B. P.; United States. Agency for International, D.; United Nations Children's, F. *Roadmap for childhood tuberculosis: towards zero deaths*; World Health Organization, 2013.

(3) Delogu, G.; Sali, M.; Fadda, G. The biology of mycobacterium tuberculosis infection. *Mediterr J Hematol Infect Dis* **2013**, *5* (1), e2013070-e2013070. DOI: 10.4084/MJHID.2013.070 PubMed.

(4) Newton, S. M.; Brent, A. J.; Anderson, S.; Whittaker, E.; Kampmann, B. Paediatric tuberculosis. *Lancet Infect Dis* **2008**, *8* (8), 498-510. DOI: 10.1016/S1473-3099(08)70182-8 PubMed.

(5) Dinkele, R.; Gessner, S.; McKerry, A.; Leonard, B.; Leukes, J.; Seldon, R.; Warner, D. F.; Wood, R. Aerosolization of Mycobacterium tuberculosis by Tidal Breathing. *Am J Respir Crit Care Med* **2022**, *206* (2), 206-216. DOI: 10.1164/rccm.202110-2378OC From NLM.

(6) Thacker, V. V.; Dhar, N.; Sharma, K.; Barrile, R.; Karalis, K.; McKinney, J. D. A lung-on-chip model of early Mycobacterium tuberculosis infection reveals an essential role for alveolar epithelial cells in controlling bacterial growth. *Elife* **2020**, *9*. DOI: 10.7554/eLife.59961 From NLM.

(7) Chandra, P.; Grigsby, S. J.; Philips, J. A. Immune evasion and provocation by Mycobacterium tuberculosis. *Nat Rev Microbiol* **2022**, *20* (12), 750-766. DOI: 10.1038/s41579-022-00763-4 From NLM.

(8) Ramos, S.; Gaio, R.; Ferreira, F.; Leal, J. P.; Martins, S.; Santos, J. V.; Carvalho, I.; Duarte, R. Tuberculosis in children from diagnosis to decision to treat. *Revista portuguesa de pneumologia* **2017**, *23* (6), 317-322. DOI: 10.1016/j.rppnen.2017.06.004 From NLM.

(9) Lee, J. Y. Diagnosis and treatment of extrapulmonary tuberculosis. *Tuberc Respir Dis (Seoul)* **2015**, *78* (2), 47-55. DOI: 10.4046/trd.2015.78.2.47 PubMed.

(10) Campbell, I. A.; Bah-Sow, O. Pulmonary tuberculosis: diagnosis and treatment. *BMJ* **2006**, *332* (7551), 1194-1197. DOI: 10.1136/bmj.332.7551.1194 PubMed.

(11) Yatim, K. M.; Lakkis, F. G. A brief journey through the immune system. *Clinical journal of the American Society of Nephrology : CJASN* **2015**, *10* (7), 1274-1281. DOI: 10.2215/cjn.10031014 From NLM.

(12) Abbas, A. K.; Lichtman, A. H.; Pillai, S.; Baker, D. L.; Baker, A. *Basic immunology : functions and disorders of the immune system*, Fifth edition. ed.; Studentconsult; Elsevier, 2016.

(13) Warrington, R.; Watson, W.; Kim, H. L.; Antonetti, F. R. An introduction to immunology and immunopathology. *Allergy, asthma, and clinical immunology : official journal of the Canadian Society of Allergy and Clinical Immunology* **2011**, *7 Suppl 1* (Suppl 1), S1. DOI: 10.1186/1710-1492-7-s1-s1 From NLM.

(14) Turvey, S. E.; Broide, D. H. Innate immunity. *The Journal of allergy and clinical immunology* **2010**, *125* (2 Suppl 2), S24-32. DOI: 10.1016/j.jaci.2009.07.016 From NLM.

(15) Ganz, T. Antimicrobial polypeptides in host defense of the respiratory tract. *J Clin Invest* **2002**, *109* (6), 693-697. DOI: 10.1172/JCI15218 PubMed.

(16) Schauber, J.; Gallo, R. L. Antimicrobial peptides and the skin immune defense system. *The Journal of allergy and clinical immunology* **2008**, *122* (2), 261-266. DOI: 10.1016/j.jaci.2008.03.027 From NLM.

(17) Strbo, N.; Yin, N.; Stojadinovic, O. Innate and Adaptive Immune Responses in Wound Epithelialization. *Advances in wound care* **2014**, *3* (7), 492-501. DOI: 10.1089/wound.2012.0435 From NLM.

(18) Mills, C. D. M1 and M2 Macrophages: Oracles of Health and Disease. *Crit Rev Immunol* **2012**, *32* (6), 463-488. DOI: 10.1615/critrevimmunol.v32.i6.10 From NLM.

(19) Guirado, E.; Schlesinger, L. S.; Kaplan, G. Macrophages in tuberculosis: friend or foe. *Seminars in immunopathology* **2013**, *35* (5), 563-583. DOI: 10.1007/s00281-013-0388-2 From NLM.

(20) Souza-Fonseca-Guimaraes, F.; Adib-Conquy, M.; Cavaillon, J. M. Natural killer (NK) cells in antibacterial innate immunity: angels or devils? *Mol Med* **2012**, *18* (1), 270-285. DOI: 10.2119/molmed.2011.00201 From NLM.

(21) Hilda, J. N.; Das, S.; Tripathy, S. P.; Hanna, L. E. Role of neutrophils in tuberculosis: A bird's eye view. *Innate Immun* **2020**, *26* (4), 240-247. DOI: 10.1177/1753425919881176 From NLM.
(22) Muefong, C. N.; Sutherland, J. S. Neutrophils in Tuberculosis-Associated Inflammation and Lung Pathology. *Frontiers in immunology* **2020**, *11*, 962. DOI: 10.3389/fimmu.2020.00962 From NLM.
(23) Brinkmann, V.; Reichard, U.; Goosmann, C.; Fauler, B.; Uhlemann, Y.; Weiss, D. S.; Weinrauch, Y.; Zychlinsky, A. Neutrophil extracellular traps kill bacteria. *Science* **2004**, *303* (5663), 1532-1535. DOI: 10.1126/science.1092385 From NLM.
(24) Howard, C. J.; Charleston, B.; Stephens, S. A.; Sopp, P.; Hope, J. C. The role of dendritic cells in shaping the immune response. *Animal health research reviews* **2004**, *5* (2), 191-195. DOI: 10.1079/ahr200468 From NLM.
(25) Bonilla, F. A.; Oettgen, H. C. Adaptive immunity. *The Journal of allergy and clinical immunology* **2010**, *125* (2 Suppl 2), S33-40. DOI: 10.1016/j.jaci.2009.09.017 From NLM.
(26) Mak, T. W.; Saunders, M. E.; Jett, B. D. Primer to The Immune Response: Second Edition. **2014**, 1-674.
(27) Laydon, D. J.; Bangham, C. R.; Asquith, B. Estimating T-cell repertoire diversity: limitations of classical estimators and a new approach. *Philos Trans R Soc Lond B Biol Sci* **2015**, *370* (1675). DOI: 10.1098/rstb.2014.0291 From NLM.
(28) Souter, M. N. T.; Eckle, S. B. G. Biased MAIT TCR Usage Poised for Limited Antigen Diversity? *Frontiers in immunology* **2020**, *11*, 1845. DOI: 10.3389/fimmu.2020.01845 From NLM.
(29) Krangel, M. S. Mechanics of T cell receptor gene rearrangement. *Curr Opin Immunol* **2009**, *21* (2), 133-139. DOI: 10.1016/j.coi.2009.03.009 From NLM.
(30) Grossman, W. J.; Verbsky, J. W.; Barchet, W.; Colonna, M.; Atkinson, J. P.; Ley, T. J. Human T regulatory cells can use the perforin pathway to cause autologous target cell death. *Immunity* **2004**, *21* (4), 589-601. DOI: 10.1016/j.immuni.2004.09.002 From NLM.
(31) Ogongo, P.; Steyn, A. J.; Karim, F.; Dullabh, K. J.; Awala, I.; Madansein, R.; Leslie, A.; Behar, S. M. Differential skewing of donor-unrestricted and γδ T cell repertoires in tuberculosis-infected human lungs. *J Clin Invest* **2020**, *130* (1), 214-230. DOI: 10.1172/jci130711 From NLM.
(32) Greenaway, H. Y.; Ng, B.; Price, D. A.; Douek, D. C.; Davenport, M. P.; Venturi, V. NKT and MAIT invariant TCRα sequences can be produced efficiently by VJ gene recombination. *Immunobiology* **2013**, *218* (2), 213-224. DOI: https://doi.org/10.1016/j.imbio.2012.04.003.
(33) Andersen, M. H.; Schrama, D.; Thor Straten, P.; Becker, J. C. Cytotoxic T cells. *The Journal of investigative dermatology* **2006**, *126* (1), 32-41. DOI: 10.1038/sj.jid.5700001 From NLM.
(34) Szabo, S. J.; Sullivan, B. M.; Stemmann, C.; Satoskar, A. R.; Sleckman, B. P.; Glimcher, L. H. Distinct effects of T-bet in TH1 lineage commitment and IFN-gamma production in CD4 and CD8 T cells. *Science* **2002**, *295* (5553), 338-342. DOI: 10.1126/science.1065543 From NLM.
(35) Pai, S. Y.; Truitt, M. L.; Ho, I. C. GATA-3 deficiency abrogates the development and maintenance of T helper type 2 cells. *Proceedings of the National Academy of Sciences of the United States of America* **2004**, *101* (7), 1993-1998. DOI: 10.1073/pnas.0308697100 From NLM.
(36) Granato, A.; Hayashi, E. A.; Baptista, B. J.; Bellio, M.; Nobrega, A. IL-4 regulates Bim expression and promotes B cell maturation in synergy with BAFF conferring resistance to cell death at negative selection checkpoints. *Journal of immunology (Baltimore, Md. : 1950)* **2014**, *192* (12), 5761-5775. DOI: 10.4049/jimmunol.1300749 From NLM.
(37) Zhu, J.; Yamane, H.; Cote-Sierra, J.; Guo, L.; Paul, W. E. GATA-3 promotes Th2 responses through three different mechanisms: induction of Th2 cytokine production, selective growth of Th2 cells and inhibition of Th1 cell-specific factors. *Cell Res* **2006**, *16* (1), 3-10. DOI: 10.1038/sj.cr.7310002 From NLM.
(38) Tesmer, L. A.; Lundy, S. K.; Sarkar, S.; Fox, D. A. Th17 cells in human disease. *Immunol Rev* **2008**, *223*, 87-113. DOI: 10.1111/j.1600-065X.2008.00628.x From NLM.
(39) Pelletier, M.; Maggi, L.; Micheletti, A.; Lazzeri, E.; Tamassia, N.; Costantini, C.; Cosmi, L.; Lunardi, C.; Annunziato, F.; Romagnani, S.; Cassatella, M. A. Evidence for a cross-talk between human

neutrophils and Th17 cells. *Blood* **2010**, *115* (2), 335-343. DOI: 10.1182/blood-2009-04-216085 From NLM.
(40) Beissert, S.; Schwarz, A.; Schwarz, T. Regulatory T cells. *The Journal of investigative dermatology* **2006**, *126* (1), 15-24. DOI: 10.1038/sj.jid.5700004 From NLM.
(41) Kaplan, M. H. The transcription factor network in Th9 cells. *Seminars in immunopathology* **2017**, *39* (1), 11-20. DOI: 10.1007/s00281-016-0600-2 From NLM.
(42) Jia, L.; Wu, C. The biology and functions of Th22 cells. *Adv Exp Med Biol* **2014**, *841*, 209-230. DOI: 10.1007/978-94-017-9487-9_8 From NLM.
(43) Choi, J.; Diao, H.; Faliti, C. E.; Truong, J.; Rossi, M.; Bélanger, S.; Yu, B.; Goldrath, A. W.; Pipkin, M. E.; Crotty, S. Bcl6 is the nexus transcription factor of T follicular helper cell (TFH) differentiation via a set of repressor-of-repressor gene circuits. *The Journal of Immunology* **2020**, *204* (1_Supplement), 76.75-76.75. DOI: 10.4049/jimmunol.204.Supp.76.5 (acccessed 6/6/2024).
(44) Martin, M. D.; Badovinac, V. P. Defining Memory CD8 T Cell. *Frontiers in immunology* **2018**, *9*, Mini Review. DOI: 10.3389/fimmu.2018.02692.
(45) Mosmann, T. R.; Li, L.; Sad, S. Functions of CD8 T-cell subsets secreting different cytokine patterns. *Semin Immunol* **1997**, *9* (2), 87-92. DOI: 10.1006/smim.1997.0065 From NLM.
(46) Joosten, S. A.; Ottenhoff, T. H. M.; Lewinsohn, D. M.; Hoft, D. F.; Moody, D. B.; Seshadri, C. Harnessing donor unrestricted T-cells for new vaccines against tuberculosis. *Vaccine* **2019**, *37* (23), 3022-3030. DOI: 10.1016/j.vaccine.2019.04.050 From NLM.
(47) Terpstra, M. L.; Remmerswaal, E. B. M.; van der Bom-Baylon, N. D.; Sinnige, M. J.; Kers, J.; van Aalderen, M. C.; Geerlings, S. E.; Bemelman, F. J. Tissue-resident mucosal-associated invariant T (MAIT) cells in the human kidney represent a functionally distinct subset. *Eur J Immunol* **2020**, *50* (11), 1783-1797. DOI: 10.1002/eji.202048644 From NLM.
(48) Lamichhane, R.; Schneider, M.; de la Harpe, S. M.; Harrop, T. W. R.; Hannaway, R. F.; Dearden, P. K.; Kirman, J. R.; Tyndall, J. D. A.; Vernall, A. J.; Ussher, J. E. TCR- or Cytokine-Activated CD8(+) Mucosal-Associated Invariant T Cells Are Rapid Polyfunctional Effectors That Can Coordinate Immune Responses. *Cell Rep* **2019**, *28* (12), 3061-3076.e3065. DOI: 10.1016/j.celrep.2019.08.054 From NLM.
(49) Bhuiyan, T. R.; Rahman, M. A.; Trivedi, S.; Afroz, T.; Al Banna, H.; Hoq, M. R.; Pop, I.; Jensen, O.; Rashu, R.; Uddin, M. I.; et al. Mucosal-Associated Invariant T (MAIT) cells are highly activated in duodenal tissue of humans with Vibrio cholerae O1 infection: A preliminary report. *PLoS Negl Trop Dis* **2022**, *16* (5), e0010411. DOI: 10.1371/journal.pntd.0010411 From NLM.
(50) Lee, Y. J.; Holzapfel, K. L.; Zhu, J.; Jameson, S. C.; Hogquist, K. A. Steady-state production of IL-4 modulates immunity in mouse strains and is determined by lineage diversity of iNKT cells. *Nature immunology* **2013**, *14* (11), 1146-1154. DOI: 10.1038/ni.2731 From NLM.
(51) Tupin, E.; Kinjo, Y.; Kronenberg, M. The unique role of natural killer T cells in the response to microorganisms. *Nat Rev Microbiol* **2007**, *5* (6), 405-417. DOI: 10.1038/nrmicro1657 From NLM.
(52) Brandes, M.; Willimann, K.; Moser, B. Professional antigen-presentation function by human gammadelta T Cells. *Science* **2005**, *309* (5732), 264-268. DOI: 10.1126/science.1110267 From NLM.
(53) Sanz, M.; Mann, B. T.; Ryan, P. L.; Bosque, A.; Pennington, D. J.; Hackstein, H.; Soriano-Sarabia, N. Deep characterization of human γδ T cell subsets defines shared and lineage-specific traits. *Frontiers in immunology* **2023**, *14*, 1148988. DOI: 10.3389/fimmu.2023.1148988 From NLM.
(54) Hong, S.; Zhang, Z.; Liu, H.; Tian, M.; Zhu, X.; Zhang, Z.; Wang, W.; Zhou, X.; Zhang, F.; Ge, Q.; et al. B Cells Are the Dominant Antigen-Presenting Cells that Activate Naive CD4+ T Cells upon Immunization with a Virus-Derived Nanoparticle Antigen. *Immunity* **2018**, *49* (4), 695-708.e694. DOI: https://doi.org/10.1016/j.immuni.2018.08.012.
(55) Tay, C.; Kanellakis, P.; Hosseini, H.; Cao, A.; Toh, B.-H.; Bobik, A.; Kyaw, T. B Cell and CD4 T Cell Interactions Promote Development of Atherosclerosis. *Frontiers in immunology* **2020**, *10*, Original Research. DOI: 10.3389/fimmu.2019.03046.
(56) Alcover, A.; Alarcón, B.; Di Bartolo, V. Cell Biology of T Cell Receptor Expression and Regulation. *Annual review of immunology* **2018**, *36*, 103-125. DOI: 10.1146/annurev-immunol-042617-053429 From NLM.

(57) Lewinsohn, D. A.; Gennaro, M. L.; Scholvinck, L.; Lewinsohn, D. M. Tuberculosis immunology in children: diagnostic and therapeutic challenges and opportunities. *The international journal of tuberculosis and lung disease : the official journal of the International Union against Tuberculosis and Lung Disease* **2004**, *8* (5), 658-674. From NLM.
(58) Takeuchi, A.; Badr Mel, S.; Miyauchi, K.; Ishihara, C.; Onishi, R.; Guo, Z.; Sasaki, Y.; Ike, H.; Takumi, A.; Tsuji, N. M.; et al. CRTAM determines the CD4+ cytotoxic T lymphocyte lineage. *The Journal of experimental medicine* **2016**, *213* (1), 123-138. DOI: 10.1084/jem.20150519 From NLM.
(59) Cooper, A. M. Cell-mediated immune responses in tuberculosis. *Annual review of immunology* **2009**, *27*, 393-422. DOI: 10.1146/annurev.immunol.021908.132703 From NLM.
(60) Thacker, V. V.; Dhar, N.; Sharma, K.; Barrile, R.; Karalis, K.; McKinney, J. D. A lung-on-chip model of early Mycobacterium tuberculosis infection reveals an essential role for alveolar epithelial cells in controlling bacterial growth. *eLife* **2020**, *9*, e59961. DOI: 10.7554/eLife.59961.
(61) Cohen, S. B.; Gern, B. H.; Delahaye, J. L.; Adams, K. N.; Plumlee, C. R.; Winkler, J. K.; Sherman, D. R.; Gerner, M. Y.; Urdahl, K. B. Alveolar Macrophages Provide an Early Mycobacterium tuberculosis Niche and Initiate Dissemination. *Cell Host Microbe* **2018**, *24* (3), 439-446.e434. DOI: 10.1016/j.chom.2018.08.001 From NLM.
(62) Godfrey, D. I.; Uldrich, A. P.; McCluskey, J.; Rossjohn, J.; Moody, D. B. The burgeoning family of unconventional T cells. *Nature immunology* **2015**, *16* (11), 1114-1123. DOI: 10.1038/ni.3298 From NLM.
(63) Griffith, J. W.; Sokol, C. L.; Luster, A. D. Chemokines and chemokine receptors: positioning cells for host defense and immunity. *Annual review of immunology* **2014**, *32*, 659-702. DOI: 10.1146/annurev-immunol-032713-120145 From NLM.
(64) de Martino, M.; Lodi, L.; Galli, L.; Chiappini, E. Immune Response to Mycobacterium tuberculosis: A Narrative Review. *Front Pediatr* **2019**, *7*, 350-350. DOI: 10.3389/fped.2019.00350 PubMed.
(65) Kleinnijenhuis, J.; Oosting, M.; Joosten, L. A.; Netea, M. G.; Van Crevel, R. Innate immune recognition of Mycobacterium tuberculosis. *Clinical & developmental immunology* **2011**, *2011*, 405310. DOI: 10.1155/2011/405310 From NLM.
(66) Podinovskaia, M.; Lee, W.; Caldwell, S.; Russell, D. G. Infection of macrophages with Mycobacterium tuberculosis induces global modifications to phagosomal function. *Cell Microbiol* **2013**, *15* (6), 843-859. DOI: 10.1111/cmi.12092 From NLM.
(67) Lee, H. J.; Woo, Y.; Hahn, T. W.; Jung, Y. M.; Jung, Y. J. Formation and Maturation of the Phagosome: A Key Mechanism in Innate Immunity against Intracellular Bacterial Infection. *Microorganisms* **2020**, *8* (9). DOI: 10.3390/microorganisms8091298 From NLM.
(68) Vergne, I.; Chua, J.; Lee, H. H.; Lucas, M.; Belisle, J.; Deretic, V. Mechanism of phagolysosome biogenesis block by viable Mycobacterium tuberculosis. *Proceedings of the National Academy of Sciences of the United States of America* **2005**, *102* (11), 4033-4038. DOI: 10.1073/pnas.0409716102 From NLM.
(69) Ramachandra, L.; Smialek, J. L.; Shank, S. S.; Convery, M.; Boom, W. H.; Harding, C. V. Phagosomal processing of Mycobacterium tuberculosis antigen 85B is modulated independently of mycobacterial viability and phagosome maturation. *Infection and immunity* **2005**, *73* (2), 1097-1105. DOI: 10.1128/iai.73.2.1097-1105.2005 From NLM.
(70) Ramachandra, L.; Noss, E.; Boom, W. H.; Harding, C. V. Processing of Mycobacterium tuberculosis antigen 85B involves intraphagosomal formation of peptide-major histocompatibility complex II complexes and is inhibited by live bacilli that decrease phagosome maturation. *The Journal of experimental medicine* **2001**, *194* (10), 1421-1432. DOI: 10.1084/jem.194.10.1421 From NLM.
(71) Okamoto Yoshida, Y.; Umemura, M.; Yahagi, A.; O'Brien, R. L.; Ikuta, K.; Kishihara, K.; Hara, H.; Nakae, S.; Iwakura, Y.; Matsuzaki, G. Essential role of IL-17A in the formation of a mycobacterial infection-induced granuloma in the lung. *Journal of immunology (Baltimore, Md. : 1950)* **2010**, *184* (8), 4414-4422. DOI: 10.4049/jimmunol.0903332 From NLM.

(72) Borkute, R. R.; Woelke, S.; Pei, G.; Dorhoi, A. Neutrophils in Tuberculosis: Cell Biology, Cellular Networking and Multitasking in Host Defense. *Int J Mol Sci* **2021**, *22* (9). DOI: 10.3390/ijms22094801 From NLM.
(73) Eum, S. Y.; Kong, J. H.; Hong, M. S.; Lee, Y. J.; Kim, J. H.; Hwang, S. H.; Cho, S. N.; Via, L. E.; Barry, C. E., 3rd. Neutrophils are the predominant infected phagocytic cells in the airways of patients with active pulmonary TB. *Chest* **2010**, *137* (1), 122-128. DOI: 10.1378/chest.09-0903 From NLM.
(74) Corleis, B.; Korbel, D.; Wilson, R.; Bylund, J.; Chee, R.; Schaible, U. E. Escape of Mycobacterium tuberculosis from oxidative killing by neutrophils. *Cell Microbiol* **2012**, *14* (7), 1109-1121. DOI: 10.1111/j.1462-5822.2012.01783.x From NLM.
(75) Ramos-Kichik, V.; Mondragón-Flores, R.; Mondragón-Castelán, M.; Gonzalez-Pozos, S.; Muñiz-Hernandez, S.; Rojas-Espinosa, O.; Chacón-Salinas, R.; Estrada-Parra, S.; Estrada-García, I. Neutrophil extracellular traps are induced by Mycobacterium tuberculosis. *Tuberculosis (Edinb)* **2009**, *89* (1), 29-37. DOI: 10.1016/j.tube.2008.09.009 From NLM.
(76) Ehlers, S. DC-SIGN and mannosylated surface structures of Mycobacterium tuberculosis: a deceptive liaison. *European Journal of Cell Biology* **2010**, *89* (1), 95-101. DOI: https://doi.org/10.1016/j.ejcb.2009.10.004.
(77) Sertl, K.; Takemura, T.; Tschachler, E.; Ferrans, V. J.; Kaliner, M. A.; Shevach, E. M. Dendritic cells with antigen-presenting capability reside in airway epithelium, lung parenchyma, and visceral pleura. *The Journal of experimental medicine* **1986**, *163* (2), 436-451. DOI: 10.1084/jem.163.2.436 From NLM.
(78) Henderson, R. A.; Watkins, S. C.; Flynn, J. L. Activation of human dendritic cells following infection with Mycobacterium tuberculosis. *Journal of immunology (Baltimore, Md. : 1950)* **1997**, *159* (2), 635-643. From NLM.
(79) Morel, C.; Badell, E.; Abadie, V.; Robledo, M.; Setterblad, N.; Gluckman, J. C.; Gicquel, B.; Boudaly, S.; Winter, N. Mycobacterium bovis BCG-infected neutrophils and dendritic cells cooperate to induce specific T cell responses in humans and mice. *Eur J Immunol* **2008**, *38* (2), 437-447. DOI: 10.1002/eji.200737905 From NLM.
(80) Blomgran, R.; Ernst, J. D. Lung neutrophils facilitate activation of naive antigen-specific CD4+ T cells during Mycobacterium tuberculosis infection. *Journal of immunology (Baltimore, Md. : 1950)* **2011**, *186* (12), 7110-7119. DOI: 10.4049/jimmunol.1100001 From NLM.
(81) Flynn, J. L.; Chan, J.; Triebold, K. J.; Dalton, D. K.; Stewart, T. A.; Bloom, B. R. An essential role for interferon gamma in resistance to Mycobacterium tuberculosis infection. *The Journal of experimental medicine* **1993**, *178* (6), 2249-2254. DOI: 10.1084/jem.178.6.2249 From NLM.
(82) Green, A. M.; Difazio, R.; Flynn, J. L. IFN-γ from CD4 T cells is essential for host survival and enhances CD8 T cell function during Mycobacterium tuberculosis infection. *Journal of immunology (Baltimore, Md. : 1950)* **2013**, *190* (1), 270-277. DOI: 10.4049/jimmunol.1200061 From NLM.
(83) Chancellor, A.; White, A.; Tocheva, A. S.; Fenn, J. R.; Dennis, M.; Tezera, L.; Singhania, A.; Elliott, T.; Tebruegge, M.; Elkington, P.; et al. Quantitative and qualitative iNKT repertoire associations with disease susceptibility and outcome in macaque tuberculosis infection. *Tuberculosis* **2017**, *105*, 86-95. DOI: https://doi.org/10.1016/j.tube.2017.04.011.
(84) Khader, S. A.; Bell, G. K.; Pearl, J. E.; Fountain, J. J.; Rangel-Moreno, J.; Cilley, G. E.; Shen, F.; Eaton, S. M.; Gaffen, S. L.; Swain, S. L.; et al. IL-23 and IL-17 in the establishment of protective pulmonary CD4+ T cell responses after vaccination and during Mycobacterium tuberculosis challenge. *Nature immunology* **2007**, *8* (4), 369-377. DOI: 10.1038/ni1449 From NLM.
(85) Cruz, A.; Fraga, A. G.; Fountain, J. J.; Rangel-Moreno, J.; Torrado, E.; Saraiva, M.; Pereira, D. R.; Randall, T. D.; Pedrosa, J.; Cooper, A. M.; Castro, A. G. Pathological role of interleukin 17 in mice subjected to repeated BCG vaccination after infection with Mycobacterium tuberculosis. *The Journal of experimental medicine* **2010**, *207* (8), 1609-1616. DOI: 10.1084/jem.20100265 From NLM.
(86) Stenger, S.; Hanson, D. A.; Teitelbaum, R.; Dewan, P.; Niazi, K. R.; Froelich, C. J.; Ganz, T.; Thoma-Uszynski, S.; Melián, A.; Bogdan, C.; et al. An antimicrobial activity of cytolytic T cells mediated by granulysin. *Science* **1998**, *282* (5386), 121-125. DOI: 10.1126/science.282.5386.121 From NLM.

(87) Jiang, J.; Chen, X.; An, H.; Yang, B.; Zhang, F.; Cheng, X. Enhanced immune response of MAIT cells in tuberculous pleural effusions depends on cytokine signaling. *Scientific Reports* **2016**, *6* (1), 32320. DOI: 10.1038/srep32320.
(88) Paquin-Proulx, D.; Costa, P. R.; Terrassani Silveira, C. G.; Marmorato, M. P.; Cerqueira, N. B.; Sutton, M. S.; O'Connor, S. L.; Carvalho, K. I.; Nixon, D. F.; Kallas, E. G. Latent Mycobacterium tuberculosis Infection Is Associated With a Higher Frequency of Mucosal-Associated Invariant T and Invariant Natural Killer T Cells. *Frontiers in immunology* **2018**, *9*, 1394. DOI: 10.3389/fimmu.2018.01394 From NLM.
(89) Chen, Y.; Bharrhan, S.; Xu, J.; Sharma, T.; Wang, Y.; Salgame, P.; Zhang, J.; Nargan, K.; Steyn, A. J. C.; Maglione, P. J.; Chan, J. B cells promote granulomatous inflammation during chronic Mycobacterium tuberculosis infection in mice. *PLoS Pathog* **2023**, *19* (3), e1011187. DOI: 10.1371/journal.ppat.1011187 From NLM.
(90) Phuah, J.; Wong Eileen, A.; Gideon Hannah, P.; Maiello, P.; Coleman, M. T.; Hendricks Matthew, R.; Ruden, R.; Cirrincione Lauren, R.; Chan, J.; Lin Philana, L.; Flynn JoAnne, L. Effects of B Cell Depletion on Early Mycobacterium tuberculosis Infection in Cynomolgus Macaques. *Infection and immunity* **2016**, *84* (5), 1301-1311. DOI: 10.1128/iai.00083-16 (acccessed 2023/08/28).
(91) du Preez, K.; Seddon, J. A.; Schaaf, H. S.; Hesseling, A. C.; Starke, J. R.; Osman, M.; Lombard, C. J.; Solomons, R. Global shortages of BCG vaccine and tuberculous meningitis in children. *Lancet Glob Health* **2019**, *7* (1), e28-e29. DOI: 10.1016/s2214-109x(18)30474-1 From NLM.
(92) Kaufmann, S. H. E. Vaccination Against Tuberculosis: Revamping BCG by Molecular Genetics Guided by Immunology. **2020**, *11*, Review. DOI: 10.3389/fimmu.2020.00316.
(93) Travieso, T.; Li, J.; Mahesh, S.; Mello, J. D. F. R. E.; Blasi, M. The use of viral vectors in vaccine development. *npj Vaccines* **2022**, *7* (1), 75. DOI: 10.1038/s41541-022-00503-y.
(94) Tameris, M. D.; Hatherill, M.; Landry, B. S.; Scriba, T. J.; Snowden, M. A.; Lockhart, S.; Shea, J. E.; McClain, J. B.; Hussey, G. D.; Hanekom, W. A.; et al. Safety and efficacy of MVA85A, a new tuberculosis vaccine, in infants previously vaccinated with BCG: a randomised, placebo-controlled phase 2b trial. *Lancet* **2013**, *381* (9871), 1021-1028. DOI: 10.1016/s0140-6736(13)60177-4 From NLM.
(95) Kochi, A. The global tuberculosis situation and the new control strategy of the World Health Organization. 1991. *Bulletin of the World Health Organization* **2001**, *79* (1), 71-75. From NLM.
(96) Salamon, H.; Kato-Maeda, M.; Small, P. M.; Drenkow, J.; Gingeras, T. R. Detection of deleted genomic DNA using a semiautomated computational analysis of GeneChip data. *Genome research* **2000**, *10* (12), 2044-2054. DOI: 10.1101/gr.gr-1529r From NLM.
(97) Skeiky, Y. A. W.; Sadoff, J. C. Advances in tuberculosis vaccine strategies. *Nature Reviews Microbiology* **2006**, *4* (6), 469-476. DOI: 10.1038/nrmicro1419.
(98) Martín, C.; Marinova, D.; Aguiló, N.; Gonzalo-Asensio, J. MTBVAC, a live TB vaccine poised to initiate efficacy trials 100 years after BCG. *Vaccine* **2021**, *39* (50), 7277-7285. DOI: https://doi.org/10.1016/j.vaccine.2021.06.049.
(99) Arbues, A.; Aguilo, J. I.; Gonzalo-Asensio, J.; Marinova, D.; Uranga, S.; Puentes, E.; Fernandez, C.; Parra, A.; Cardona, P. J.; Vilaplana, C.; et al. Construction, characterization and preclinical evaluation of MTBVAC, the first live-attenuated M. tuberculosis-based vaccine to enter clinical trials. *Vaccine* **2013**, *31* (42), 4867-4873. DOI: https://doi.org/10.1016/j.vaccine.2013.07.051.
(100) Tameris, M.; Mearns, H.; Penn-Nicholson, A.; Gregg, Y.; Bilek, N.; Mabwe, S.; Geldenhuys, H.; Shenje, J.; Luabeya, A. K. K.; Murillo, I.; et al. Live-attenuated Mycobacterium tuberculosis vaccine MTBVAC versus BCG in adults and neonates: a randomised controlled, double-blind dose-escalation trial. *The Lancet Respiratory Medicine* **2019**, *7* (9), 757-770. DOI: https://doi.org/10.1016/S2213-2600(19)30251-6.
(101) Nieuwenhuizen, N. E.; Kulkarni, P. S.; Shaligram, U.; Cotton, M. F.; Rentsch, C. A.; Eisele, B.; Grode, L.; Kaufmann, S. H. E. The Recombinant Bacille Calmette-Guérin Vaccine VPM1002: Ready for Clinical Efficacy Testing. *Frontiers in immunology* **2017**, *8*, 1147. DOI: 10.3389/fimmu.2017.01147 From NLM.

(102) Grode, L.; Ganoza, C. A.; Brohm, C.; Weiner, J.; Eisele, B.; Kaufmann, S. H. E. Safety and immunogenicity of the recombinant BCG vaccine VPM1002 in a phase 1 open-label randomized clinical trial. *Vaccine* **2013**, *31* (9), 1340-1348. DOI: https://doi.org/10.1016/j.vaccine.2012.12.053.
(103) Tait, D. R.; Hatherill, M.; Van Der Meeren, O.; Ginsberg, A. M.; Van Brakel, E.; Salaun, B.; Scriba, T. J.; Akite, E. J.; Ayles, H. M.; Bollaerts, A.; et al. Final Analysis of a Trial of M72/AS01E Vaccine to Prevent Tuberculosis. *New England Journal of Medicine* **2019**, *381* (25), 2429-2439. DOI: 10.1056/NEJMoa1909953.
(104) La Manna, M. P.; Orlando, V.; Tamburini, B.; Badami, G. D.; Dieli, F.; Caccamo, N. Harnessing Unconventional T Cells for Immunotherapy of Tuberculosis. **2020**, *11*, Perspective. DOI: 10.3389/fimmu.2020.02107.
(105) Musvosvi, M.; Huang, H.; Wang, C.; Xia, Q.; Rozot, V.; Krishnan, A.; Acs, P.; Cheruku, A.; Obermoser, G.; Leslie, A.; et al. T cell receptor repertoires associated with control and disease progression following Mycobacterium tuberculosis infection. *Nat Med* **2023**, *29* (1), 258-269. DOI: 10.1038/s41591-022-02110-9 From NLM.
(106) Mazzotti, L.; Gaimari, A.; Bravaccini, S.; Maltoni, R.; Cerchione, C.; Juan, M.; Navarro, E. A.; Pasetto, A.; Nascimento Silva, D.; Ancarani, V.; et al. T-Cell Receptor Repertoire Sequencing and Its Applications: Focus on Infectious Diseases and Cancer. *Int J Mol Sci* **2022**, *23* (15). DOI: 10.3390/ijms23158590 From NLM.
(107) Garibyan, L.; Avashia, N. Polymerase chain reaction. *The Journal of investigative dermatology* **2013**, *133* (3), 1-4. DOI: 10.1038/jid.2013.1 From NLM.
(108) Sanders, R.; Huggett, J. F.; Bushell, C. A.; Cowen, S.; Scott, D. J.; Foy, C. A. Evaluation of Digital PCR for Absolute DNA Quantification. *Analytical Chemistry* **2011**, *83* (17), 6474-6484. DOI: 10.1021/ac103230c.
(109) Zoutman, W. H.; Nell, R. J.; Versluis, M.; van Steenderen, D.; Lalai, R. N.; Out-Luiting, J. J.; de Lange, M. J.; Vermeer, M. H.; Langerak, A. W.; van der Velden, P. A. Accurate Quantification of T Cells by Measuring Loss of Germline T-Cell Receptor Loci with Generic Single Duplex Droplet Digital PCR Assays. *J Mol Diagn* **2017**, *19* (2), 236-243. DOI: 10.1016/j.jmoldx.2016.10.006 From NLM.
(110) Hegenbarth, J.-C.; Lezzoche, G.; De Windt, L. J.; Stoll, M. Perspectives on Bulk-Tissue RNA Sequencing and Single-Cell RNA Sequencing for Cardiac Transcriptomics. *Frontiers in Molecular Medicine* **2022**, *2*, Review. DOI: 10.3389/fmmed.2022.839338.
(111) Nyaruaba, R.; Mwaliko, C.; Kering, K. K.; Wei, H. Droplet digital PCR applications in the tuberculosis world. *Tuberculosis* **2019**, *117*, 85-92. DOI: https://doi.org/10.1016/j.tube.2019.07.001.
(112) Roederer, M. How many events is enough? Are you positive? *Cytometry Part A* **2008**, *73A* (5), 384-385. DOI: https://doi.org/10.1002/cyto.a.20549.
(113) Estévez, O.; Anibarro, L.; Garet, E.; Martínez, A.; Pena, A.; Barcia, L.; Peleteiro, M.; González-Fernández, Á. Multi-parameter flow cytometry immunophenotyping distinguishes different stages of tuberculosis infection. *The Journal of infection* **2020**, *81* (1), 57-71. DOI: 10.1016/j.jinf.2020.03.064 From NLM.
(114) Tembhare, P.; Yuan, C. M.; Xi, L.; Morris, J. C.; Liewehr, D.; Venzon, D.; Janik, J. E.; Raffeld, M.; Stetler-Stevenson, M. Flow cytometric immunophenotypic assessment of T-cell clonality by Vβ repertoire analysis: detection of T-cell clonality at diagnosis and monitoring of minimal residual disease following therapy. *Am J Clin Pathol* **2011**, *135* (6), 890-900. DOI: 10.1309/ajcpv2d1ddsgjdbw From NLM.
(115) O'Donnell, E. A.; Ernst, D. N.; Hingorani, R. Multiparameter flow cytometry: advances in high resolution analysis. *Immune Netw* **2013**, *13* (2), 43-54. DOI: 10.4110/in.2013.13.2.43 From NLM.
(116) Esmael, A.; Abebe, T.; Mihret, A.; Mussa, D.; Neway, S.; Ernst, J.; Rengarajan, J.; Wassie, L.; Howe, R. Mycobacterium tuberculosis antigen-specific T-cell responses in smear-negative pulmonary tuberculosis patients. *Clin Exp Immunol* **2022**, *209* (1), 99-108. DOI: 10.1093/cei/uxac049 From NLM.
(117) Mupfumi, L.; Mpande, C. A. M.; Reid, T.; Moyo, S.; Shin, S. S.; Zetola, N.; Mogashoa, T.; Musonda, R. M.; Kasvosve, I.; Scriba, T. J.; et al. Immune Phenotype and Functionality of Mtb-Specific T-Cells in

HIV/TB Co-Infected Patients on Antiretroviral Treatment. *Pathogens* **2020**, *9* (3). DOI: 10.3390/pathogens9030180 From NLM.
(118) Adekambi, T.; Ibegbu, C. C.; Cagle, S.; Kalokhe, A. S.; Wang, Y. F.; Hu, Y.; Day, C. L.; Ray, S. M.; Rengarajan, J. Biomarkers on patient T cells diagnose active tuberculosis and monitor treatment response. *J Clin Invest* **2015**, *125* (5), 1827-1838. DOI: 10.1172/jci77990 From NLM.
(119) Henriquez, J.; Zhou, J.; Li, J.; Crawford, R.; Kaminski, N. Application of gene specific mRNA level determinations in individual cells using flow cytometry-based PrimeFlow™ in immunotoxicology. *Toxicol Appl Pharmacol* **2017**, *337*, 39-44. DOI: 10.1016/j.taap.2017.10.021 From NLM.
(120) Croce, A. C.; Bottiroli, G. Autofluorescence spectroscopy and imaging: a tool for biomedical research and diagnosis. *Eur J Histochem* **2014**, *58* (4), 2461. DOI: 10.4081/ejh.2014.2461 From NLM.
(121) Mpande, C. A. M.; Rozot, V.; Mosito, B.; Musvosvi, M.; Dintwe, O. B.; Bilek, N.; Hatherill, M.; Scriba, T. J.; Nemes, E. Immune profiling of Mycobacterium tuberculosis-specific T cells in recent and remote infection. *EBioMedicine* **2021**, *64*, 103233. DOI: 10.1016/j.ebiom.2021.103233 From NLM.

Supplementary Material

Supplementary Table 1: The Beta TCR Vβ antibody kit composition and associated Vbeta according to Wei *et al*.

Tube	Conjugate	Vbeta	Optimal volume (µl)
A	PE FITC+PE FITC	VB5.3 VB7.1 VB3	2.5
B	PE FITC+PE FITC	VB9 VB17 VB16	2.5
C	PE FITC+PE FITC	VB18 VB5.1 VB20	2.5
D	PE FITC+PE FITC	VB13.1 VB13.6 VB8	3.75
E	PE FITC+PE FITC	VB5.2 VB2 VB12	2.5
F	PE FITC+PE FITC	VB23 VB1 VB21.3	2.5
G	PE FITC+PE FITC	VB11 VB22 VB14	2.5
H	PE FITC+PE FITC	VB13.2 VB4 VB7.2	5

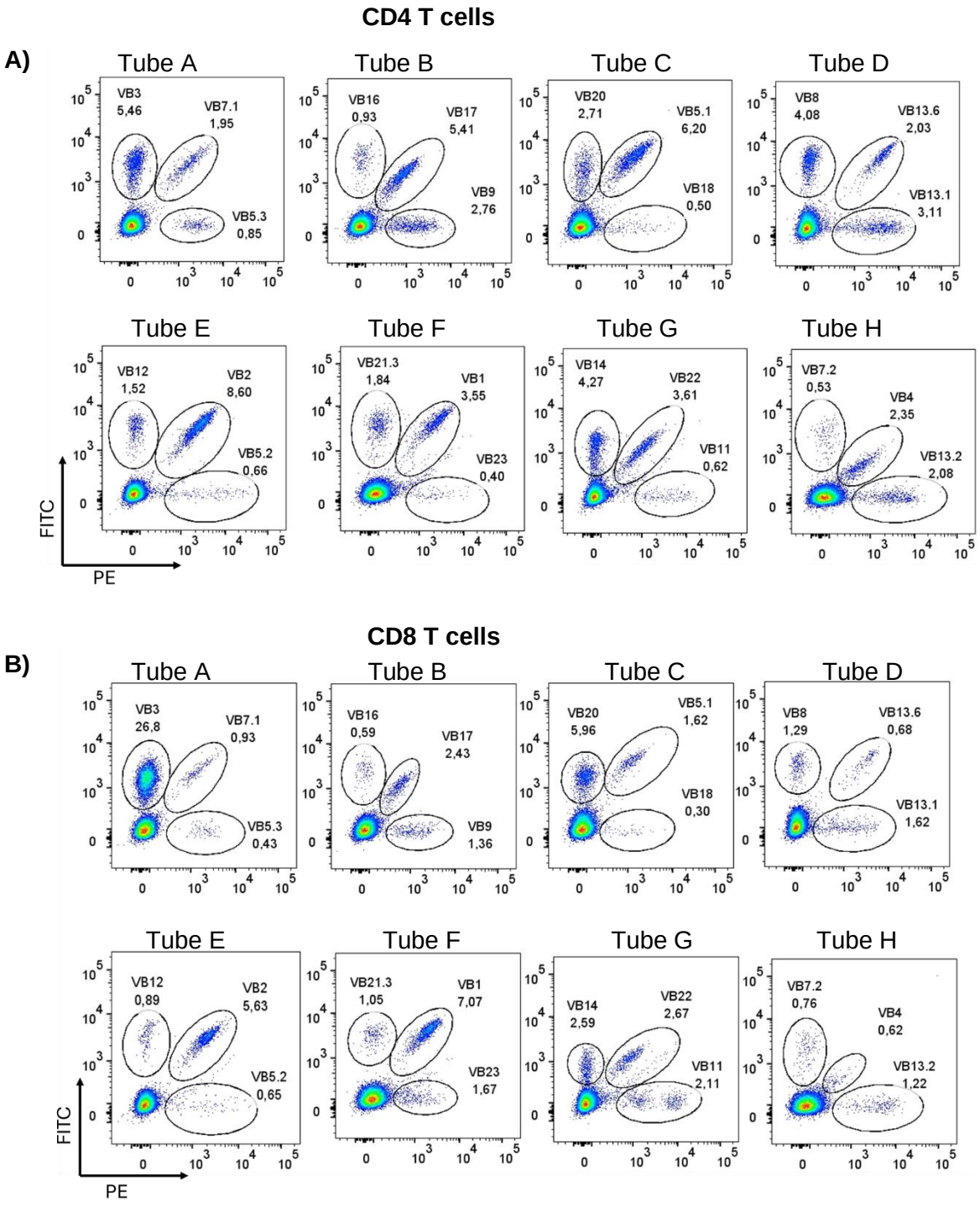

Supplementary Figure 1: Optimal antibody volumes allow detection of different Vβ sequences expressed by CD4 and CD8 T cells. Frequencies of CD4 **(A)** and **(B)** CD8 T cells expressing the different Vβ sequences. A total of one million cells was used to test each tube.